Aymptotic Safety in the Standard Model and Beyond

Carlos Mauricio Nieto Guerrero[1,2]

PhD Thesis

Supervisor
Roberto Percacci[1]

[1] Scuola Internazionale Superiore di Studi Avanzati - SISSA

[2] Abdus Salam International Centre for Theoretical Physics - ICTP

Scuola Internazionale Superiore di Studi Avanzati
Theoretical Particle Physics Section
Trieste, Italy
2019

Abstract

TITLE: Aymptotic Safety in the Standard Model and Beyond [i].

AUTHOR: NIETO GUERRERO, Carlos Mauricio[ii].

KEYWORDS: Asymptotic Safety, Standard Model, Gravity, Yukawa couplings.

DESCRIPTION: We study the evolution of the Standard Model couplings in the framework of Asymptotic Safety. We explore the dynamics of Gauge-Yukawa systems, which has been proven to be successful in the generation of UV fixed points . With an extensive analysis, we examine the UV properties of the Standard Model under the extension of its fermionic sector. Considering also the compelling the evidence of Asymptotic Safety in gravity, we take the into account the gravitational effects in the running of gauge and quark Yukawa matrices. Special attention is given to the gravitationally-induced hierarchy in the mass spectrum of the quarks.

[i] PhD Thesis

[ii] Theoretical Particle Physics Section, SISSA. Supervisor: Roberto Percacci.

Contents

Introduction

In the early days of quantum field theory, renormalizability was used as a criterion to select physically viable models. It was later understood that effective field theories can be useful and predictive in their domain of validity even if not renormalizable. Current particle physics is largely based on this paradigm. However, it leaves an enormous freedom. One would like to have a more restrictive framework to guide the search for physics beyond the Standard Model. Non-perturbative renormalizability, also known as *asymptotic safety* (AS), provides such a framework. A quantum field theory is AS if all its couplings, running along the renormalization group (RG) flow, reach a fixed point in the ultraviolet (UV) limit [1, 2]. The fixed point can be interacting or free (Gaussian). In the latter case, AS reduces to asymptotic freedom (AF). In both cases, the theory is well behaved and predictive at all energies. UV completeness is by itself a rather abstract notion, being untestable in practice. The real bonus of AS is that when a suitable fixed point exists, typically there are only a finite number of relevant directions that determines the dimension of the surface where the couplings live. This greatly restricts the infrared physics.

While AF theories have been studied in great detail and for a long time, work on AS models for particle physics has only begun quite recently. For some early references based on the use of the functional renormalization group see [3, 4, 5, 6, 7, 8]. A breakthrough came with the work of Litim and Sannino, who constructed gauge-Yukawa systems admitting interacting fixed points that are under perturbative control [9] (see also [10]). In these models the fixed point arises from a cancellation between one- and two-loop terms in the β-functions. The crucial ingredient is the Veneziano limit, providing the small expansion parameter

$$\epsilon = \frac{N_f}{N_c} - \frac{11}{2} \ ,$$

where N_c and N_f are the numbers of colors and flavors respectively. It is reasonable to expect that there may exist AS models also for finite values of ϵ. General conditions for the existence

of such fixed points have been discussed in [11, 9]. Applications of these ideas to BSM physics have appeared [12, 13, 14, 15, 16, 17].

The Standard Model (SM) by itself is not AS because of the Landau pole in the $U(1)$ gauge coupling [18, 19] and the uncertain fate of the Higgs quartic interaction [20]. The Landau pole can only be avoided by assuming that the gauge coupling is identically zero at all energies. This is known as the triviality problem.

In this work, we focus on two different forms of turning the SM into an AS theory. Either we extend the matter content, or we take into account the gravitational corrections to the running of all the SM couplings. Regarding the modification of the matter content of the SM, the simplest (and most studied) extension consists of multiple generations of vector-like fermions carrying diverse representations under the SM gauge group. Vector-like fermions have the property of not giving rise to gauge anomalies and being technically natural. The authors of [14] have studied the β-functions to two-loop order in the simplified case of $SU(3) \times SU(2)$ gauge interactions and a Yukawa-like interaction among the vector-like fermions. They find several UV fixed points, which they match to the low-energy SM in a number of benchmark cases. In a parallel development, the authors of [15, 16] studied AS for the full SM gauge group, again extended by vector-like fermions, by means of a resummation of the perturbative series of the β-functions. They find several UV fixed points, which however cannot be matched to the low-energy SM in a consistent manner [16].

To move forward in this program, we report our results for a large class of models based on the SM matter content and with $SU_c(3) \times SU_L(2) \times U_Y(1)$ gauge interactions, retaining only the top Yukawa coupling and the Higgs quartic self-interaction; in addition, the models contain vector-like fermions coupled to the SM which have Yukawa interactions with a new set of scalar fields. The restriction to the top Yukawa makes the form of the β-functions more manageable—and is in line with earlier investigations. Our models differ in the number of copies of the vector-like fermions and in the representation of the gauge groups that they carry.

In contrast to [15, 16] we do not use resummed β-functions. Instead, we compare the results of the two-loop gauge β-functions considered so far in the literature with the three loop results. As explained in Chapter 3, the β-functions for the Yukawa and scalar couplings are retained always at one- and two-loops less than the gauge couplings, respectively. By comparing the results of these two different approximation schemes, we are able to assess quantitatively the impact of radiative corrections and therefore to decide whether a given fixed point is within the perturbative domain or not. This selection is supported by the use of other tests of perturbativity that the fixed points must satisfy, as discussed in sections 3.2 and 3.3.

We have made a systematic search of reliable fixed points in a large grid parameterized by the number of vector-like fermions N_f and their $SU(3)_c \times SU(2)_L \times U(1)_Y$ quantum numbers [21]. We first find all the zeros of the β-functions for each model in the grid. We then test each fixed point under two conditions:

- The fixed point must occur in a region in which the perturbative expansion is reliable. At the very least, this implies that it must be possible to reasonably trace its value at some order in the perturbative expansion back to that of the previous order. We see *a posteriori* that this can be done only when the values of the couplings and of the scaling exponents (the eigenvalues of the linearized expansion around the fixed point) are sufficiently small and the fixed point satisfies all the criteria introduced in Chapter 3.
- The fixed point must be connected to the SM at low energy. In general this would require a delicate numerical analysis of the trajectories emanating from it. However, we find that a rough necessary condition is sufficient for our purposes: the fixed point must not have any coupling that is zero and irrelevant, because such couplings must be identically zero at all scales to avoid Landau poles.

These two requirements taken together, that we consider to be quite reasonable, are very restrictive. As a matter of fact, we are not able to identify *any* choice for the group representations and number of generations of the vector-like fermions that would make the extension of the SM reliably AS. This does not mean that such an extension does not exist: it only means that if such an AS extension of the SM exists, it must either be different from those that we have considered, or else it must have a fixed point that lies outside the reach of perturbation theory.

Having explored the matter extensions of the SM, we move on and ask whether gravitational corrections modify the general picture of the previous analysis. Studies of gravitational systems within the framework of functional renormalization group suggest that there exists a stable fixed-point with a finite number of relevant directions [22, 23, 24, 25, 26, 27, 28, 29, 30, 31, 32, 33, 34, 35, 36, 37, 38]. Effects of vector, fermion and scalar degrees of freedom have been also studied in the literature [28]. From these studies, it seems that the SM degrees of freedom do not spoil the AS picture in gravity. The general consensus is that the SM degrees of freedom does not affect the AS properties of gravity. Conversely, studies of gravitational effects on matter couplings have been also carried out [39, 40, 41, 42]. For our discussion, it is relevant to note the nature of the corrections induced by gravity in gauge and Yukawa interactions. Due to the universality of the gravitational interactions, the corrections to the running of a given gauge (g) and Yukawa (y) couplings take the form

$$\beta_{g,y} = \beta_{g,y}^{Matter} + f_{g,y} g(y),$$

where $f_{g,y}$ are functions of the gravitational couplings. These new set of RG equations open the possibility of rendering the Standard Model asymptotically safe. In fact, there have been attempts trying to exploit the properties of the modified beta functions [43, 44, 45, 46, 47, 48, 49]. Here, we go one step further and explore the structure of the corrected beta functions in the full quark sector of the SM.

In this context we have studied the set of quark Yukawa couplings and mixing parameters below and beyond the Planck scale. Since the AS paradigm in gravity tells us that quantum corrections are important beyond the Planck scale, we expect to have modifications to the running of the SM parameters at very high energies. In particular, we look for non-trivial fixed points for which the dimension of the critical hypersurface is smaller than the total number of couplings. Thus, the gravitational corrections induce predictions in the set of SM couplings. Since at least one of the Yukawa couplings might be predicted by the presence of such a fixed point, there is the possibility of explaining, at least in part, the hierarchy in the spectrum of masses in the quark sector. If the SM can be embedded in a AS theory, then it depends on fewer parameters than in the usual formulation. Another important aspect of this analysis is the avoidance of the triviality problem in the $U(1)$ sector. In fact, it is the exclusion of the Landau pole in g_1 that allows us to talk about predictions in the Yukawa couplings because the theory becomes UV finite. The gravitational effects give a solution to the problem that was not found with the inclusion of vector-like fermions. In Chapter 4, we describe the main features of the mechanism behind the generation of the non-trivial fixed point in the gauge and Yukawa sector. Going from one to three generations of quarks, we illustrate how the predictions arise and how the RG flow of the couplings get modified.

List of Publications

The discussion presented in this text is based on the following works:

- C. M. Nieto, R. Percacci, V. Skrinjar, "Split Weyl Transformations in Quantum Gravity", Phys. Rev. vol. D96, no. 10, p. 106019, 2017.
- D. Barducci, M. Fabbrichesi, C. M. Nieto, R. Percacci, V. Skrinjar, "In search of a UV completion of the standard model - 378.000 models that don't work", JHEP, vol. 11, p. 057, 2018.
- R. Alkofer, A. Eichhorn, A. Held, C. M. Nieto, R. Percacci, M. Schröfl, "Quark masses and mixings from UV completion within a minimal parametrization of BSM physics", *In preparation.*

Chapter 1

The Concept of Asymptotic Safety

In this chapter we describe the general procedure that we follow in the rest of this work. This allows us to motivate better the requirements that we impose on the fixed points in order for them to be considered as physical. We recommend [50] as a general reference on RG flows.

1.1. The fixed points of the β-functions

Consider a theory with generic (gauge, fermion or scalar) fields and (generally dimensionful) couplings $\bar{g}_i$ characterizing the interactions among them. In the study of the renormalization group (RG) flows it is customary to use dimensionless couplings g_i. We define these dimensionless couplings as $g_i = \mu^{-d_i}\bar{g}_i$, where d_i is the mass dimension of $\bar{g}_i$, and μ is the sliding energy scale. The renormalization of the theory is completely characterized by its β-functions

$$\beta_i(g_j) \equiv \mu \frac{dg_i}{d\mu}\,, \tag{1.1.1}$$

A fixed point of this theory, denoted g_j^*, is defined by the vanishing of the β-functions of all couplings:

$$\beta_i(g_j^*) = 0\,. \tag{1.1.2}$$

When the couplings g_j assume the values g_j^*, their flow has stopped. In general, a given fixed point can be reached either in the UV or in the IR limit. The space of couplings is filled with trajectories flowing towards or away from fixed points . In the next section, we discuss some properties of the theory space and the information we can obtain about it.

1.2. Linearized flow

Once we have a candidate fixed point, we can study the flow in its immediate neighborhood. We first introduce the coordinates $y_i \equiv g_i - g_i^*$ that quantify the closeness to the fixed point . Then, we study the RG evolution via the linearized the β-functions

$$\frac{dy_i}{dt} = M_{ij} y_j \,, \tag{1.2.1}$$

where $M_{ij} \equiv \partial\beta_i/\partial g_j$ is referred to as the *stability matrix*. In order to better understand the fate of each coupling in theory space, we diagonalize the linear system by going to the variables $z_i = (S^{-1})_{ij} y_j$. The matrix S is defined such that it diagonalizes M

$$(S^{-1})_{ij} M_{jl} S_{ln} = \delta_{in} \theta_n \,, \tag{1.2.2}$$

Thus, the new β-functions and their solutions take the simple form

$$\frac{dz_i}{dt} = \theta_i z_i \quad \text{and} \quad z_i(t) = c_i \, e^{\theta_i t} = c_i \left(\frac{\mu}{\mu_0}\right)^{\theta_i} . \tag{1.2.3}$$

We see that the evolution of each new variable z_i depends on its eigenvalue or scaling exponent θ_i. Depending on the sign of θ_i we can have three different situations

- For $\theta_i > 0$, as we increase μ we are pushed away from the fixed point and z_i increases without control; the direction z_i is said to be *irrelevant*.
- If $\theta_i < 0$, as we increase μ we are pulled back to the fixed point; the direction z_i is called a *relevant* direction.
- If $\theta_i = 0$, we do not know the fate of z_i and we have to go beyond the linear order as explained below; the direction z_i is called *marginal* in this case.

The notion of relevance/irrelevance is independent of the direction of the flow and of the choice of basis. The eigendirections in (1.2.3) define a linear space (shown in Figure 1.1 as a white plane) around the fixed point . In the same figure we depict in blue the full UV critical surface, defined as the surface of points that are pulled to the fixed point at high energies. The points that are not on the critical surfacet would generally flow towards infinite values. In order for the couplings g_i to be finite, our coupling constants must lie on the critical surface. As a consequence, some or the couplings will not be independent. The non-trivial equation defining the critical surface sets non-trivial relations among couplings, for instance, $g_i = f(g_j)$. This is

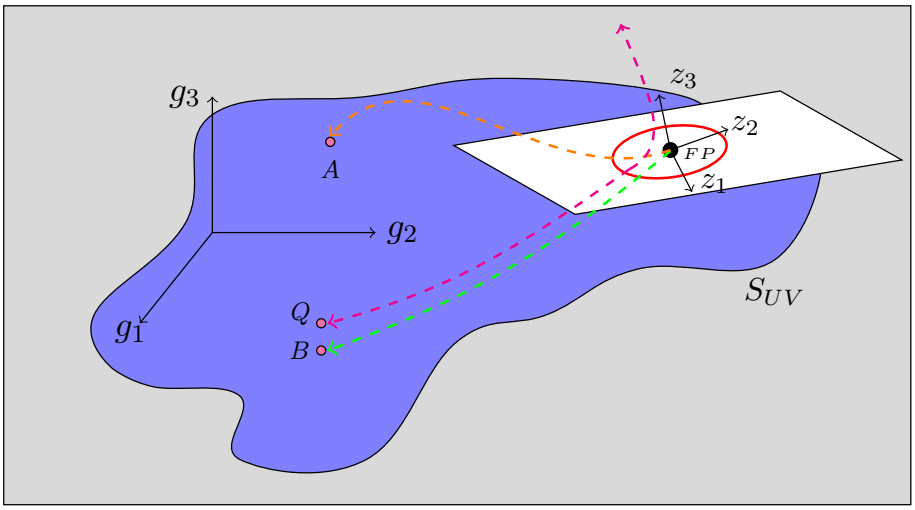

Figure 1.1: Theory space of couplings g_i where only 3 axes are shown for simplicity. For a given fixed point we show the UV safe surface S_{UV} (blue region), the approximated UV critical surface around the fixed point (white plane), the new set of coordinates z_i, a small region of possible initial points for the flow (red circle) and two UV safe trajectories ending at a given matching scale $\mathcal{M}$ (green and orange lines). We also show a trajectory starting close to the point B but outside S_{UV}. This trajectory approaches the fixed point but goes to inifinite values at very high energies (magenta line).

source of the predictive power of AS theories. We see here that finiteness of $d_{S_{UV}}$, the dimension of the critical surface, constrains the theory at all energy scales. The smaller the dimension of the critical surface, the larger the number of prediction that can be made. In Chapter 4 we exploit this property and use it to understand important features of the SM of particle physics. It is an key question throughout this work to ask whether the SM couplings at low energies lie or not on a critical surface.

The eigenvalues θ_i have the property of being universal quantities—meaning that they are invariant under a general coordinate transformation in the space of couplings [10]. We know that in general, from dimensional analysis, the β-function for a dimensionful coupling $\bar{g}_i$, we have $\beta_i(\bar{g}_j, k) = k^{d_i}\alpha_i(g_j)$ where $\alpha_i(g_j)$ contains the non-trivial dependence on the dimensionless couplings. Then, the beta functions for the dimensionless couplings are given by

$$\beta_i = -d_i g_i + \alpha_i(g_j), \tag{1.2.4}$$

where $\alpha_i(g_j)$ encodes the pure quantum contributions to the β-functions and the first term represents the classical scaling. Therefore, the stability matrix is given by

$$M_{ij} = -d_i\delta_{ij} + \frac{\partial\alpha}{\partial g_j}. \tag{1.2.5}$$

Thus, the eigenvalues θ_i can be written as the sum of $-d$, coming from the classical scaling, plus quantum corrections.

1.3. Marginal couplings

If one of the eigenvalues is equal to zero, the linear approximation does not give us information about the RG behavior in the direction associated to it. Then we have to go further in the expansion. At second order in the couplings y_i, the β-functions take the form

$$\frac{dy_i}{dt} = M_{ij}y_j + P_{ijk}y_j y_k\,, \quad \text{where} \quad P_{ijk} = \frac{\partial^2 \beta_i}{\partial g_j \partial g_k}. \tag{1.3.1}$$

The structure of these quadratic flows is quite complicated to describe in full generality. The fate of a specific trajectory depends strongly on the position of the initial point in the neighborhood of the fixed point.

However, marginal couplings do not generally occur for a fully interacting fixed point: in the models considered here they can always be identified with some coupling that is itself zero at the fixed point. We show in Appendix A that the structure of the β-functions is such that the flow of the marginal couplings near the fixed point is of the form

$$\frac{dy_i}{dt} = P_{iii}y_i^2\,, \tag{1.3.2}$$

(no summation implied). Our beta functions in Chapter 3 will be written always in terms of $\alpha_i = \frac{g_i^2}{(4\pi)^2}$, which are bound to be positive. Therefore, marginal directions α_i with $P_{iii} < 0$ are UV attractive and are called *marginally relevant* (a well-known example being the QCD gauge coupling) while those with $P_{iii} > 0$ are UV repulsive and are called *marginally irrelevant*. Altogether, the UV critical surface is thus spanned by the relevant and marginally relevant directions.

1.4. Infrared matching

Once we have an understanding of the fixed point structure—and the conditions on the couplings α_i and the scaling exponents θ_i are satisfied—there remains to find the trajectory connecting a given fixed point to the IR physics. This is accomplished in the following manner. First, we define IR scale which depends on the problem we deal with. In Chapter 3 we take it to be

1.83 TeV, while in Chapter 4 it is equal to 173.21 GeV. This defines the target for the flow to the IR from the UV fixed point. The RG flow is started from a point belonging to the UV critical surface, infinitesimally close to the fixed point (red circle in Figure 1.1). This guarantees that, to high precision, the flow towards the UV ends at the fixed point. The system is then allowed to flow by means of the full β-functions of the theory towards the IR. The initial point of the flow is varied until, ideally, the trajectory hits exactly the desired IR values.

For most of the models that we consider in Chapter 3, this laborious procedure is not necessary. For all their fixed points that can be regarded as being in the perturbative domain, the hypercharge is zero at the fixed point and is also a marginally irrelevant coupling. This means that in order to reach the fixed point in the UV limit, the hypercharge must be zero at all energies. All other trajectories have a Landau pole. These models are thus excluded by a version of the triviality problem. On the other hand, in Chapter 4 we do need to perform a matching. The analysis is quite involved but we are able to test the fixed-point regime and obtain IR values that are close to the measured ones. In the next Chapters, we study two different approaches that attempt to render the SM dimensionless couplings finite in the far UV. The two analyses have different nature. Therefore, we need to introduce new concepts in each of those studies. The first one is about perturbation theory, which is given in section 1.5. The other one is about asymptotically safe gravity, introduced in Chapter 2.

1.5. Perturbative Asymptotic Safety

When we work in the framework of perturbation theory, extra conditions should be imposed in the resulting quantities associated to a fixed point . This is necessary in order to remain within the domain of perturbative accuracy. Therefore, we demand that all the couplings at the fixed point g_i^* are sufficiently small. In practice this means that the transition from one order to the next in the loop expansion should not change appreciably the position of the fixed point, neither its global properties. We will see that this implies that the numerical value of the fixed points must satisfy the condition

$$0 < \left(\frac{g_i^*}{4\pi}\right)^2 < 1\,, \tag{1.5.1}$$

The condition in Eq. (1.5.1) suffices to keep the perturbative expansion within its limits of validity. However, this is true if the coefficients in the perturbative expansions are of the same order and not too large. Otherwise, the loop expansion does not converge. Every new loop expansion would introduce a larger and larger modification. This is the main motivation for checking all our results at two different loop orders. In section 3.2 we will expand on perturbative stability and it will become more clear why the requirement (1.5.1) is a good

indicator of perturbative realiability.

On the other hand, we have the universal quantity θ_i. Its value quantifies how fast we flow towards the fixed point . Moreover, for canonically marginal couplings (having $d_i = 0$), we note that the scaling exponents have a fully quantum origin. Thus, we ask for the following

$$|\theta_i| < O(1)\,. \tag{1.5.2}$$

As a disgression, we recall that the β-function of a single coupling is independent of the gauge choice in dimensional regularization. It is regularization scheme-independent up to two-loops. If there are several couplings running together, their β-functions depend on the scheme already at the two-loops [51]. There is therefore a degree of ambiguity in the position of the fixed points we are going to discuss because their position could be moved by changing the scheme. We assume that these changes are small if the fixed point is found within the perturbative regime. One should however bear in mind this problem of scheme dependence in all the discussions to follow.

Chapter 2

Asymptotic Safety in Gravity

In this chapter, we discuss the concept of Asymptotic Safety for gravity. We start by analyzing pure gravity. Then, we move to systems including gravity and matter. The latter case is of particular relevance in our examination of the UV completeness of the Standard Model. It is known that Einstein gravity is not renormalizable at the perturbative level [52, 53, 54, 55]. That is, we need to fit an infinite number of free parameters in order to cancel the divergences appearing at every loop order in the perturbative expansion. Consequently, the theory is valid up to some physical scale (namely, the Planck scale). Quantum corrections to the Einstein action are suppressed by powers of the Planck scale M_{pl}. Below this energy scale, and at a given order in the momentum expansion, only a finite number of counterterms are needed and the theory is predictive as an Effective Field Theory (EFT) [56, 57, 58, 59]. The breakdown of the perturbative quantum treatment of Einstein gravity makes us wonder whether the issue lies in gravity itself or in the perturbative analysis. It is possible that the theory is renormalizable in a non-perturbative sense and therefore valid at all energies. Actually, if by means of non-perturbative methods we are able to find a UV fixed point with the properties described in Chapter 1, we can say we have found a quantum description of gravity in the framework of Quantum Field Theory [22, 60, 61, 23, 24, 25, 26, 27, 62, 28, 29, 30, 31, 32, 34, 37, 37]. In the following, we describe the main features of AS gravity.

2.1. Functional Renormalization Group Framework

Most of the studies of AS in gravity are carried out in the framework of Functional Renormalization Group, which allows for a non-perturbative treatment. In particular, the

Wetterich equation is used in order to determine the beta functions of any theory [63, 64, 65]. The scale dependence in the couplings is introduced in the definition of the generating functional through an infrared cutoff R_k. The main idea of this approach is to provide an exact RG equation that is valid in the perturbative, as well as in the non-perturbative regime. Here, we outline the central notions of this framework for a scalar theory; then, we extend it to gravity in order to discuss the current status of the field of AS. We start by modifying the quadratic part of the action S in the definition of the generating functional of connected correlation functions W_k. Introducing the so called 'cutoff' or 'regulator' action depending on an operator Δ

$$\Delta S_k(\phi) = \frac{1}{2}\int dx \phi R_k(\Delta)\phi, \tag{2.1.1}$$

we write

$$e^{W_k[j]} = \int (d\phi) e^{-S-\Delta S_k + \int dx j\phi}. \tag{2.1.2}$$

It is useful to call z the argument of R_k. This variable can be regarded as the eigenvalue of the operator Δ. The term (2.1.1) in (2.1.2) has the impact of modifying the quadratic part of modes with eigenvalues λ_n less than k. That is, it guarantees that only modes with eigenvalues larger than k are integrated out. The other modes are decoupled since they acquire a mass of order k. In order fit the above requirements, R_k must satisfy some general conditions. First, we require that $R_k \to 0$ for $k \to 0$ (for any value of z), in order to get the full quantum effective action in the IR. Similarly, we demand $R_k(z)$ to increase monotonically as a function of k for fixed z, and to decrease monotonically with z for at fixed k. Then, for $z > k$ the regulator goes to zero fast enough so that it only suppress the IR modes. Finally, as a normalization condition, we ask for $R_k(0) = k^2$. To sum up, we see that the k plays the role of an IR cutoff. However, R_k was used only to introduce an explicit scale dependence in the generating functional. In our final result, we will see how the Wetterich equation will be UV and IR finite.

We can apply the Legendre transform to (2.1.2) to obtain

$$\tilde{\Gamma}_k(\varphi) = -W_k(j_\varphi) + \int dx j_\varphi \varphi, \tag{2.1.3}$$

where we have introduced the expectation value of ϕ

$$\varphi(x)_j = \langle \phi(x) \rangle = \frac{\partial W}{\partial j(x)}. \tag{2.1.4}$$

The quantity j_φ is obtained by inverting Eq. (2.1.4); that is, j_φ becomes a function of φ. Finally, we define the Effective Average Action (EAA) $\Gamma_k(\varphi)$ by subtracting the cutoff action from $\tilde{\Gamma}_k(\varphi)$

$$\Gamma_k(\varphi) = \tilde{\Gamma}_k(\varphi) - \Delta S_k(\varphi). \tag{2.1.5}$$

In some sense, the subtraction of the cutoff action compensates its introduction done in the generating functional. Now, the significance of EAA is that its flow equation presents a simple and compact form. In fact, we can derive a flow equation for Γ_k that is valid regardless of the use of perturbation theory.

Defining $t = \text{Ln } k$, the scale derivative of W_k is written as

$$\frac{dW_k}{dt} = -\frac{d}{dt}\langle \Delta S_k \rangle = -\frac{1}{2} Tr \langle \phi\phi \rangle \frac{dR_k}{dt}, \tag{2.1.6}$$

where the trace stands for an integration over coordinate and momentum space. Now, from the definition of φ, we obtain

$$\begin{aligned} \frac{d\Gamma_k}{dt} =& -\frac{dW_k}{dt} - \frac{d\Delta S_k[\varphi]}{dt}, \\ =& \frac{1}{2}\text{Tr}\left(\langle\phi\phi\rangle - \langle\phi\rangle\langle\phi\rangle\right)\frac{dR_k}{dt}, \\ =& \frac{1}{2}\text{Tr}\,\frac{\delta^2 W_k}{\delta j \delta j}\frac{dR_k}{dt}. \end{aligned} \tag{2.1.7}$$

From the Legendre transform of $W_k[j]$, we see that

$$\frac{\delta \bar{\Gamma}_k}{\delta \varphi} = j, \tag{2.1.8}$$

and, therefore

$$\frac{\delta^2 W_k}{\delta j \delta j} = \left(\frac{\delta^2 \bar{\Gamma}_k}{\delta\varphi\delta\varphi}\right)^{-1}. \tag{2.1.9}$$

Thus, transforming our results in terms of Γ_k, we arrive at the equation [63]

$$\frac{d\Gamma_k}{dt} = \frac{1}{2}\text{Tr}\left(\frac{\delta\Gamma_k}{\delta\phi\delta\phi} + R_k\right)^{-1}\frac{dR_k}{dt}. \tag{2.1.10}$$

Eq. (2.1.10) is referred to as the Wetterich equation, Exact Renormalization Group Equation (ERGE) or Functional Renormalization Group Equation (FRGE). It has the structure of a one-loop equation whose graphic representation is given in Fig. 2.1. That representation comes from the fact that in $\partial_k\Gamma$ we have the exact propagator $\left(\frac{\delta\Gamma_k}{\delta\phi\delta\phi} + R_k\right)^{-1}$, which is depicted as a continuous line in 2.1.

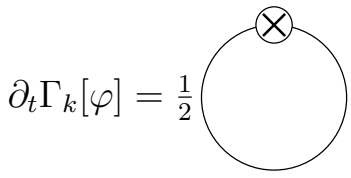

Figure 2.1: Representation of the FRG equation (2.1.10). The continuous line symbolize the complete propagator. The crossed circle stands for the insertion of $\partial_k R_k$

We observe that the flow equation for Γ_k depends only on Γ_k itself, there is no reference to the bare action S. That is, the derivative of Γ_k at a scale k depends only on the physics at the scale k and below. We do not need information about the UV. Additionally, we note that (2.1.10) is UV finite. The insertion of $\frac{dR_k}{dt}$ makes the trace finite since we know that the cutoff decreases fast for $z > k^2$, and then $\frac{dR_k}{dt}$ also does. In other words, in (2.1.10) we have difference of two EAA at slightly different k, therefore divergences in both expressions cancel out leaving us the finite part only.

We saw before that our flow equation is free of UV and IR divergences, even though W_k and Γ_k themselves are not. Therefore, it is useful to use Eq. (2.1.10) in order to study particular QFT. We explain now how to proceed in this regard. We bring in the idea of 'theory space' as the space of all functionals of φ. Then, we write the most general EAA constructed with all the functionals $\mathcal{O}_i(\varphi)$ in the theory space respecting the symmetries of the system

$$\Gamma_k(\varphi) = \sum_i g_i(k)\mathcal{O}_i(\varphi), \tag{2.1.11}$$

where $g_i(k)$ stand for the running coupling constants. Differentiating with respect to t we have

$$\frac{d\Gamma_k}{dt} = \sum_i \beta_i \mathcal{O}_i(\varphi), \text{ where } \beta_i(g_j, k) = \frac{dg_i}{dt}. \tag{2.1.12}$$

The quantities $\beta_i(g_j, k)$ are the beta functions of the theory. They can be computed by expanding the r.h.s. of (2.1.10) on the basis of operators $\mathcal{O}_i(\varphi)$, and comparing each side of the equation.

2.2. FRG in Gravity

The Wetterich equation can be used also for gauge theories, in particular, it is useful in the study of Yang-Mills theory and Gravity. The extension for those cases share similar elements. Therefore we focus on gravity since it is the most relevant for the upcoming chapters. The functional integral in (2.1.2) depends strongly on the operator Δ because it helps us classifying modes according to their eigenvalues and k. Clearly Δ is defined in some spacetime setting. For a scalar theory, we usually work in a flat space. For gravity, however, spacetime is dynamical itself so the notion of a fixed operator is doomed. A way out of this is by means of the Background Field Method. If we split the metric into background and fluctuation

$$g_{\mu\nu} = \bar{g}_{\mu\nu} + h_{\mu\nu}, \tag{2.2.1}$$

we can use $\bar{g}_{\mu\nu}$ to construct an operator $\bar{\Delta}$ whose set of eigenvalues can be used to sort different modes in $h_{\mu\nu}$. Although we have separated the metric in two parts and diffeomorphism invariance is lost, we can still write the functional integral in a background gauge invariant way.

In this gravitational context, the functional integral in (2.1.2) has to be readjusted to include the gauge-fixing and ghost action, S_{GF} and S_{gh}. Moreover, new sources terms appear in the integration. In a compact form, the new generating functional is

$$e^{W_k[j,J,\bar{J},\bar{g}]} = \int (dhdCd\bar{C}) e^{-S(h,C,\bar{C};\bar{g})-\Delta S_k(h,C,\bar{C};\bar{g})+\int dx\sqrt{\bar{g}}(j^{\mu\nu}h_{\mu\nu}+J^{\mu}C_{\mu}+\bar{J}^{\mu}\bar{C}_{\mu})}, \tag{2.2.2}$$

where $S(h, C, \bar{C}; \bar{g})$ contains the gauge-fixing and ghost contribution

$$S(h, C, \bar{C}; \bar{g}) = S(h; \bar{g}) + S_{GF}(h; \bar{g}) + S_{gh}(C, \bar{C}; \bar{g}), \tag{2.2.3}$$

and the new cutoff term is written as

$$\Delta S_k(h, C, \bar{C}; \bar{g}) = \frac{1}{2}\int dx\sqrt{\bar{g}} h_{\mu\nu} R_k^{\mu\nu\rho\sigma}(\bar{g}) h_{\rho\sigma} + \int dx\sqrt{\bar{g}}\bar{C}_{\mu}\bar{g}^{\mu\nu}R_k^{gh}(\bar{g})C_{\nu}. \tag{2.2.4}$$

It is worth noting that the cutoff action (2.2.4) is constructed with the background metric, and the cutoff function for the fluctuation $h_{\mu\nu}$ contains now spacetime indices. In a similar manner as before, we define the EAA by the Legendre transform of W_k, minus the cutoff action

$$\Gamma_k(h, C, \bar{C}; \bar{g}) = -W_k(j, J, \bar{J}; \bar{g}) + \int dx\sqrt{\bar{g}}(j^{\mu\nu}h_{\mu\nu} + J^{\mu}C_{\mu} + \bar{J}^{\mu}\bar{C}_{\mu}) - \Delta S_k(h, C, \bar{C}; \bar{g}), \tag{2.2.5}$$

where we have used the same names for the expectation value of the fields, e.g., $h_{\mu\nu} = \langle h_{\mu\nu}\rangle$. Following the same lines as before, we obtain the new ERGE

$$\frac{d\Gamma_k(\varphi;\bar{g})}{dt} = \frac{1}{2}\mathrm{Tr}\left(\frac{\delta^2(\Gamma_k + \Delta S_k)}{\delta\varphi\delta\varphi}\right)^{-1}\frac{d}{dt}\frac{\delta^2\Delta S_k}{\delta\varphi\delta\varphi}. \tag{2.2.6}$$

We have collected the metric fluctuations and ghosts in the expression $\varphi = (h_{\mu\nu}, C_{\mu}, \bar{C}_{\mu})$. It is important to point out the double dependence of Γ_k on the background and fluctuation metric. Physical properties or global characteristics of a theory must be independent of the choice of $\bar{g}_{\mu\nu}$. The broken shift symmetry of the full metric, $\bar{g}_{\mu\nu} \to \bar{g}_{\mu\nu} + \epsilon_{\mu\nu}$ and $h_{\mu\nu} \to h_{\mu\nu} - \epsilon_{\mu\nu}$, has been considered in order to understand background independence in quantum gravity [66, 67, 68, 69, 70].

Leaving aside the discussion of background dependence, we focus now on more computational aspects of FRG in gravity. Studies of Eq. (2.2.6) are carried out in the same spirit as case of scalar case. The idea consists in writing an effective action with a given number of operators $\mathcal{O}(g)$. Due to computational reasons, people usually take truncations in theory space. That is, a finite set of operators is retained in Γ_k, in order to study the RG properties of the all the couplings constants. In particular, we search for non-trivial fixed points in the gravitational couplings defining a critical hypersurface of small dimensionality d. As explained in Chapter

1, d is given by the number of relevant directions. In this case, however, (1.5.1) and (1.5.2) do not apply because perturbation theory is not needed. Considering that a finite number of operators can be considered at once, the stability or reliance of the global properties of quantum gravity is investigated by comparing results in different truncations. For instance, the number of relevant operators or dimension of the critical surface should not change when enlarging the set of invariants in Γ_k. The effective action is commonly written as

$$\begin{aligned}\Gamma_k = &-\frac{1}{16\pi G_N}\int dx\sqrt{g}(R-2\Lambda)+\Gamma_k^{\text{Higher}-\text{Order}}\\ &+\frac{1}{32\pi G_N\alpha}\int dx\sqrt{\bar{g}}\bar{g}^{\mu\nu}\left(\bar{D}^\rho h_{\mu\rho}-\frac{1+\beta}{4}\bar{D}_\mu h\right)\left(\bar{D}^\lambda h_{\nu\lambda}-\frac{1+\beta}{4}\bar{D}_\nu h\right)\\ &-\sqrt{2}\int dx\sqrt{\bar{g}}\bar{C}_\mu\left((\bar{g}^{\mu\rho}\bar{D}^\lambda g_{\rho\nu}D_\lambda+\bar{D}^\lambda g_{\lambda\nu}D_\rho)-\frac{1+\beta}{2}\bar{D}^\mu D_\nu\right)C^\nu,\end{aligned} \tag{2.2.7}$$

where G_N is the Newton coupling, Λ the cosmological constant, and $\Gamma_k^{\text{Higher}-\text{Order}}$ represents higher order terms. The second line corresponds to the gauge-fixing action, parametrized by α and β; while the third line is the Faddeev-Popov operator. Work on the Einstein-Hilbert (EH) truncation ($\Gamma_k^{\text{Higher}-\text{Order}}=0$) has been proven successful in determining the existence of a non-trivial fixed point in the space G_N-Λ [23]. Stability of the results within the FRG framework has been tested by analyzing different gauge-fixing conditions (different α and β) [71], cutoff actions ΔS_k [23], and parametrizations for the metric fluctuations [71, 72, 73]. So far, the results in EH suggest that there exists a fixed point with G_N and Λ relevant, that is, with two relevant directions ($d_{S_{UV}}=2$). Higher order truncations put forward the conjecture that the actual dimension of S_{UV} is $d_{S_{UV}}=3$. Such extensions include powers of R up to 70 [74], the operators $R_{\mu\nu}R^{\mu\nu}$, $C^{\mu\nu\rho\sigma}C_{\mu\nu\rho\sigma}$ and beyond [31, 27, 34]. Although the stability matrix is diagonalized by a mixture of different directions (or operators) in theory space, there are hints indicating that 1, R, and a combination of R^2 and $R_{\mu\nu}R^{\mu\nu}$ are the relevant operators in quantum gravity [75]. Higher order operators seem to be dominated by their canonical dimension. This indicates that gravity displays a non-trivial fixed point with a finite number of relevant directions ($d_{S_{UV}}<\infty$). In order to have an idea about the fate of the couplings at high energies, we plot in Fig. 2.2 the RG flow of the dimensionless Newton coupling $g_N=G_Nk^2$ for the Einstein-Hilbert truncation [47]. In that figure, we can see that g_N goes to a fixed point value beyond the Planck scale, while it decreases considerably fast below M_{pl}. We might be then allowed to neglect g_N at low energies. The behavior of the dimensionful coupling G_N is precisely the opposite as g_N. That is, it presents a nearly constant behavior below the Planck scale, while it decreases afterwards.

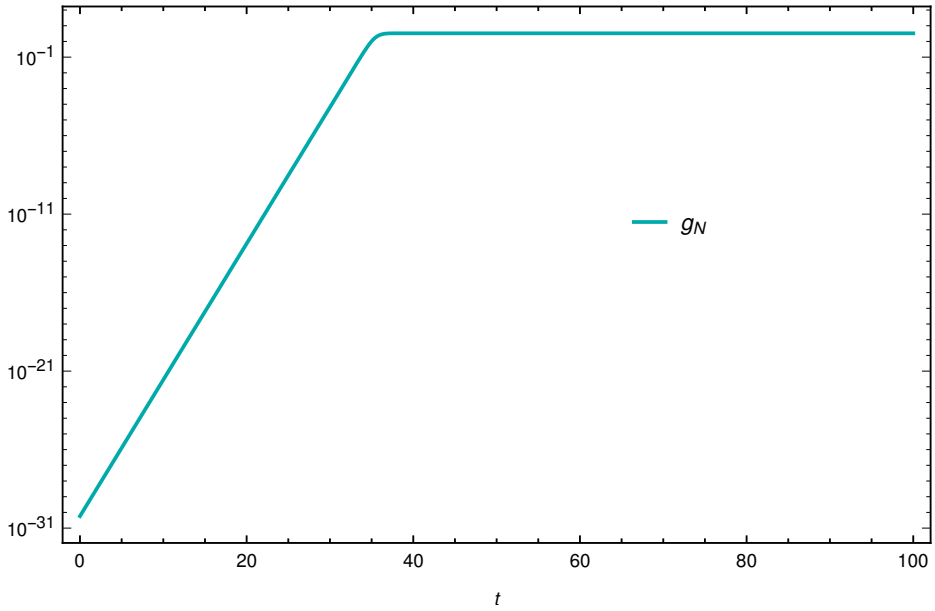

Figure 2.2: RG flow of the dimensionless Newton coupling g_N in the EH truncation.

2.3. Split Weyl Transformations in Quantum Gravity

We briefly present here the results of a very particular choice of $\epsilon_{\mu\nu}$ in the shift transformation $\bar{g}_{\mu\nu} \to \bar{g}_{\mu\nu} + \epsilon_{\mu\nu}$ and $h_{\mu\nu} \to h_{\mu\nu} - \epsilon_{\mu\nu}$. If we take $\epsilon_{\mu\nu} = \epsilon\bar{g}_{\mu\nu}$, we deal with the so called Split Weyl (SW) transformations. As we can see, it corresponds to a Weyl transformation of the background metric. Since the main source of split symmetry breaking in the context of FRG is the cutoff action, we can try to solve the flow equation and the resulting Ward identity coming from the breaking. By combining these two equations, we can rewrite the double dependence in a single metric dependence. In the case of Split Weyl transformations, we do not recover the full single metric dependence, only the part associated to the group action.

In order to discuss the effects of Split Weyl transformations, we use the exponential parametrization, which can be written schematically as $g = \bar{g}e^h$ instead of using the usual *linear* parametrization ($g = g + h$). We also discuss first a simpler scenario in which the metric belongs to a single conformal class, the conformally reduced case (CORE). That is, fixing a "fiducial" metric in this class, every other metric can be obtained by a Weyl transformation

$$g_{\mu\nu} = e^{2\sigma}\hat{g}_{\mu\nu}. \tag{2.3.1}$$

As the metric $\hat{g}_{\mu\nu}$ is kept fixed, we see that gravity is reduced to a scalar field theory. For the

field σ, we have the split transformation as

$$\sigma = \bar{\sigma} + \omega \ . \tag{2.3.2}$$

Thus, we can define a background metric

$$\bar{g}_{\mu\nu} = e^{2\bar{\sigma}} \hat{g}_{\mu\nu}, \tag{2.3.3}$$

and therefore the full metric is obtained from the background metric by means of the Weyl transformation

$$g_{\mu\nu} = e^{2\omega} \bar{g}_{\mu\nu} \ . \tag{2.3.4}$$

Under a SW transformation, the conformal factors transform as $\delta\bar{\sigma} = \epsilon$, $\delta\omega = -\epsilon$, while the full factor σ remains invariant.

In CORE gravity, the general form of the cutoff action is

$$\Delta S_k = \frac{1}{2} \int dx \sqrt{\bar{g}} \ \omega \mathcal{R}_k(\bar{\sigma}, \hat{g}) \omega. \tag{2.3.5}$$

The cutoff kernel R_k is a function of a Laplace-type operator $\mathcal{O}$ constructed with the fiducial metric and the background conformal factor. We start considering the cutoff constructed with $\mathcal{O} = \bar{\Delta}$, where $\bar{\Delta} = -\bar{g}^{\mu\nu} \bar{\nabla}_\mu \bar{\nabla}_\nu$ is the Laplacian of the background metric. For dimensional reasons, it can be written as

$$\mathcal{R}_k(\bar{\Delta}) = k^d r(y), \tag{2.3.6}$$

where r is a dimensionless function of the dimensionless variable $y = \bar{\Delta}/k^2$. The result of the Split Weyl transformations discussed in the previous section is

$$\begin{aligned} \delta^{(S)} \Delta S_k = & -\frac{1}{2} \int d^d x \sqrt{\bar{g}} (\epsilon \mathcal{R}_k \omega + \omega \mathcal{R}_k \epsilon) \\ & + \frac{1}{2} \int d^d x \sqrt{\bar{g}} \omega \left[\epsilon d \mathcal{R}_k + \epsilon \frac{\partial \mathcal{R}_k}{\partial \bar{\sigma}} + \partial_\mu \epsilon \frac{\partial \mathcal{R}_k}{\partial (\partial_\mu \bar{\sigma})} + \dots \right] \omega. \end{aligned} \tag{2.3.7}$$

In order to derive a simple expression for the modified Split Weyl Ward identity (mSWWI), we introduce a SW-covariant derivative. We find that $D_\mu \omega = \partial_\mu \omega + \partial_\mu \bar{\sigma}$ is invariant under SW transformations. Thus, the new Laplacian $\bar{\Delta}^W = -\bar{g}^{\mu\nu} D_\mu D_\nu$ defined with D_μ transforms simply as $\delta \bar{\Delta}^W = -2\epsilon \bar{\Delta}^W$. It is also useful to consider an "extended" transformation $\delta^{(E)}$ which agrees with δ on all fields but acts also on the cutoff by

$$\delta^{(E)} k = -\epsilon k \ , \tag{2.3.8}$$

as dictated by dimensional analysis. Thus, acting on any functional of the fields and k,

$$\delta^{(E)} = \delta - \int dx \, \epsilon \, k \frac{\delta}{\delta k} \ . \tag{2.3.9}$$

Note that since ϵ is generally not constant, we cannot assume that k is constant either. This fact can be taken just as a mathematical fact in order to derive the mSWWI.

The cutoff is now a function

$$\mathcal{R}_k(\bar{\Delta}^W) = k^d r(y), \quad \text{with} \quad y = \bar{\Delta}^W/k^2 \ . \tag{2.3.10}$$

leading to the transformation

$$\delta\Delta S_k = \int dx \epsilon k \frac{\delta}{\delta k}\Delta S_k - \frac{1}{2}\int d^dx\sqrt{\bar{g}}(\epsilon\mathcal{R}_k\omega + \omega r_0\epsilon), \tag{2.3.11}$$

It will become clear later that transformations involving linear terms in ω do not contribute to the variation of the effective average action, so they are harmless for the derivation of a Ward identity. On the other hand, the transformations involving the functional derivative with respect to k lead to Ward identities with a known and compact form.

The derivation of a modified Ward identity follows the same lines as the derivation of the Wetterich equation given in Sec. 2.1. We start from the generating functional W_k, defined by

$$e^{W_k(j,\bar{\sigma};\hat{g})} = \int \mathcal{D}\omega e^{-S-\Delta S_k+\int j\omega}, \tag{2.3.12}$$

Taking into account that S is invariant under δ, the variation of W_k is

$$\delta W_k(j,\hat{g},\bar{\sigma}) = -\langle\delta\Delta S_k\rangle + \int d^dx\sqrt{\bar{g}}j\epsilon. \tag{2.3.13}$$

From definition of the effective average action Γ_k, we have

$$\Gamma_k[\langle\omega\rangle,\bar{\sigma};\hat{g}] = -W_k + \int d^dx\sqrt{\bar{g}}j\langle\omega\rangle - \Delta S_k(\langle\omega\rangle). \tag{2.3.14}$$

Its transformation is

$$\delta\Gamma_k = -\delta W_k + \int d^dx\sqrt{\bar{g}}j\epsilon - \delta\Delta S_k(\langle\omega\rangle). \tag{2.3.15}$$

The terms coming from the source cancel in the final variation of Γ_k, and we end up just with

$$\delta\Gamma_k = -\langle\delta\Delta S_k\rangle - \delta\Delta S_k(\langle\omega\rangle). \tag{2.3.16}$$

Similarly, the linear terms in ω coming from $\delta\Delta S_k$ cancel out, and we find

$$\delta\Gamma_k = \frac{1}{2}Tr\left(\frac{\delta^2\Gamma_k}{\delta\omega\delta\omega} + R_k\right)^{-1}\int dx\epsilon k\frac{\delta R_k}{\delta k}, \tag{2.3.17}$$

where we have used the relation $\left(\frac{\delta^2\Gamma_k}{\delta\omega\delta\omega}+R_k\right)^{-1}=\langle\omega(x)\omega(y)\rangle-\langle\omega(x)\rangle\langle\omega(y)\rangle$, and the trace means double integration in spacetime. Equation (2.3.17) tells us that the split symmetry in S is broken at the quantum level due to the introduction of the cutoff action. On the other hand, the local version of the Wetterich equation (Eq. 2.1.10) tells us that the effective action, for an x-dependent scale, satisfies the flow equation

$$\int dx\delta k\frac{\delta\Gamma_k}{\delta k}=\frac{1}{2}Tr\left(\frac{\delta^2\Gamma_k}{\delta\omega\delta\omega}+R_k\right)^{-1}\int dx\delta k\frac{\delta R_k}{\delta k}. \tag{2.3.18}$$

Therefore, the variation of the effective action with respect to the transformation δ is proportional to the functional derivative with respect to the scale k

$$\delta\Gamma_k=\int dx\epsilon k\frac{\delta\Gamma_k}{\delta k}. \tag{2.3.19}$$

This last expression states that Γ_k is invariant under the extended transformation $\delta^{(E)}$

$$\delta^{(E)}\Gamma_k=0. \tag{2.3.20}$$

Thus, the effective average action can be written in terms of the invariant quantities $\hat{k}=e^{\bar{\sigma}}k$ and $\sigma=\bar{\sigma}+\langle\omega\rangle$ as

$$\Gamma_k[\langle\omega\rangle,\bar{\sigma},\hat{g}]=\hat{\Gamma}_{\hat{k}}[\sigma,\hat{g}]. \tag{2.3.21}$$

We observe that we can reduce the number of variables that Γ_k depends upon. Namely, we have reduced by one the number of independent variables. The extension to full gravity is straightforward since we still consider the specific case of SW transformations. That is, we deal only with one function ϵ characterizing the transformation. In that case, there are extra sources of SW breaking coming from the gauge fixing. However, choosing the appropriate gauge-fixing term, it is possible to include all the symmetry breaking terms in the cutoff action.

In the full gravity case, the metric is written as

$$g_{\mu\nu}=\bar{g}_{\mu\rho}(e^{\mathbf{X}})^{\rho}{}_{\nu}\quad\text{where}\quad X^{\rho}{}_{\nu}=\bar{g}^{\rho\sigma}h_{\sigma\nu}\ . \tag{2.3.22}$$

Using matrices to represent two-index tensors, we have that $\mathbf{g}=\bar{\mathbf{g}}e^{\mathbf{X}}$ and $\mathbf{X}=\bar{\mathbf{g}}^{-1}\mathbf{h}$. Now, decomposing the fluctuation field into its trace-free and trace part, we obtain

$$\mathbf{X}=\mathbf{X}^T+2\omega\mathbf{1}, \tag{2.3.23}$$

where $\mathbf{X}^T$ is traceless and we have defined $\omega=h/2d$, with $h=\mathrm{Tr}\,\mathbf{X}=\bar{g}^{\mu\nu}h_{\mu\nu}$. For the particular case considered before, i.e., metrics belonging to a single conformal equivalence class, we have that

$$\mathbf{g}=\bar{\mathbf{g}}e^{2\omega}e^{\mathbf{X}^T}=\hat{\mathbf{g}}e^{2(\bar{\sigma}+\omega)}e^{\mathbf{X}^T}=\bar{\mathbf{g}}e^{2\sigma}e^{\mathbf{X}^T}, \tag{2.3.24}$$

where e^{σ} is the conformal factor of the full metric, which is decomposed into a background part $e^{\bar{\sigma}}$ and a quantum contribution e^{ω}. Under the SW transformation, the fields transform as

$$\delta h^T_{\mu\nu} = 2\epsilon h^T_{\mu\nu},\ \delta\omega = -\epsilon,\ \delta\bar{\sigma} = \epsilon, \bar{g}_{\mu\nu} = 2\epsilon\bar{g}_{\mu\nu}. \tag{2.3.25}$$

In [70], we describe how to follow a similar procedure to the one for the CORE case. We just need to include the gauge-fixing term, and therefore the ghosts fields. At the end, we find a similar statement: $\delta_{(E)}\Gamma_k = 0$. That is, we can write the effective action in terms of quantities that are invariant under the SW transformations As expected the mSWWI eliminates the dependence of the EAA on the dynamical variable ω and on the background variable $\bar{\sigma}$, replacing them by the single invariant σ. In the process one also has to redefine the background as well as the cutoff. In order to work out the Ward identity for more complicated forms of $\epsilon_{\mu\nu}$, we need to consider groups more complicated than the Weyl group. That is, we need a richer structure in split transformations. This is an open question that we leave for future.

2.4. Gravity and Matter

Since gravity cannot be described alone, we need to include matter degrees of freedom in order to get a more realistic picture of a quantum theory for all fundamental forces of nature. Then two questions naturally arise at this point: how do matter degrees of freedom alter the pattern portrayed in the previous section? How do AS gravity affect the fate of the couplings in the matter sector? In the specific case of the SM, we have $N_S = 4$ scalars, $N_F = 24$ fermions and $N_V = 12$ vector fields. Effects of matter degrees of freedom in AS gravity have been studied in [76, 28, 77, 78, 79]. It is found that for a small number of matter fields, the interacting fixed point is still present. For a larger number of fields, the fixed point might be lost, although higher truncations might be needed in order to have a more precise conclusion. For the Newton coupling, we can see how the matter fields affect the existence of a fixed point. Assuming that g_N reaches an interacting fixed point in pure gravity, we can write the matter contributions as

$$\beta_{g_N} = \beta^{\text{Grav}}_{g_N} + \beta^{\text{Matter}}_{g_N},\ \text{with}\ \beta^{\text{Matter}}_{g_N} = (N_S a_S + N_F a_F + N_V a_V) g_N^2, \tag{2.4.1}$$

where the sign of a_i, $i = S, F, V$ determine the screening or antiscreening effects of each fields.

It is also expected that gravity modifies the running of the matter couplings. The specific form of such effects depends on the truncation, and the other free elements in the FRG analysis. Even though a definite answer might be far from being obtained, several calculations of the new matter beta functions have been carried out. In the gauge sector: [44, 45, 80, 46, 48, 81]. In the Yukawa sector: [39, 82, 40, 42, 41]. They all agree on the fact that the structure of gravity

effects on a given canonicallly marginal coupling is

$$\beta_{g_j} = \beta_{g_j}^{\text{Matter}} + \beta_{g_j}^{\text{Grav}}, \text{ with } \beta_{g_j}^{\text{Grav}} = -f_{g_j} g_j, \tag{2.4.2}$$

where f_{g_j} is a function of the gravitational couplings, and g_j is a gauge or Yukawa coupling. For the gauge couplings g, the value of f_g is still unclear but there are hints in favour of a positive function, $f_g \geq 0$. The sign of the new contributions is important since it can destroy or introduce a non-trivial fixed point . In Chapter 4, we explain the implications of having $f_g \geq 0$. There, we use the loop-expanded beta functions for the matter contributions since the arising fixed points lie at small enough values.

For the Yukawa couplings of the SM, Eq. (2.4.2) also applies, so we have an extra function f_y. This gravity contribution is the same for all the Yukawa couplings because gravity is a flavour-blind interaction. Assuming that AS exists for gravity, and that it is not destroyed by matter degrees of freedom, we can explore the consequences of (2.4.2) in the fate of SM couplings. Exploiting the constant behavior of f_g, f_y beyond the Planck scale (see Fig. 2.2 for g_N), we can aim at finding an interacting fixed point in the matter sector. As sketched in Fig. 1.1, the presence of an interacting fixed point can provide low-energy predictions. This last aspect of asymptotically safe gravity is the key point to be discussed in Chapter 4.

Chapter 3

Asymptotic Safety Beyond the Standard Model

In this chapter, we study in detail the extensions of the SM via vector-like fermions described in the Introduction. Here, besides the notion of perturbativity in terms of the fixed-point values of the coupling constants and scaling exponents, we need to introduce additional concepts that are useful throughout the text. We also clarify what approximation scheme we use in the remaining part of the chapter. This is important because we make use of the perturbative loop expansion in all the work presented here.

3.1. Approximation schemes

The perturbative β-functions of the SM and its extensions have a natural hierarchy originating from the Weyl consistency conditions [83, 84, 85, 86, 87]:

$$\frac{\partial \beta^j}{\partial g_i} = \frac{\partial \beta^i}{\partial g_j} \,. \tag{3.1.1}$$

A consistent solution of eq. (3.1.1) relates different orders in the perturbative expansion and indicates that the gauge couplings must have the highest order in the loop expansion, while the Yukawa coupling must be computed at one order less, and the quartic interaction one further order less. This leaves us in practice with two approximations for the running of the couplings:

- the `210` approximation scheme, in which the gauge couplings are renormalized at the two-loop order (NLO), the Yukawa coupling only at one-loop order (LO) and the quartic

interaction is not renormalized; and

- the 321 approximation scheme, in which the gauge couplings are renormalized at the three-loop order (NNLO), the Yukawa coupling at two-loop order (NLO) and the quartic interaction at one-loop order (LO).

By comparing the two approximations it is possible to test the stability of the fixed point against radiative corrections and the overall reliability of the perturbative computation.

Other approximation schemes are also possible, for example retaining all β-functions at the same order or keeping only the gauge β-functions one order higher than the others. These different choices do not satisfy eq. (3.1.1). They are analysed in [88] where they respective merits (and shortcomings) are discussed.

Perturbative β-functions: A digest of the literature

The perturbative study of the β-functions of the SM, together with some of its possible extensions, has been a collective endeavor covering many years. We collect here the main stepping stones in this ongoing computation.

The one-loop (LO) β-function for a non-abelian gauge group was computed in the classic papers [89] and [90] where AF was discovered. The LO β-function for the Yukawa coupling was presented in [91] and that for the quartic Higgs interaction in [92]. The two-loop (NLO) β-functions for the gauge groups have been calculated in [93, 94, 95, 96], those for the Yukawa couplings in [97, 98, 99] and that for the quartic Higgs interaction in [100, 99, 101]. The case of the SM has been discussed in [102]. Mistakes in some of these results were corrected in [103, 104] where they were also generalized to arbitrary representations of non-simple groups. The three-loop (NNLO) β-functions of a gauge theory with simple groups were given partially in [105], then in [106]. The full NNLO β-functions for the SM were presented in [107] and those for generic representations of non-simple gauge groups in [108]. In this last paper, some contributions from the Yukawa and quartic Higgs interactions were not included. For these terms we have used currently unpublished results of L. Mihaila [109]. The NNLO β-functions for the Yukawa and quartic Higgs couplings were partially computed in [110] and fully in [111, 112]. We will not need them here.

3.2. Another test of perturbativity

Besides the smallness of the couplings and scaling exponents, there is another simple test that we use to assess whether a fixed point is in the perturbative domain. In the remaining part of this chapter, we use the variables

$$\alpha_i = \frac{g_i^2}{(4\pi)^2} \text{ for } i = 1, 2, 3, \quad \text{and} \quad \alpha_t = \frac{y_t^2}{(4\pi)^2}\,, \tag{3.2.1}$$

where g_i are the SM gauge couplings, and y_t is the top Yukawa coupling.

Let us write the β-functions of the gauge couplings α_i in the schematic form

$$\beta_i = \Big(A^{(i)} + B_r^{(i)}\alpha_r + C_{rs}^{(i)}\alpha_r\alpha_s\Big)\alpha_i^2, \tag{3.2.2}$$

where A, B and C are the one-, two- and three-loops coefficients. At a fixed point we can split each beta function in the following way

$$0 = \beta_i = A_*^{(i)} + B_*^{(i)} + C_*^{(i)}\ , \tag{3.2.3}$$

where $A_*^{(i)} = A^{(i)}\alpha_{i*}^2$, $B_*^{(i)} = B_r^{(i)}\alpha_{r*}\alpha_{i*}^2$ and $C_*^{(i)} = B_{rs}^{(i)}\alpha_{r*}\alpha_{s*}\alpha_{i*}^2$. When we insert the values of the fixed point calculated in the `321` approximation scheme, we expect the three contributions to be ordered as $C_*^{(i)} < B_*^{(i)} < A_*^{(i)}$, or equivalently

$$\rho_i < \sigma_i < 1\ , \quad \text{where} \quad \rho_i = |C_*^{(i)}/A_*^{(i)}| \quad \text{and} \quad \sigma_i = |B_*^{(i)}/A_*^{(i)}|\ . \tag{3.2.4}$$

Every time we work in the `321` approximation scheme, we compute ρ and σ for the non-trivial gauge coupling at the fixed point . Our analysis will show us that the fixed points present in both `210` and `321` approximations satisfy the bound $\rho_i < \sigma_i < 1$.

3.3. Testing fixed points with central charges

At a fixed point the theory is a conformal field theory (CFT). As explained in appendix B, one can estimate the size of the relative changes of the central charges of the CFT to decide whether a fixed point is within the domain of perturbation theory. These relative changes are obtained in terms of the function $a = a_{free} + a_q$ (a_q refers to the contribution of quantum corrections) and of the c-function as

$$\delta a \equiv \frac{a - a_{free}}{a_{free}} = \frac{a_q}{a_{free}} \quad \text{and} \quad \delta c \equiv \frac{c - c_{free}}{c_{free}} = \frac{c_q}{c_{free}}\,. \tag{3.3.1}$$

If δa or δc become smaller than -1 the fixed point is unphysical because it cannot correspond to a CFT (since $c > 0$ and $a > 0$ are guaranteed for CFT). A fixed point for which δc or δa is of order 1 should be discarded as well, since quantum corrections are then comparable in size to the free-theory contribution.

The central charges in the `210` approximation scheme can be easily computed by embedding the models in the general gauge-Yukawa Lagrangian of [113]. Computation in the `321` approximation scheme is significantly more complicated due to a major increase in complexity of the Zamolodchikov metric. We do not pursue the `321` computation for that reason and also because the results in the `210` approximation scheme are enough to confirm that our other perturbativity criteria are compatible with the CFT tests.

3.4. Procedure summary

Given a model, we first look for all the fixed-point solutions of the β-functions. Since the β-functions are given in the form of a Taylor expansion, they will have several zeroes that are mere artifacts of the expansion, and we have to select those that have a chance of being physical. The criteria we apply are: stability under radiative corrections and matching to the SM at low energy (see Sec. 1.4).

We begin by analyzing the fixed points of the `210` approximation scheme. In the first step, we retain only those fixed points that can be reasonably assumed to be within the perturbative regime, that is, those for which the couplings and the scaling exponents satisfy the bounds in eq. (1.5.1) and eq. (1.5.2). We use the criteria discussed in sections 3.2 and 3.3 to confirm that these bounds are indeed reasonable indicators of radiative stability.

We then compare with the results of the same analysis in the `321` approximation scheme. We retain only those fixed points that can be reasonably identified in both approximations. Their number is quite small. We find that the identification is only possible if the couplings and scaling exponents are sufficiently small.

Finally, for the fixed points that are radiatively stable in the sense just described, we look for the possibility of matching to the SM at low energy. If all these conditions are satisfied, we have a fixed point that can be considered as physical. Otherwise, the fixed point should be rejected and deemed unphysical.

3.5. The fate of the Standard Model couplings

The running of the SM couplings, when extended to high energies, presents two important features: partial gauge coupling unification and a Landau pole in the abelian gauge coupling. Since this singularity appears beyond the Planck scale, where gravitational effects are important, it might well happen that there will be no divergence and that all couplings are well-behaved once we consider a full theory of gravity and matter (see Chapter 4). Nevertheless, it is interesting to investigate whether such infinities could be avoided within the matter sector.

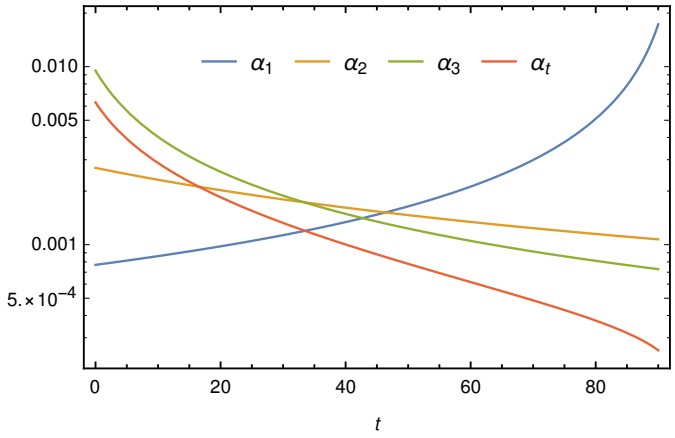

Figure 3.1: Running of the gauge couplings α_i and Yukawa α_t for the SM in the `321` approximation scheme. On the horizontal axis $t = \ln(\mu/M_Z)$. Just above $t \simeq 40$ the three gauge couplings come close together. At larger values of t, α_1 begins its ascent towards the Landau pole.

Throughout this chapter, we shall consider a simplified version of the SM where only the top-Yukawa coupling y_t is retained. The remaining Yukawa couplings are set to zero. For simplicity we will keep calling this the SM. However, we stress that the degrees of freedom that enter the flow are not only those of the top quark but the full SM matter content (*i.e.*, the number of fermions that enter in loops counts all the quarks and leptons).

3.5.1. The 210 approximation scheme

The first question is whether the β-functions of the SM have fixed points. We then consider the beta functions in the 210 approximation scheme, which are given by

$$\begin{aligned}
\beta_1^{\rm NLO} &= \alpha_1^2\left(\frac{41}{3}+\frac{199}{9}\alpha_1+9\alpha_2+\frac{88}{3}\alpha_3-\frac{17}{3}\alpha_t\right),\\
\beta_2^{\rm NLO} &= \alpha_2^2\left(-\frac{19}{3}+3\alpha_1+\frac{35}{3}\alpha_2+24\,\alpha_3-3\,\alpha_t\right),\\
\beta_3^{\rm NLO} &= \alpha_3^2\left(-14+\frac{11}{3}\alpha_1+9\,\alpha_2-52\,\alpha_3-4\,\alpha_t\right),\\
\beta_t^{\rm LO} &= \alpha_t\left(-\frac{17}{6}\alpha_1-\frac{9}{2}\alpha_2-16\,\alpha_3+9\,\alpha_t\right),
\end{aligned} \tag{3.5.1}$$

The set of β-functions in eq. (3.5.1) admits several zeroes. They are given by the last column of Table C.1 in Appendix C. However, only two of them (solutions P_{16} and P_{17}) have all α_i positive. Their properties are summarized in Table 3.1.

	α_1^*	α_2^*	α_3^*	α_t^*	θ_1	θ_2	θ_3	θ_4
FP_1	0	0.543	0	0	3.44	−2.44	0	0
FP_2	0	0.623	0	0.311	5.21	2.21	0	0

Table 3.1: Fixed points and their scaling exponents for the SM in the 210 approximation scheme.

Although less than 1, the values for the couplings constants are quite sizeable and we may suspect that they lie outside the perturbative domain. Considering that scaling exponents are classically zero, we see that the quantum correction are quite large. The values of θ_i indicates the breakdown of the perturbative validity, as we will see in the next subsection. If we decide to ignore the breaking of the perturbative regime and insist on looking for trajectories connecting one of the fixed points to the IR regime, the requirement of lying on the UV critical surface implies that there is always a coupling that vanishes at all scales. Namely, given that $\alpha_1^* = 0$, and that the β-function for α_1 is proportional to a power of α_1 itself, this coupling does not run at all. In other words, the coupling α_1 is frozen at zero at all scales and the $U(1)$ gauge interaction is trivial. Clearly there are no physical fixed point within the SM in the 210 expansion: the problem of the Landau pole is still present even when the gauge couplings are taken at three loops.

3.5.2. The 321 approximation scheme

To check the perturbative stability of the two fixed points of the previous section, we now study the β-functions to the next order. In the 321 approximation scheme, the β-functions take the form [87]

$$\begin{aligned}
\beta_1^{\rm NNLO} &= \beta_1^{\rm NLO} + \alpha_1^2\left[-\frac{388613}{2592}\alpha_1^2 + \frac{205}{48}\alpha_1\alpha_2 + \frac{1315}{32}\alpha_2^2 - \frac{274}{27}\alpha_1\alpha_3 - 2\,\alpha_2\alpha_3 + 198\,\alpha_3^2\right.\\
&\quad \left. - \left(\frac{2827}{144}\alpha_1 + \frac{785}{16}\alpha_2 + \frac{58}{3}\alpha_3\right)\alpha_t + \frac{315}{8}\alpha_t^2 + \frac{3}{2}\Big(\alpha_1 + \alpha_2 - \alpha_\lambda\Big)\alpha_\lambda\right],\\
\beta_2^{\rm NNLO} &= \beta_2^{\rm NLO} + \alpha_2^2\left[-\frac{5597}{288}\alpha_1^2 + \frac{291}{16}\alpha_1\alpha_2 + \frac{324953}{864}\alpha_2^2 - \frac{2}{3}\alpha_1\alpha_3 + 78\,\alpha_2\alpha_3 + 162\,\alpha_3^2\right.\\
&\quad \left. - \left(\frac{593}{48}\alpha_1 + \frac{729}{16}\alpha_2 + 14\alpha_3\right)\alpha_t + \frac{147}{8}\alpha_t^2 + \frac{1}{2}\Big(\alpha_1 + 3\alpha_2 - 3\alpha_\lambda\Big)\alpha_\lambda\right],\\
\beta_3^{\rm NNLO} &= \beta_3^{\rm NLO} + \alpha_3^2\left[-\frac{2615}{108}\alpha_1^2 + \frac{1}{4}\alpha_1\alpha_2 + \frac{109}{4}\alpha_2^2 + \frac{154}{9}\alpha_1\alpha_3 + 42\,\alpha_2\alpha_3 + 65\,\alpha_3^2\right.\\
&\quad \left. - \left(\frac{101}{12}\alpha_1 + \frac{93}{4}\alpha_2 + 80\alpha_3\right)\alpha_t + 30\,\alpha_t^2\right],\\
\beta_t^{\rm NLO} &= \beta_t^{\rm LO} + \alpha_t\left[+\frac{1187}{108}\alpha_1^2 - \frac{3}{2}\alpha_1\alpha_2 - \frac{23}{2}\alpha_2^2 + \frac{38}{9}\alpha_1\alpha_3 + 18\,\alpha_2\alpha_3 - 216\,\alpha_3^2\right.\\
&\quad \left. + \left(\frac{131}{8}\alpha_1 + \frac{225}{8}\alpha_2 + 72\alpha_3\right)\alpha_t - 24\,\alpha_t^2 - 12\,\alpha_t\alpha_\lambda + 3\,\alpha_\lambda^2\right],\\
\beta_\lambda^{\rm LO} &= 12\alpha_\lambda^2 - \Big(3\alpha_1 + 9\alpha_2\Big)\alpha_\lambda + \frac{9}{4}\left(\frac{1}{3}\alpha_1^2 + \frac{2}{3}\alpha_1\alpha_2 + \alpha_2^2\right) + 12\,\alpha_t\alpha_\lambda - 12\,\alpha_t^2,
\end{aligned} \tag{3.5.2}$$

where the quartic Higgs coupling

$$\alpha_\lambda = \frac{\lambda}{(4\pi)^2} \tag{3.5.3}$$

is now renormalized.

Due to the higher order of the equations, there are more fixed points than the two found in the 210 approximation scheme. They are listed in Table 3.2.

	α_1^*	α_2^*	α_3^*	α_t^*	α_λ^*	θ_1	θ_2	θ_3	θ_4	θ_5
FP_1	0	0	0	0.297	0.184	8.32	−2.57	0	0	0
FP_2	0	0.120	0	0.0695	0.0575	1.46	1.18	0.495	0	0
FP_3	0	0.124	0	0.333	0.230	8.82	−2.52	1.38	0	0
FP_4	0.436	0.146	0	0.648	0.450	−27.0	17.3	−7.85	2.19	0
FP_5	0.433	0	0	0.573	0.377	−25.6	15.7	−6.85	0	0

Table 3.2: Fixed points and their scaling exponents for the SM in the 321 approximation scheme.

Consistently with the discussion in the case of the `210` approximation scheme, neither the couplings nor the exponents are small. Moreover, it is not possible to recognize among the new fixed points those of the `210` approximation scheme: the values change dramatically, contrary to what would be expected in a well-behaved perturbative expansion.

The criterion of perturbativity introduced in section 3.2 confirms the instability of the fixed points . In the `210` approximation scheme, for the two fixed points of Table 3.1, we have $B_*^{(2)} = 1.87$ and $B_*^{(2)} = 2.46$, respectively, while $C_*^{(2)} = 32.7$ and $C_*^{(2)} = 53.9$, respectively. For both fixed points the ratio ρ_2 is of order 10, grossly violating the bound (3.2.4). It therefore appears that we are outside the domain where perturbation theory can be trusted. We conclude that the SM (at least in the simplified form considered here) does not have a physical fixed point within perturbation theory. In the next section, we study a family of models that represents the simplest extension to the SM content with the potential of generating perturbative fixed points.

3.6. Standard Model extensions

In this section, we consider (minimal) extensions of the SM by adding new matter fields charged under the SM group $SU_c(3) \times SU_L(2) \times U_Y(1)$. The gauge sector is not modified. Following [11, 9, 14, 114], we take N_f families of vector-like fermions minimally coupled to the SM. The idea is to consider a new type of Yukawa interactions among the vector-like fermions such that their contribution generate new zeros in the gauge β-functions. Accordingly, new scalar fields must be included as well. These scalars are taken to be singlets of the SM group while the fermions carry the representations R_3 under $SU_c(3)$, R_2 under $SU_L(2)$, and have hypercharge Y of the gauge group $U_Y(1)$. Denoting S_{ij} the matrix formed with N_f^2 complex scalar fields, the Lagrangian characterizing this minimal BSM extension is

$$\mathcal{L} = \mathcal{L}_{SM} + \mathrm{Tr}\,(\bar{\psi} i \not{D} \psi) + \mathrm{Tr}\,(\partial_\mu S^\dagger \partial_\mu S) - y \mathrm{Tr}\,(\bar{\psi}_L S \psi_R + \bar{\psi}_R S^\dagger \psi_L). \tag{3.6.1}$$

In eq. (3.6.1), $\mathcal{L}_{SM}$ stands for the SM lagrangian, y is the BSM Yukawa coupling, which we assume to be the same for all fermions, the trace sums over the SM representation indices as well as the flavour indices, and we have decomposed ψ as $\psi = \psi_L + \psi_R$ with $\psi_{R/L} = \frac{1}{2}(1 \pm \gamma_5)\psi$. We neglect the role of quartic self interactions of the scalars S_{ij} as well as portal couplings of the latter to the Higgs sector.

This extension of the SM is simple enough to allow explicit computations while giving rise to new features in the RG flow. The vector-like fermions are a proxy for more elaborated extensions; they do not introduce gauge anomalies and do not induce a large renormalization of the Higgs mass: they are technically natural.

3.6.1. The β-functions

Within the model defined by the Lagrangian (3.6.1), we look for fixed points satisfying the requirements discussed in section 3.4. We start the analysis in the 210 approximation scheme and write the β-functions of the system (3.6.1) in terms of the quantities in eq. (3.2.1) augmented by the new coupling $\alpha_y = \frac{y^2}{(4\pi)^2}$.

In the following, as in section 3.5, we keep only the top-Yukawa coupling. The β-functions will depend on the dimensions of the fermion representations d, their Casimir invariants C and Dynkin indices S, which are defined in general as

$$\begin{aligned} d_{R_2} &= 2\ell + 1, & d_{R_3} &= \frac{1}{2}(p+1)(q+1)(p+q+2), \\ C_F^{(2)} &= C_{R_2} = \ell(\ell+1), & C_F^{(3)} &= C_{R_3} = p + q + \frac{1}{3}(p^2+q^2+pq), \\ S_F^{(2)} &= S_{R_2} = \frac{d_{R_2} C_{R_2}}{3}, & S_F^{(3)} &= S_{R_3} = \frac{d_{R_3} C_{R_3}}{8}. \end{aligned} \tag{3.6.2}$$

Here, $\ell = 0, 1/2, 1, 3/2, \ldots$ denotes the highest weight of R_2, and (p, q) (with $p, q = 0, 1, 2 \ldots$) the weights of R_3.

In the 210 approximation scheme, the β-functions are given by [96, 98, 100, 103]

$$\begin{aligned} \beta_1^{\rm NLO} &= \left(B_1 + M_1\alpha_1 + H_1\alpha_2 + G_1\alpha_3 - D_1\alpha_y - \frac{17}{3}\alpha_t \right) \alpha_1^2, \\ \beta_2^{\rm NLO} &= \left(-B_2 + M_2\alpha_2 + H_2\alpha_1 + G_2\alpha_3 - D_2\alpha_y - 3\,\alpha_t \right) \alpha_2^2, \\ \beta_3^{\rm NLO} &= \left(-B_3 + M_3\alpha_3 + H_3\alpha_1 + G_3\alpha_2 - D_3\alpha_y - 4\,\alpha_t \right) \alpha_3^2, \\ \beta_t^{\rm LO} &= \left(9\alpha_t - \frac{17}{6}\alpha_1 - \frac{9}{2}\alpha_2 - 16\,\alpha_3 \right) \alpha_t, \\ \beta_y^{\rm LO} &= \left(T\alpha_y - F_1\alpha_1 - F_2\alpha_2 - F_3\alpha_3 \right) \alpha_y, \end{aligned} \tag{3.6.3}$$

where we have included the gauge and matter contributions in the coefficients B_i, M_i, H_i, G_i and D_i, for $i = 1, 2, 3$. These coefficient are expressed in terms of d_{R_2}, d_{R_3}, C_{R_2}, C_{R_3}, S_{R_2}, S_{R_3}, Y and N_f as follows. For the diagonal and mixing gauge contributions to the gauge β-functions

we have

$$
\begin{aligned}
B_1 &= \frac{41}{3} + \frac{8}{3} N_f Y^2 d_{R_2} d_{R_3}, & M_1 &= \frac{199}{9} + 8 Y^4 N_f d_{R_2} d_{R_3}, \\
H_1 &= 9 + 8 Y^2 N_f C_{R_2} d_{R_2} d_{R_3}, & G_1 &= \frac{88}{3} + 8 N_f Y^2 C_{R_3} d_{R_2} d_{R_3}, \\
B_2 &= \frac{19}{3} - \frac{8}{3} N_f S_{R_2} d_{R_3}, & M_2 &= \frac{35}{3} + 4 N_f S_{R_2} d_{R_3} \left(2\, C_{R_2} + \frac{20}{3} \right), \\
H_2 &= 3 + 8 N_f Y^2 S_{R_2} d_{R_3}, & G_2 &= 24 + 8 N_f S_{R_2} C_{R_3} d_{R_3}, \\
B_3 &= 14 - \frac{8}{3} N_f S_{R_3} d_{R_2}, & M_3 &= -52 + 4 N_f S_{R_3} d_{R_2} (2\, C_{R_3} + 10), \\
G_3 &= 9 + 8 N_f S_{R_3} C_{R_2} d_{R_2}, & H_3 &= \frac{11}{3} + 8 N_f Y^2 S_{R_3} d_{R_2}.
\end{aligned}
\tag{3.6.4}
$$

For the Yukawa contribution to the gauge β-functions we have

$$
D_1 = 4 N_f^2 Y^2 d_{R_2} d_{R_3}, \;\; D_2 = \frac{1}{3} 4 N_f^2 C_{R_2} d_{R_2} d_{R_3}, \;\; D_3 = \frac{1}{8} 4 N_f^2 C_{R_3} d_{R_2} d_{R_3}, \tag{3.6.5}
$$

whereas the running of the new coupling α_y is characterized by the coefficients

$$
T = 2(N_f + d_{R_2} C_{R_3}), \quad F_1 = 12\, Y^2, \;\; F_2 = 12\, C_{R_2}, \;\; F_3 = 12\, C_{R_3}. \tag{3.6.6}
$$

All the new contributions to the gauge couplings running are multiplied by N_f, meaning that we can go back to the SM by taking the $N_f \to 0$ limit.

Due to the simplicity of the β-functions to this order in perturbation theory, we can find analytic solutions of the equations $\beta_i^{\text{NLO}} = \beta_t^{\text{LO}} = \beta_y^{\text{LO}} = 0$ as functions of Y, ℓ, p, q and N_f. All these solutions are listed in Table C.1 and can be split in two categories according to whether they depend on the hypercharge Y or not. Those independent of Y have $\alpha_1^* = 0$.

For the gauge couplings, the β-functions in the 321 approximation scheme are given by

$$\begin{aligned}
\beta_1^{\rm NNLO} &= \beta_1^{\rm NLO} + \Big[-M_{11}\alpha_1^2 + M_{12}\alpha_1\alpha_2 - M_{13}\alpha_1\alpha_3 - G_{23}\alpha_2\alpha_3 + H_{11}\alpha_2^2 + G_{11}\alpha_3^2 \\
&\quad + \frac{315}{8}\alpha_t^2 + K_{y1}\alpha_y^2 - \frac{2827}{144}\alpha_1\alpha_t - \frac{785}{16}\alpha_2\alpha_t - \frac{58}{3}\alpha_3\alpha_t \\
&\quad - (K_{11}\alpha_1 + K_{12}\alpha_2 + K_{13}\alpha_3)\,\alpha_y + \frac{3}{2}(\alpha_1 + \alpha_2 - \alpha_\lambda)\,\alpha_\lambda\Big]\,\alpha_1^2, \\
\beta_2^{\rm NNLO} &= \beta_2^{\rm NLO} + \Big[- M_{22}\alpha_2^2 + M_{21}\alpha_2\alpha_1 - M_{23}\alpha_2\alpha_3 - G_{13}\alpha_1\alpha_3 - H_{22}\alpha_1^2 + G_{22}\alpha_3^2 \\
&\quad + \frac{147}{8}\alpha_t^2 + K_{y2}\alpha_y^2 - \frac{729}{16}\alpha_2\alpha_t - \frac{593}{48}\alpha_1\alpha_t - 14\,\alpha_3\alpha_t \\
&\quad - (K_{22}\alpha_2 + K_{21}\alpha_1 + K_{23}\alpha_3)\,\alpha_y + \frac{1}{2}(\alpha_1 + 3\,\alpha_2 - 3\,\alpha_\lambda)\,\alpha_\lambda\Big]\,\alpha_2^2, \qquad (3.6.7) \\
\beta_3^{\rm NNLO} &= \beta_3^{\rm NNLO} + \Big[-M_{33}\alpha_3^2 + M_{31}\alpha_3\alpha_1 - M_{32}\alpha_3\alpha_2 - G_{12}\alpha_1\alpha_2 - H_{33}\alpha_2^2 + G_{33}\alpha_2^2 \\
&\quad + 30\,\alpha_t^2 + K_{3y}\alpha_y^2 - 80\,\alpha_3\alpha_t - \frac{101}{12}\alpha_1\alpha_t - \frac{93}{4}\alpha_2\alpha_t \\
&\quad - (K_{33}\alpha_3 + K_{31}\alpha_1 + K_{32}\alpha_2)\,\alpha_y\Big]\,\alpha_3^2\,.
\end{aligned}$$

For the Yukawa and quartic Higgs couplings, the β-functions are given by

$$\begin{aligned}
\beta_t^{\rm NLO} &= \beta_t^{\rm LO} + \Big[-24\,\alpha_t^2 + 3\,\alpha_\lambda^2 - 12\,\alpha_t\alpha_\lambda + \Big(\frac{131}{8}\alpha_1 + \frac{225}{8}\alpha_2 + 72\,\alpha_3\Big)\,\alpha_t \\
&\quad + \frac{1187}{108}\alpha_1^2 + \frac{3}{2}\alpha_1\alpha_2 - \frac{23}{2}\alpha_2^2 + \frac{38}{9}\alpha_1\alpha_3 + 18\,\alpha_2\alpha_3 - 216\,\alpha_3^2 \\
&\quad + \frac{58}{27}B_{t1}\alpha_1^2 + 2B_{t2}\alpha_2^2 + \frac{160}{9}B_{t3}\alpha_3^2\Big]\,\alpha_t \qquad (3.6.8) \\
\beta_y^{\rm NLO} &= \beta_y^{\rm LO} + \big[(4-V)\alpha_y^2 + (V_1\alpha_1 + V_2\alpha_2 + V_3\alpha_3)\,\alpha_y \\
&\quad + W_1\alpha_1^2 + W_2\alpha_2^2 + W_3\alpha_3^2 - W_{12}\alpha_1\alpha_2 - W_{13}\alpha_1\alpha_2 - W_{23}\alpha_2\alpha_3\big]\alpha_y, \\
\beta_\lambda^{\rm LO} &= 12\,\alpha_\lambda^2 - (3\,\alpha_1 + 9\,\alpha_2)\,\alpha_\lambda + \frac{9}{4}\Big(\frac{1}{3}\alpha_1^2 + \frac{2}{3}\alpha_1\alpha_2 + \alpha_2^2\Big) + 12\,\alpha_t\alpha_\lambda - 12\,\alpha_t^2\,.
\end{aligned}$$

In eqs. (3.6.7)–(3.6.8), we have introduced several coefficients containing the gauge and Yukawa contributions which depend on N_f and the group representations of the SM and new vector-like fermions. These coefficients are given in appendix D.

It is not possible to find analytic solutions for the fixed points in the 321 approximation scheme. The system $\beta_i^{\rm NNLO} = \beta_t^{\rm NLO} = \beta_y^{\rm NLO} = \beta_\lambda^{\rm LO} = 0$ must be solved numerically, separately for each given choice of (N_f, Y, p, q, ℓ). No separation between Y-independent and dependent solutions can be established before solving the equations.

3.6.2. Results

In order to find fixed points satisfying the conditions (1.5.1) and (1.5.2), we generate a grid in the space spanned by the quantum numbers (N_f, ℓ, Y) for three specific $SU_c(3)$ representations: colorless ($p = q = 0$), fundamental ($p = 1, q = 0$) and adjoint ($p = q = 1$). For each of these representations, we consider the following values for the number of vector-like fermions, their isospin and hypercharge: $N_f \in [1, 300]$ in steps of size 1, $\ell \in [1/2, 10]$ and $Y \in [0, 10]$ both in steps of size 1/2. This amounts to 126,000 points for each representation of $SU_c(3)$.

Colorless vector-like fermions

Colorless vector-like fermions are the least phenomenologically restricted and therefore the most attractive candidates for a successful extension of the SM. In the `210` approximation scheme we find that only the Y-independent set of solutions contains fixed points fulfilling the required conditions ($\alpha < 1$, $|\theta| < O(1)$).

To set the precise bound on $|\theta|$, we plot in Figure 3.2 the largest eigenvalues of the stability matrix M_{ij}. For the Y-independent solutions there is a gap between 2.21 and 62.6; for the Y-dependent solutions there are no eigenvalues less than 9.63. Accordingly, we decide to consider fixed points with $|\theta| < 3$. In this way we probably include some fixed points that are not within perturbation theory, but we prefer to err on this side than to miss potentially interesting fixed points. In this way we discard all the Y-dependent fixed points since there is always an eigenvalue which is at least of order 10.

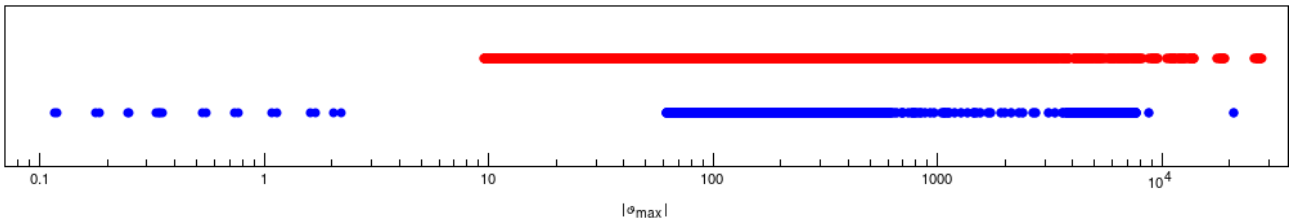

Figure 3.2: Distribution of the largest eigenvalues $\theta_{\max}$ of the stability matrix associated to the colorless models. Blue dots: eigenvalues for the Y-independent solutions: there is a gap between 2.21 and 62.6. Red dots: eigenvalues for the Y-dependent solutions: there is no gap, the eigenvalues start around 10.

After having applied all the criteria discussed in subsection 3.4 we find that, for any value of the hypercharge Y, the only representations producing satisfactory candidate fixed points are those collected, together with the corresponding eigenvalues, in Table 3.3. The eigenvalues of the stability matrix turn out to be Y-independent as well.

(N_f, ℓ)	α_1^*	α_2^*	α_3^*	α_t^*	α_y^*	θ_1	θ_2	θ_3	θ_4	θ_5	
$(1, \frac{1}{2})$	0	0.200	0	0	0.300	2.04	−0.900	0.884	0	0	P_{16}
	0	0.213	0	0.106	0.319	2.21	1.19	0.743	0	0	P_{17}
	0	0.179	0	0	0	−1.61	0.893	−0.804	0	0	P_{18}
	0	0.189	0	0.0943	0	−1.70	1.15	0.697	0	0	P_{19}
$(1, 1)$	0	0.0137	0	0	0.0411	0.333	−0.0616	0.0135	0	0	P_{16}
	0	0.0140	0	0.0070	0.0420	0.341	0.0633	0.0137	0	0	P_{17}
	0	0.0103	0	0	0	−0.247	−0.0464	0.0103	0	0	P_{18}
	0	0.0105	0	0.0052	0	−0.251	0.0473	0.0104	0	0	P_{19}
$(2, \frac{1}{2})$	0	0.104	0	0	0.117	1.0833	−0.467	0.328	0	0	P_{16}
	0	0.108	0	0.0542	0.122	1.14	0.525	0.315	0	0	P_{17}
	0	0.0827	0	0	0	−0.744	−0.372	0.303	0	0	P_{18}
	0	0.0856	0	0.0428	0	−0.770	0.427	0.283	0	0	P_{19}
$(3, \frac{1}{2})$	0	0.0525	0	0	0.0472	0.530	−0.236	0.109	0	0	P_{16}
	0	0.0543	0	0.0272	0.0489	0.552	0.251	0.109	0	0	P_{17}
	0	0.0385	0	0	0	−0.346	−0.173	0.0897	0	0	P_{18}
	0	0.0394	0	0.0197	0	−0.355	0.182	0.0896	0	0	P_{19}
$(4, \frac{1}{2})$	0	0.0189	0	0	0.0141	0.179	−0.0849	0.0179	0	0	P_{16}
	0	0.0194	0	0.0097	0.0146	0.185	0.0880	0.0182	0	0	P_{17}
	0	0.0130	0	0	0	−0.117	−0.0584	0.0130	0	0	P_{18}
	0	0.0132	0	0.0066	0	−0.119	0.0599	0.0132	0	0	P_{19}

Table 3.3: Set of fixed points and eigenvalues for colorless vector-like fermions in the `210` approximation scheme. We highlight in green the fixed points that appear also in the `321` approximation. The labels in the second to the last last column refer to the list in Table C.1.

The bounds on N_f and ℓ come from the behavior of the eigenvalues as functions of these parameters. If we plot one of the eigenvalues as a function of N_f for several values of l, we observe that it increases very fast. From Figure 3.3, we see that only models with small N_f produce sufficiently small eigenvalues.

It is important to note that the large scaling dimensions of models with large N_f frustrate the apparently promising strategy of increasing N_f in order to increase the NLO term in the gauge β-functions to cancel the (N_f-independent) LO term with smaller (and therefore more perturbative) values of the couplings α_i.

The above selection of the viable fixed points is confirmed by the study of their CFT central charges. There are 20 Y-independent fixed points with eigenvalues up to about ± 2. The fixed point with least variation in the central charges is that with $(N_f, \ell) = (1, 1)$, having $\delta a \simeq -0.0007$ and $\delta c \simeq 0.08$. The one with the largest change is that with $(N_f, \ell) = (1, 1/2)$, having $\delta a \simeq -0.2$ and $\delta c \simeq 0.8$. All these fixed points (except for the one corresponding to $(N_f, \ell, Y) = (1, 1/2, 0)$) pass the collider bounds test (see appendix B). There are 69 Y-dependent fixed points with eigenvalues up to ± 10. None of them have positive a or c with δa and δc being of $O(1)$. They should all be discarded. These results confirm our classification of the fixed points in Table 3.3 according to the size of their eigenvalues and the ratio ρ.

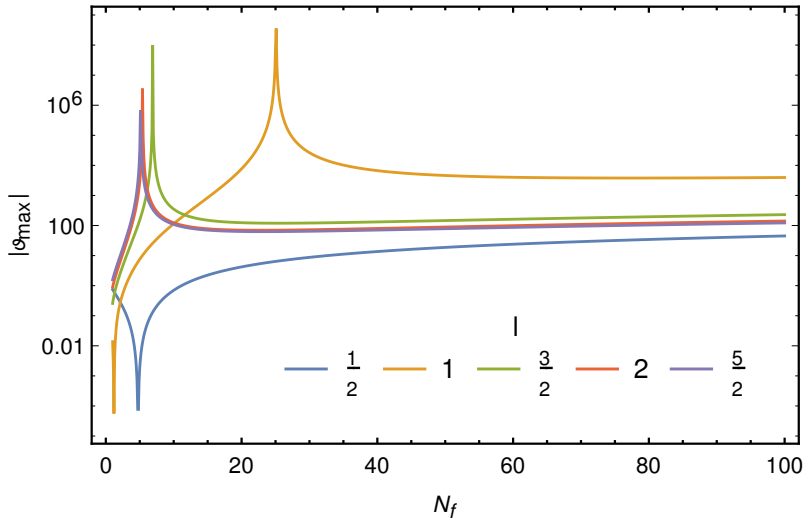

Figure 3.3: Behaviour of a given eigenvalue $|\theta|$ as a function of N_f for several values of ℓ in the colorless case. The scaling dimension increases very fast with N_f, and only small values of N_f, ℓ produce $|\theta| < O(1)$.

Now that we have isolated the candidates to study, we check whether these fixed points can be connected to the SM via the RG flow. We note that β_1 is proportional to α_1^2 and so, in order to avoid Landau poles, α_1 has to vanishes at all energy scales. In conclusion, although we have perturbative fixed points, these cannot be matched to the SM because we know that g_1 is different from zero at the TeV scale.

We then perform a similar search in the `321` approximation scheme. Here, we stick to solutions having $|\theta| < 1$. We find that the same combinations of N_f and ℓ that provide perturbative fixed points in the `210` case also give viable solutions here. Moreover, the solutions turn out to be Y-independent as well.

In Table 3.4 we show the fixed point solutions satisfying the criteria in eq. (1.5.1) and eq. (1.5.2). All the fixed points in Table 3.4 can be traced back to fixed points that were already present in the `210` approximation scheme and listed in Table 3.3. Notice that for a given pair (N_f, ℓ), not all the fixed points in `210` persist. For those that do, the values of α^* and θ change by relatively small amount. We can then claim that the solutions given in Table 3.4 are radiatively stable fixed points.

Unfortunately, when we look at trajectories lying on the UV critical surface, we find again that the coupling α_1 must be zero at all scales in all the models. The abelian interactions suffer from the triviality problem and no matching to the SM is possible if asymptotic safety is assumed. All these colorless models are therefore ruled out.

(N_f, l)	α_1^*	α_2^*	α_3^*	α_t^*	α_y^*	α_λ^*	θ_1	θ_2	θ_3	θ_4	θ_5	θ_6	σ_2	ρ_2
$(1,1)$	0	0.0096	0	0.0048	0	0.0039	−0.244	0.0655	0.0430	0.0103	0	0	0.918	0.0821
	0	0.0119	0	0.0060	0.0343	0.0048	0.301	0.0813	0.0531	0.0134	0	0	0.8601	0.140
$(2, \frac{1}{2})$	0	0.0498	0	0.0259	0	0.0211	−0.592	0.382	0.282	0.200	0	0	0.581	0.418
	0	0.0567	0	0.0296	0.0734	0.0242	0.696	0.442	0.314	0.224	0	0	0.5012	0.499
$(3, \frac{1}{2})$	0	0.0291	0	0.0148	0	0.0120	−0.306	0.2080	0.132	0.0827	0	0	0.737	0.263
	0	0.0362	0	0.0184	0.0353	0.0150	0.403	0.262	0.165	0.100	0	0	0.645	0.354
$(4, \frac{1}{2})$	0	0.0117	0	0.0059	0	0.0048	−0.112	0.0804	0.052	0.0130	0	0	0.887	0.113
	0	0.0162	0	0.0081	0.0125	0.0066	0.161	0.112	0.0723	0.0179	0	0	0.823	0.177

Table 3.4: Fixed points and eigenvalues for colorless vector-like fermions, in the `321` approximation scheme. The last two columns give the values of the ratios σ_2 and ρ_2 (see 3.2.4).

Vector-like fermions in the fundamental of $SU_c(3)$

For the fundamental representation ($p = 1$ and $q = 0$ or vice-versa) we follow the same procedure as before and generate 126,000 models by scanning the same grid in the (N_f, ℓ, Y) space. We split the solutions in two families depending on whether they depend on the value of their hypercharge Y or not. The distribution of the largest eigenvalues given in Figure 3.4 shows that there are no fixed points with $|\theta| < 52.1$ for the Y-dependent solutions, whereas for the Y-independent solutions there is a gap between 10.8 and 372.

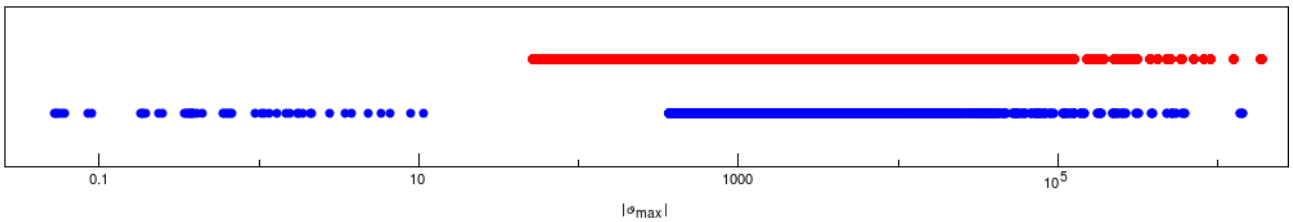

Figure 3.4: Distribution of the largest eigenvalues $\theta_{\max}$ of the stability matrix of the fixed points of the $SU(3)$ fundamental representation. Blue dots: eigenvalues for the Y-independent solutions: there is a gap between 10.8 and 372. Red dots: eigenvalues for the Y-dependent solutions: there is no gap, the eigenvalues start at 52.1.

Accordingly, we eliminate all Y-dependent solutions and impose the bound $|\theta| < 11$ for those that are Y-independent. In this way, even more than in the preceding section, we include models that are probably unreliable, but these can be eliminated at a later stage. For the Y-independent solutions, we find the combinations of N_f and ℓ in Tables 3.5 and 3.6 that generate satisfactory candidate fixed points.

This selection is confirmed by the study of the central charges for these models. Among the 49 distinct Y-independent fixed points with eigenvalues up to ± 10, all have positive c-function, but 6 of them have a negative a-function (with one more being borderline acceptable). The CFT

test seems to work well here: all fixed points with reasonable scaling exponents pass it, whereas the ones with relatively large exponents do not. An unexpected fact is that the separation between large and small exponents seems to be around a maximum value of $|\theta|$ around 3. For these perturbative and "semi-perturbative" fixed points, we also notice that the a-function is generically pushed toward 0 ($a_q < 0$) whereas the c function is generically shifted to larger values ($c_q > 0$). This is why the fixed points with negative a-function still seem to pass the c-function test. If one considers δc instead, then for most of these fixed points $\delta c > 1$, but apparently not for all. Finally, if one also studies the collider bounds one finds that ten more fixed points are excluded, usually those which just barely satisfied one or both of the a and c tests. The collider bounds tests seem to be the most stringent.

When one tries to match these fixed points to the SM at low energies, it turns out that the abelian gauge coupling α_1 must again be zero at all scales. None of these fixed points is physically viable.

In the `321` approximation scheme, there exist fixed points that can be reasonably traced back to those in the `210` approximation scheme. These solutions are shown in Table 3.7, where we have included only fixed points with $|\theta| < 1$ in order to get small ratios ρ_i and σ_i. However, they all have at least one coupling that has to be zero at all scales, thus preventing a proper matching to the SM. We conclude that also all the models with the vector-like fermions in the fundamental representation of $SU_c(3)$ cannot provide an AS extension to the SM.

Vector-like fermions in higher representations of $SU_c(3)$

For the adjoint representation (with $p = q = 1$), the search over the same grid of values for (N_f, ℓ, Y) (and thus 126,000 further models) does not produce any fixed point within the perturbative domain. This is true both in the `210` and in the `321` approximation scheme.

In Figure 3.5, we show the distribution the largest eigenvalues of the stability matrix for the `210` approximation scheme. We clearly see that the eigenvalues are rather large. In fact, the minimum eigenvalue in the Y-independent set of solutions is 1342, while in the Y-dependent set is 426.

This problem is confirmed by the study of the central charges. For the Y-independent fixed points we find for all fixed points δa of $O(1000)$. Similarly, the Y-dependent the fixed points have δa of $O(100)$. Tests of the c-function confirm these results, even though the a-function seems to be more sensitive, in the sense that it suffers greater relative change.

Again, we come up empty handed. The models with the vector-like fermions in the adjoint

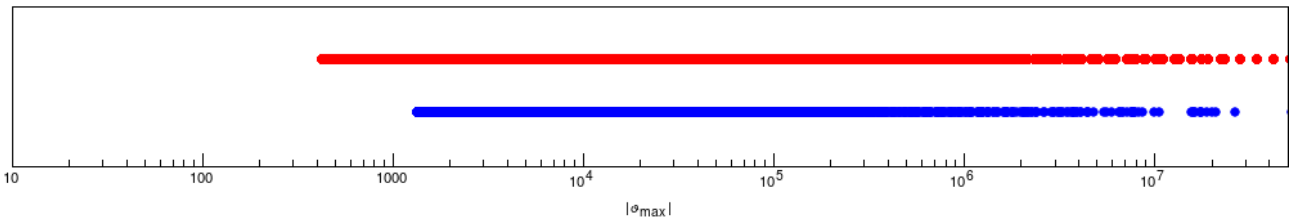

Figure 3.5: Distribution of the largest eigenvalue $\theta_{\max}$ of the stability matrix associated to the fixed points of the $SU(3)$ adjoint representation. Blue: eigenvalues for the Y-independent solutions. Red: eigenvalues for the Y-dependent solutions. In both cases, there is no gap and the distribution starts at very large values.

representation of $SU_c(3)$ do not provide a viable AS extension to the SM. Higher $SU_c(3)$ representations are disfavored by experimental constraints because of the early onset of the modifications in the α_3 running.

A model that almost works

Having ruled out all possible candidates, one may wonder if the criteria in (1.5.1) and (1.5.2) might be too stringent and make us miss some potentially interesting models. In the case at hand, we can indeed find additional fixed points that naively seem to be good candidates for an asymptotically safe extension of the SM. This is achieved if we allow for larger values of θ and relinquish the condition (1.5.2).

As an example, consider the case of colorless vector-like fermions with quantum numbers $N_f = 3$, $\ell = 1/2$ and $Y = 3/2$. Its fixed points and eigenvalues are given in Table 3.8.

(N_f, ℓ, Y)	α_1^*	α_2^*	α_3^*	α_t^*	α_y^*	θ_1	θ_2	θ_3	θ_4	θ_5
$(3, 1/2, 3/2)$	0.188	0	0	0	0.778	33.2	-3.36	-0.817	0	0

Table 3.8: Values of the couplings and eigenvalues at the promising fixed point for the model that almost works (`210` approximation scheme).

This example provides a very interesting (and non-trivial) extension of the SM which includes non-trivial fixed point value for the gauge coupling α_1, as well as the Yukawa coupling α_y. We see that some of the scaling exponents θ_i are large and the criterion (1.5.2) is accordingly violated. Nonetheless, let us momentarily suspend disbelief and apply the formula in (1.5.1). We do not find any coupling frozen to zero and therefore a SM matching seems plausible. In fact, taking the IR scale $M = M_Z \exp(3) \simeq 1.83 TeV$ – where the SM couplings have the values

$\alpha_1 = 0.000795$, $\alpha_2 = 0.00257$, $\alpha_3 = 0.00673$, $\alpha_t = 0.00478$ – we find a good matching, with an error of the order of per mille, see Figure 3.6.

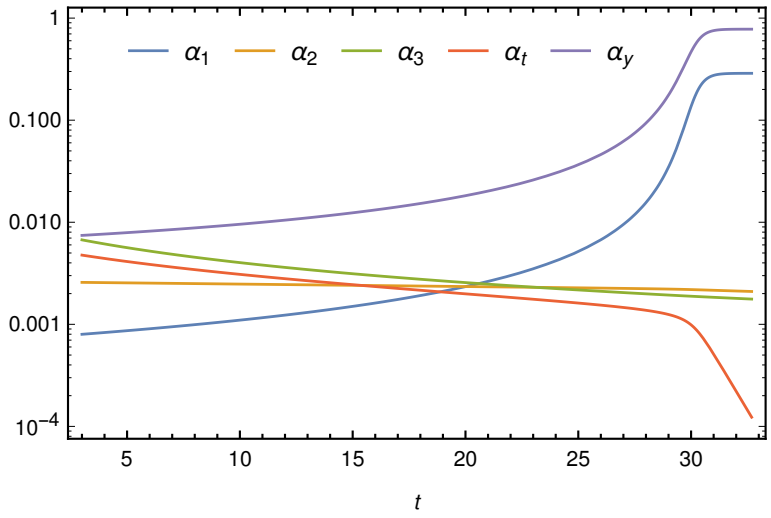

Figure 3.6: Evolution of the couplings with t in a logarithmic scale for the fixed point in Table 3.8. This running provides a trajectory in the theory space connecting the fixed point and the physics at a matching scale around 2 TeV.

Ignoring the large scaling exponents, this model seems to provide a very promising candidate for an AS extension of the SM. However, it is not radiatively stable. The `321` approximation scheme β-functions generate very different fixed points that cannot be easily traced back to those in the `210` approximation scheme. This example shows us the power of our criteria used so far. It is not just enough to find a fixed point and connect it to the IR physics. We have to make sure that we are not violating important properties of our theory.

Five benchmark models studied in the literature

The authors of [14] find that it is possible to generate asymptotically safe extensions to the SM in the subsystem $(\alpha_2, \alpha_3, \alpha_y)$ of the couplings. The five benchmark models discussed in [14] (labeled as A, B, C, D and E) are not among those in our scan because they do not include hypercharge, top Yukawa and quartic interaction. We analyzed them separately.

The hypercharge Y can easily be added to these models. The charge Y must be larger than a minimal value in order for the corresponding direction in the UV critical surface to be marginally relevant. This does not change the behavior of the models.

Similar to what happens to the model in section 3.6.2, all these models have at least one

large scaling exponent (See Tab. 3.9). The large values of θ imply that the fixed points are not in the perturbative domain even though they can be connected to the SM in the IR regime. In fact, the fixed points in the `210` approximation scheme cannot be identified with those in the `321` approximation scheme because of their instability against radiative corrections. We can see how the structure of the fixed points changes by comparing Table 3.9 to Table 3.10. The eigenvalues are always large in both tables.

	(R_3, R_2, N_f)	α_2^*	α_3^*	α_y^*	θ_1	θ_2	θ_3
A	$(1, 4, 12)$	0.241	0	0.338	210	-1.90	0
B	$(10, 1, 30)$	0	0.129	0.116	338	-2.06	0
		0.277	0.129	0.116	341	-2.08	0.897
C	$(10, 4, 80)$	0	0.332	0.0995	23258	-2.18	0
		0.0753	0.0503	0.0292	1499	328	-2.77
		0.800	0	0.150	145193	-2.12	0
D	$(3, 4, 290)$	0.0615	0.0416	0.0057	943	45.3	-2.29
		0.0896	0	0.0067	1984	-2.11	0
E	$(3, 3, 72)$	0.218	0.150	0.0471	896	112	-1.78

Table 3.9: Couplings and eigenvalues for the benchmark models in [14] for the `210` approximation scheme.

	(R_3, R_2, N_f)	α_2^*	α_3^*	α_y^*	θ_1	θ_2	θ_3	ρ_3
A	$(1, 4, 12)$	0	0	0.1509	-4.83	0	0	–
B	$(10, 1, 30)$	0	0.0138	0	-20.02	2.24	0	3.14
		0	0	0.0594	-4.75	0	0	–
C	$(10, 4, 80)$	0	0	0.0187	-4.501	0	0	–
		0	0.0036	0	-49.4	2.28	0	9.29
D	$(3, 4, 290)$	0	0	0.0115	-6.95	0	0	–
		0	0.0108	0	-36.7	1.015	0	5.81
E	$(3, 3, 72)$	0	0	0.0357	-5.79	0	0	–
		0	0.0305	0	-21.8	1.098	0	2.66

Table 3.10: Couplings, eigenvalues and the ratio ρ_3 for the benchmark models in [14] for the `321` approximation scheme.

If we take the fixed points in the `321` approximation scheme at their face value and try to match them to the SM, we always encounter a coupling, α_2 in almost all the cases (see Table 3.10), that is frozen to its vanishing value: the theory is trivial in the coupling α_2 and it cannot be matched to the SM. In other words, the benchmark models in [14] suffer from the same pathology of the models in our scan. Unlike those models, in this case it is a non-abelian coupling that is trivial.

Two more benchmark models studied in the literature

The authors of [15] study three models where the fermions are in the representations $(N_f, \ell, Y) = (3, 2, 1/6)$, $(3, 1, 0) \oplus (1, 2, 1/2)$ and $(3, 1, 0) \oplus (1, 3, 0) \oplus (1, 1, 1)$, respectively. Further models (with Majorana fermions charged under only one gauge group at the time) are introduced in [16]. In both papers, they consider the large N_f limit and the zeros of the β-functions are found after resumming the blob diagrams of the perturbative theory.

Resummed β-functions could help in discussing the AS of a theory, yet there is no available procedure that is free of the ambiguities derived from summing over a particular class of diagrams. Moreover, a large number of new states must be included to be within the regime of validity of the resummation scheme which—from the phenomenological point of view—is unappealing.

It is difficult to compare these results to ours because of the non-perturbative nature of the resummation procedure. In our approach these models are all ruled out because of the larger scaling dimensions arising from the large values of N_f (see Figure 3.3 and the discussion in section 3.6). The fixed points obtained in the approach of [15] and [16] are probably linked to essential singularities in the complete resummation [115] and no perturbative treatment—like expanding around the fixed point values to search for the trajectory back to the SM—is possible.

While these models provide interesting examples of AS theories, it is difficult to see them as viable candidate for extensions of the SM because the low-energy matching is problematic: to wit, even assuming that the fixed point found are physical, the authors of [16] conclude (in the published version of their paper) that there is no matching because of the persistence of the Landau pole in the $U(1)$ coupling (which can only be avoided at the price of making the vacuum of the model unstable because of the running of the quartic Higgs interaction).

Combining more than one representation

Combining vector-like fermions in different representations (as done, for instance, in [15, 16]) provides other examples of models that almost work. In the simplest scenario, we can try to construct a model with two types of vector-like fermions. In that case, we duplicate the last three terms in Eq. (3.6.1) for fermions $\tilde{\psi}$ and scalars $\tilde{S}$. We call the extra Yukawa coupling z with, as usual,

$$\alpha_z = \frac{z^2}{(4\pi)^2} \tag{3.6.9}$$

and assume no mixing between the two families.

Since many of the BSM extensions attempt to describe dark matter, we take one of the possible minimal models discussed in [116], and identify some of the vector-like fermions with dark matter. We take N_{f_2} vector-like fermions with quantum numbers $p = q = 0$, $\ell = 2$ and $Y = 0$. That is, we take colorless quintuplets with no hypercharge. Additionally, we consider 3 colorless vector-like fermions in the $(1, 2, 3/2)$ representation. Within the `210` approximation scheme, for the combination $(1, 2, 3/2) \oplus (1, 5, 0)$, we realize that fixed points split in two categories: fixed points that depend on the number of quintuplets N_{f_2} and fixed points that do not. For the latter we have that $\alpha_y = 0$, and the conditions to lie on the critical surface defined by the fixed points imply that $\alpha_2 = 0$. This feature makes the corresponding N_{f_2}-independent fixed points uninteresting.

α_1^*	α_2^*	α_3^*	α_t^*	α_y^*	α_z^*	θ_1	θ_2	θ_3	θ_4	θ_5	θ_6
0.226	0.193	0	0	0.778	0.534	241	24.2	−2.85	−2.28	−1.51	0

Table 3.11: Values of the couplings at the fixed point of interest and eigenvalues for the model combining 3 fields in the representation $(1, 2, 3/2)$ and 8 fields in the representation $(1, 5, 0)$ (`210` approximation scheme).

For the N_{f_2}-dependent fixed points, we find that in order to have $\alpha_i < 1$ for all couplings, the minimum number of quintuplets should be equal to eight. Taking the minimal case of $N_{f_2} = 8$, we find 6 fixed points, all of them having one large eigenvalue around 250. Thus, according to our requirement about perturbation theory, these fixed points are not reliable since there is always one θ which is much larger than 1. This is similar to what happens in section 3.6.2. Nevertheless, we can find a matching with the SM. The only difference with respect to the model in section 3.6.2 is that, in the present case, two matching scales are needed—the reason being that the large number of quintuplets makes α_2 decrease fast so that these fields must be decoupled at very high energies. In Figure 3.7 we show the logarithmic running of the couplings and the two different matching scales. The quintuplets decouple at an energy scale $O(10^{13})$ TeV (and must be considered *wimpzilla* dark matter [117]), the doublets at the energy scale of 1.83 TeV. All the couplings flow to the fixed point in Table 3.11

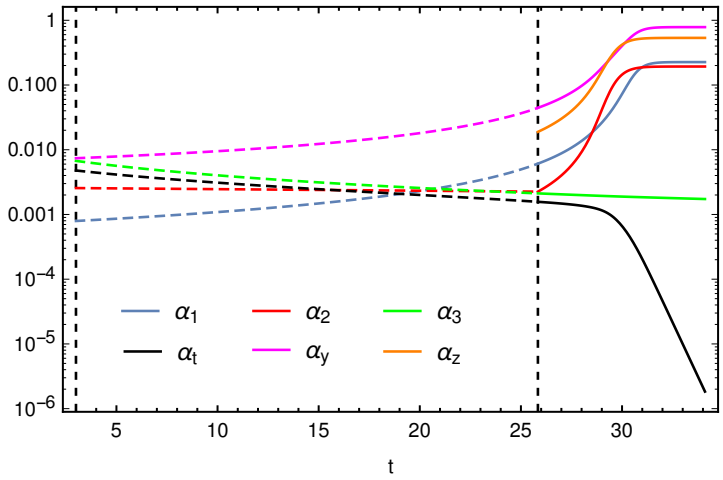

Figure 3.7: Evolution of the couplings with t for the fixed point in Table 3.11 within the `210` approximation with 3 fields in $(1, 2, 3/2)$ and 8 fields in $(1, 5, 0)$. This running provides a trajectory in the theory space connecting the fixed point to a matching scale around 2 TeV passing through another scale (for the quintuplets) at about 10^{13} TeV.

Even though Figure 3.7 shows a nice flow of the coupling constants towards the SM, the size of the eigenvalues implies a breakdown of perturbation theory. Indeed, the fixed point analysed does not survive in the `321` approximation scheme. The results of this chapter reveal us that extensions of the SM via vector-like fermion are unlikely to feature asymptotic safety. This is certainly true in perturbation theory. Beyond perturbation theory different things might happen. Since the main obstacle for a successful extension comes from the Landau pole in the $U(1)$ sector of the SM, we ask ourselves how to render g_1 finite at very high energies. In the next chapter we explore a different approach to the problem. Namely, we consider the effects of gravity on the running of the SM couplings. Substantial attention is given to the $U(1)$ gauge coupling and the quark Yukawa couplings.

(N_f, l)	α_1^*	α_2^*	α_3^*	α_t^*	α_y^*	θ_1	θ_2	θ_3	θ_4	θ_5	
$(1, \frac{1}{2})$	0	0.0411	0	0	0.0264	0.378	−0.185	0.0936	0	0	P_{16}
	0	0.0422	0	0.0211	0.0271	0.389	0.195	0.0936	0	0	P_{17}
	0	0.0385	0	0	0	−0.346	−0.173	0.0897	0	0	P_{18}
	0	0.0394	0	0.0197	0	−0.355	0.182	0.0896	0	0	P_{19}
$(1, 1)$	0	0	0.417	0	0	−6.67	−6.67	4.17	0	0	P_{11}
	0	0	0.521	0	0.417	10.8	−8.33	4.00	0	0	P_9
$(1, \frac{3}{2})$	0	0	0.176	0	0	−2.81	−2.81	1.52	0	0	P_{11}
	0	0	0.205	0.365	0	3.84	−3.28	1.52	0	0	P_{10}
	0	0	0.195	0	0.120	3.49	−3.12	1.51	0	0	P_9
	0	0	0.232	0.413	0.143	4.83	3.72	1.55	0	0	P_8
$(1, 2)$	0	0	0.0982	0	0	−1.57	−1.57	0.720	0	0	P_{11}
	0	0	0.108	0.193	0	1.88	−1.74	0.735	0	0	P_{10}
	0	0	0.105	0	0.0526	1.78	−1.68	0.730	0	0	P_9
	0	0	0.117	0.208	0.0586	2.15	1.88	0.749	0	0	P_8
$(1, \frac{5}{2})$	0	0	0.0600	0	0	−0.960	−0.960	0.360	0	0	P_{11}
	0	0	0.0646	0.115	0	1.08	−1.03	0.371	0	0	P_{10}
	0	0	0.0632	0	0.0266	1.04	−1.01	0.368	0	0	P_9
	0	0	0.0683	0.121	0.0288	1.18	1.09	0.380	0	0	P_8
$(1, 3)$	0	0	0.0412	0.0733	0.0150	0.689	0.660	0.184	0	0	P_8
	0	0	0.0388	0	0.0141	0.632	−0.621	0.178	0	0	P_9
	0	0	0.0395	0.0702	0	0.647	−0.632	0.180	0	0	P_{10}
	0	0	0.0372	0	0	−0.596	−0.596	0.174	0	0	P_{11}
$(1, \frac{7}{2})$	0	0	0.0221	0	0	−0.354	−0.354	0.0737	0	0	P_{11}
	0	0	0.0232	0.0413	0	0.376	−0.371	0.0764	0	0	P_{10}
	0	0	0.0229	0	0.0073	0.370	−0.366	0.0756	0	0	P_9
	0	0	0.0241	0.0428	0.0077	0.394	0.385	0.0784	0	0	P_8
$(1, 4)$	0	0	0.0114	0	0	−0.182	−0.182	0.0235	0	0	P_{11}
	0	0	0.0118	0.0210	0	0.191	−0.189	0.0235	0	0	P_{10}
	0	0	0.0117	0	0.0033	0.188	−0.187	0.0233	0	0	P_9
	0	0	0.0122	0.0217	0.0035	0.197	0.195	0.0242	0	0	P_8
$(1, \frac{9}{2})$	0	0	0.0033	0	0	−0.0530	−0.0530	0.0022	0	0	P_{11}
	0	0	0.0034	0.0061	0	0.0550	−0.0549	0.0023	0	0	P_{10}
	0	0	0.0034	0	0.0009	0.0544	−0.0544	0.0023	0	0	P_9
	0	0	0.0035	0.0063	0.0009	0.0566	0.0564	0.0023	0	0	P_8

Table 3.5: Fixed points and eigenvalues for vector-like fermions in the fundamental representation of $SU_c(3)$, in the 210 approximation scheme, with $N_f = 1$. We highlight in green the fixed points that appear also in the 321 approximation scheme. The labels in the second to the last last column refer to the list in Table C.1.

(N_f, l)	α_1^*	α_2^*	α_3^*	α_t^*	α_y^*	θ_1	θ_2	θ_3	θ_4	θ_5	
$(2, \frac{1}{2})$	0	0	0.176	0	0	-2.81	-2.81	1.52	0	0	P_{11}
	0	0	0.205	0.365	0	3.84	-3.28	1.52	0	0	P_{10}
	0	0	0.260	0	0.260	5.91	-4.16	1.59	0	0	P_9
	0	0	0.330	0.588	0.330	8.99	5.29	1.68	0	0	P_8
$(2, 1)$	0	0	0.0600	0	0	-0.960	-0.960	0.360	0	0	P_{11}
	0	0	0.0646	0.115	0	1.08	-1.03	0.371	0	0	P_{10}
	0	0	0.0727	0	0.0529	1.30	-1.16	0.390	0	0	P_9
	0	0	0.0795	0.141	0.0578	1.50	1.27	0.405	0	0	P_8
$(2, \frac{3}{2})$	0	0	0.0221	0	0	-0.354	-0.354	0.0737	0	0	P_{11}
	0	0	0.0232	0.0413	0	0.376	-0.371	0.0764	0	0	P_{10}
	0	0	0.0252	0	0.0144	0.417	-0.403	0.0810	0	0	P_9
	0	0	0.0266	0.0473	0.0152	0.448	0.426	0.0842	0	0	P_8
$(2, 2)$	0	0	0.0033	0	0	-0.0530	-0.0530	0.0022	0	0	P_{11}
	0	0	0.0034	0.0061	0	0.0550	-0.0549	0.0023	0	0	P_{10}
	0	0	0.0036	0	0.0017	0.0587	-0.0584	0.0024	0	0	P_9
	0	0	0.0038	0.0068	0.0018	0.0612	0.0608	0.0025	0	0	P_8
$(3, \frac{1}{2})$	0	0	0.0600	0	0	-0.960	-0.960	0.360	0	0	P_{11}
	0	0	0.0646	0.115	0	1.08	-1.03	0.371	0	0	P_{10}
	0	0	0.0882	0	0.0784	1.77	-1.41	0.423	0	0	P_9
	0	0	0.0985	0.175	0.0876	2.10	1.58	0.443	0	0	P_8
$(3, 1)$	0	0	0.0114	0	0	-0.182	-0.182	0.0227	0	0	P_{11}
	0	0	0.0118	0.0210	0	0.191	-0.189	0.0235	0	0	P_{10}
	0	0	0.0143	0	0.0095	0.237	-0.229	0.0276	0	0	P_9
	0	0	0.0150	0.0267	0.0100	0.252	0.241	0.0288	0	0	P_8
$(4, \frac{1}{2})$	0	0	0.0221	0	0	-0.354	-0.354	0.0737	0	0	P_{11}
	0	0	0.0232	0.0413	0	0.376	-0.371	0.0764	0	0	P_{10}
	0	0	0.0335	0	0.0268	0.607	-0536	0.0987	0	0	P_9
	0	0	0.0361	0.0642	0.0289	0.670	0.577	0.104	0	0	P_8
$(5, \frac{1}{2})$	0	0	0.0033	0	0	-0.0530	-0.530	0.0022	0	0	P_{11}
	0	0	0.0343	0.0061	0	0.0550	-0.0549	0.0023	0	0	P_{10}
	0	0	0.0052	0	0.0038	0.0850	-0.0829	0.0034	0	0	P_9
	0	0	0.0055	0.0097	0.0040	0.0903	0.0878	0.035	0	0	P_8

Table 3.6: Same as Table 3.5, with $N_f > 1$.

(N_f, l)	α_1^*	α_2^*	α_3^*	α_t^*	α_y^*	α_λ^*	θ_1	θ_2	θ_3	θ_4	θ_5	θ_6	σ	ρ
$(1, \frac{1}{2})$	0	0.0291	0	0.0148	0	0.0120	−0.306	0.208	0.132	0.0827	0	0	0.737	0.263
	0	0.0305	0	0.0155	0.0209	0.0126	0.322	0.219	0.139	0.0863	0	0	0.719	0.281
$(1, \frac{5}{2})$	0	0	0.0346	0	0	0	−0.748	−0.748	0.295	0	0	0	0.577	0.423
	0	0	0.0355	0	0.0167	0	−0.774	0.768	0.304	0	0	0	0.559	0.441
$(1, 3)$	0	0	0.0252	0	0	0	−0.501	−0.501	0.156	0	0	0	0.676	0.323
	0	0	0.0258	0	0.0101	0	−0.516	0.514	0.160	0	0	0	0.664	0.336
$(1, \frac{7}{2})$	0	0	0.0171	0	0	0	−0.315	−0.315	0.0670	0	0	0	0.771	0.228
	0	0	0.0177	0.0358	0	0.0221	0.969	−0.329	0.290	0.0723	0	0	0.758	0.242
	0	0	0.0175	0	0.0058	0	−0.324	0.324	0.0717	0	0	0	0.763	0.237
	0	0	0.0182	0.0368	0.0061	0.0227	0.998	0.334	0.298	0.0742	0	0	0.748	0.252
$(1, 4)$	0	0	0.098	0	0	0	−0.170	−0.170	0.0223	0	0	0	0.864	0.136
	0	0	0.0102	0.0193	0	0.0119	0.521	−0.177	0.165	0.0231	0	0	0.856	0.144
	0	0	0.0101	0	0.0029	0	−0.175	0.175	0.0229	0	0	0	0.859	0.141
	0	0	0.0104	0.0198	0.0030	0.0123	0.536	0.182	0.170	0.0237	0	0	0.8505	0.149
$(1, \frac{9}{2})$	0	0	0.0032	0	0	0	−0.0519	−0.0519	0.0022	0	0	0	0.955	0.0451
	0	0	0.0033	0.0059	0	0.0037	0.159	−0.0537	0.0526	0.0023	0	0	0.952	0.0476
	0	0	0.0032	0	0.0008	0	−0.0532	0.0532	0.0023	0	0	0	0.953	0.0469
	0	0	0.0033	0.0061	0.0009	0.00038	0.1635	0.0551	0.0540	0.0023	0	0	0.9505	0.0495
$(2, 1)$	0	0	0.346	0	0	0	−0.748	−0.748	0.295	0	0	0	0.577	0.423
	0	0	0.0381	0	0.0319	0	−0.846	0.824	0.326	0	0	0	0.5077	0.492
$(2, \frac{3}{2})$	0	0	0.0171	0	0	0	−0.315	−0.315	0.0699	0	0	0	0.771	0.228
	0	0	0.0177	0.0358	0	0.0221	0.969	−0.329	0.295	0.0723	0	0	0.758	0.242
	0	0	0.0187	0	0.0113	0	−0.350	0.349	0.0767	0	0	0	0.737	0.263
$(2, 2)$	0	0	0.0032	0	0	0	−0.0519	−0.0519	0.0022	0	0	0	0.955	0.0451
	0	0	0.0033	0.0059	0	0.0037	0.159	−0.0537	0.0526	0.0023	0	0	0.952	0.0476
	0	0	0.0035	0	0.0016	0	−0.0570	0.0570	0.0024	0	0	0	0.948	0.0521
	0	0	0.0036	0.0065	0.0017	0.0040	0.1756	0.0592	0.0579	0.0025	0	0	0.945	0.552
$(3, \frac{1}{2})$	0	0	0.0346	0	0	0	−0.748	−0.748	0.295	0	0	0	0.577	0.423
	0	0	0.0417	0	0.0440	0	−0.950	0.913	0.359	0	0	0	0.431	0.569
$(3, 1)$	0	0	0.0098	0	0	0	−0.170	−0.170	0.0223	0	0	0	0.864	0.136
	0	0	0.0102	0.0193	0	0.119	0.521	−0.177	0.165	0.0231	0	0	0.856	0.144
	0	0	0.0118	0	0.0081	0	0.208	−0.208	0.0270	0	0	0	0.819	0.181
	0	0	0.0123	0.0237	0.0085	0.0147	0.641	0.218	0.200	0.0281	0	0	0.8062	0.194
$(4, \frac{1}{2})$	0	0	0.0171	0	0	0	−0.315	−0.315	0.0699	0	0	0	0.771	0.228
	0	0	0.0177	0.0358	0	0.0221	0.969	−0.329	0.290	0.0723	0	0	0.758	0.242
	0	0	0.0226	0	0.0196	0	0.439	−0.437	0.0931	0	0	0	0.647	0.353
$(5, \frac{1}{2})$	0	0	0.0033	0	0	0	−0.0519	−0.0519	0.0022	0	0	0	0.955	0.0451
	0	0	0.0033	0.0059	0	0.0037	0.159	−0.0537	0.0526	0.0023	0	0	0.952	0.0476
	0	0	0.0048	0	0.0035	0	0.0798	−0.0793	0.0034	0	0	0	0.914	0.0859
	0	0	0.0050	0.0092	0.0037	0.0057	0.248	0.0843	0.0809	0.0035	0	0	0.9066	0.0934

Table 3.7: Fixed points and eigenvalues for vector-like fermions in the fundamental representation of $SU_c(3)$, in the `321` approximation scheme. The last two columns give the values of the ratio σ and ρ for α_2 or α_3 depending on which coupling is non-zero (see 3.2.4).

Chapter 4

Gravitational Corrections to the Running of Standard Model Couplings

4.1. General beta functions

With the discussion of the the previous chapters about gravity and matter, we move forward and study the compound system in more detail. The purpose of this chapter is to determine a possible effects of quantum gravity on the running of the Standard Model couplings. In particular, we focus on the subset of gauge and quark Yukawa couplings. An extension to the lepton sector is straightforward. For completeness, we write here the known Yukawa Lagrangian for the quark sector in the SM

$$\mathcal{L} = -Y^D_{ij}\bar{q}^i_L H d^j_R - Y^U_{ij}\bar{q}^i_L \tilde{H} u^j_R. \tag{4.1.1}$$

In this Lagrangian, H is the Higgs doublet, $\tilde{H}$ is the coujugate Higgs doublet ϵH^* (being ϵ the Levi-Civita symbol in two dimensions), q_L is the quark doublets, d_R the right-handed down quarks and u_R the right-handed up quarks. The last three fields contain an additional index labeling the specific generation, i.e., the number of copies we have for each field. Therefore, the matrices Y^D, Y^U represent the general interaction among all the fields present in the SM.

Following the discussion started in section 2.4, we recall, given the the universality of gravitational interactions, all the gauge couplings beta functions in the SM get modified in the same way. Thus, the 2-loops beta functions for the three SM gauge couplings $\beta_i = \frac{dg_i}{dt}$ are [96, 103, 104]

$$\beta_1 = g_1\left(\tfrac{41}{6}g_1^2\frac{\varepsilon 1}{(4\pi)^2} + g_1^2\Big[\tfrac{199}{18}g_1^2 + \tfrac{9}{2}g_2^2 + 44g_3^2 - \tfrac{17}{6}U - \tfrac{5}{6}D\Big]\frac{\varepsilon 2}{(4\pi)^4} - f_g\right), \tag{4.1.2}$$

$$\beta_2 = g_2\left(-\tfrac{19}{6}g_2^2\frac{\varepsilon 1}{(4\pi)^2} + g_2^2\Big[\tfrac{3}{2}g_1^2 + \tfrac{35}{6}g_2^2 + 12g_3^2 - \tfrac{3}{2}(U+D)\Big]\frac{\varepsilon 2}{(4\pi)^4} - f_g\right), \tag{4.1.3}$$

$$\beta_3 = g_3\left(-7g_3^2\frac{\varepsilon 1}{(4\pi)^2} + g_3^2\Big[\tfrac{11}{6}g_1^2 + \tfrac{9}{2}g_2^2 - 26g_3^2 - 2(U+D)\Big]\frac{\varepsilon 2}{(4\pi)^4} - f_g\right), \tag{4.1.4}$$

where $\varepsilon_1, \varepsilon_2 = 0, 1$ represent the $1, 2$-loop contributions respectively. We have also used the traces $U = Tr(Y_U Y_U^\dagger)$ and $D = Tr(Y_D Y_D^\dagger)$ of the up and down Yukawa matrices. Similar equations for the gauge beta functions for a more simplified system were given (3.6.3).

Analogously, the modification of all the Yukawa beta functions will have the same form. At very high energies, we can write the corrected beta functions for the two Yukawa matrices (Y_U, Y_D) in the quark sector of the SM as [98, 103, 104]

$$\begin{aligned}\beta_{Y_U} = \frac{dY_U}{dt} = \Big[Y_2(S) - G_U + \tfrac{3}{2}\left(Y_U Y_U^\dagger - Y_D Y_D^\dagger\right)\Big] Y_U\frac{\varepsilon_1}{(4\pi)^2} + \Big[\tfrac{3}{2}(Y_U Y_U^\dagger)^2 - \tfrac{1}{4}Y_U Y_U^\dagger Y_D Y_D^\dagger \\ + \quad - Y_D Y_D^\dagger Y_U Y_U^\dagger + \tfrac{11}{4}(Y_D Y_D^\dagger)^2 + A_{UU}Y_U Y_U^\dagger + A_{UD}Y_D Y_D^\dagger + B_U\Big] Y_U\frac{\varepsilon_2}{(4\pi)^4} - f_y Y_U,\end{aligned} \tag{4.1.5}$$

$$\begin{aligned}\beta_{Y_D} = \frac{dY_D}{dt} = \Big[Y_2(S) - G_D + \tfrac{3}{2}\left(Y_D Y_D^\dagger - Y_U Y_U^\dagger\right)\Big] Y_D\frac{\varepsilon_1}{(4\pi)^2} + \Big[\tfrac{3}{2}(Y_D Y_D^\dagger)^2 - \tfrac{1}{4}Y_D Y_D^\dagger Y_U Y_U^\dagger \\ + \quad - Y_U Y_U^\dagger Y_D Y_D^\dagger + \tfrac{11}{4}(Y_U Y_U^\dagger)^2 + A_{DD}Y_D Y_D^\dagger + A_{DU}Y_U Y_U^\dagger + B_D\Big] Y_D\frac{\varepsilon_2}{(4\pi)^4} - f_y Y_D.\end{aligned} \tag{4.1.6}$$

In the previous expressions, we have introduced the following pure gauge 1-loop contributions

$$G_U = \frac{17}{12}g_1^2 + \frac{9}{4}g_2^2 + 8g_3^2, \quad G_D = \frac{5}{12}g_1^2 + \frac{9}{4}g_2^2 + 8g_3^2, \tag{4.1.7}$$

as well as the pure trace factor

$$Y_2(S) = \mathrm{Tr}\left(3Y_U Y_U^\dagger + 3Y_D Y_D^\dagger\right). \tag{4.1.8}$$

On the other hand, for the 2-loops contribution we have

$$A_{UU} = \left(\tfrac{223}{48}g_1^2 + \tfrac{135}{16}g_2^2 + 16g_3^2\right) - \tfrac{9}{4}Y_2(S), \tag{4.1.9}$$

$$A_{UD} = \tfrac{5}{4}Y_2(S) - \left(\tfrac{43}{48}g_1^2 - \tfrac{9}{16}g_2^2 + 16g_3^2\right), \tag{4.1.10}$$

$$A_{DD} = \left(\tfrac{187}{48}g_1^2 + \tfrac{135}{16}g_2^2 + 16g_3^2\right) - \tfrac{9}{4}Y_2(S), \tag{4.1.11}$$

$$A_{DU} = \tfrac{5}{4}Y_2(S) - \left(\tfrac{79}{48}g_1^2 - \tfrac{9}{16}g_2^2 + 16g_3^2\right), \tag{4.1.12}$$

$$\begin{aligned}B_U = -\chi_4(S) + \left(\tfrac{1}{8} + \tfrac{145}{81}N_{sm}\right)g_1^4 - \left(\tfrac{35}{4} - N_{sm}\right)g_2^4 - \left(\tfrac{404}{3} - \tfrac{80}{9}N_{sm}\right)g_3^4 \\ - \tfrac{3}{4}g_1^2 g_2^2 + \tfrac{19}{9}g_1^2 g_2^3 + 9g_2^2 g_3^2 + \tfrac{5}{2}Y_4(S),\end{aligned} \tag{4.1.13}$$

$$B_D = -\chi_4(S) - \left(\tfrac{29}{72} + \tfrac{5}{81}N_{sm}\right) g_1^4 - \left(\tfrac{35}{4} - N_{sm}\right) g_2^4 - \left(\tfrac{404}{3} - \tfrac{80}{9}N_{sm}\right) g_3^4 - \tfrac{9}{4} g_1^2 g_2^2 + \tfrac{31}{9} g_1^2 g_2^3 + 9 g_2^2 g_3^2 + \tfrac{5}{2} Y_4(S), \tag{4.1.14}$$

$$\chi_4(S) = \tfrac{9}{4}\mathrm{Tr}\left[3(Y_U Y_U^\dagger)^2 + 3(Y_D Y_D^\dagger)^2 - \tfrac{2}{3} Y_U Y_U^\dagger Y_D Y_D^\dagger\right], \tag{4.1.15}$$

$$Y_4(S) = (\tfrac{17}{12} g_1^2 + \tfrac{9}{4} g_2^2 + 8 g_3^2)\mathrm{Tr}\,(Y_U Y_U^\dagger) + (\tfrac{5}{12} g_1^2 + \tfrac{9}{4} g_2^2 + 8 g_3^2)\mathrm{Tr}\,(Y_D Y_D^\dagger), \tag{4.1.16}$$

where N_{sm} is the number of families we have in the Standard Model. In the set of gauge and Yukawa beta functions we have included the gravitational correction (f_g, f_y) which are independent the quantum numbers of the fermions/scalars of the SM. In principle, f_g and f_y depend on all the relevant gravitational couplings of the theory, as we explained in Sec. 2.4. From our discussion on asymptotically safe gravity, we learned that the gravitational couplings, and their effects, are small at low energies. On the contrary, at energies beyond the Planck scale, the gravitational sector goes to a non-trivial fixed point, and therefore the couplings approach a constant value. Thus, we can assume that (f_g, f_y) are constant beyond M_{pl} and zero below M_{pl}. The transition between the two regimes is ignored for now, and we believe that its particular form does not affect the global picture of the present scenario.

We transform now the Yukawa beta functions to the basis of standard Yukawa couplings and CKM elements, in order to make a connection with the quantities studied experimentally. We start by defining two hermitian matrices out of Y_U and Y_D

$$M_U = Y_U Y_U^\dagger, \;\; M_D = Y_D Y_D^\dagger. \tag{4.1.17}$$

At a given scale μ, these matrices are diagonalized by two unitary matrices V_L^U, V_L^D as follows

$$\begin{aligned} V_L^U M_U V_L^{U\dagger} &= D_U^2 = diag[y_u^2, y_c^2, y_t^2], \\ V_L^D M_D V_L^{D\dagger} &= D_D^2 = diag[y_d^2, y_s^2, y_b^2]. \end{aligned} \tag{4.1.18}$$

However, at another scale μ' these matrices M are not diagonalized by same transformations any more. Consequently, the diagonal entries will change with the energy scale. Our goal is to find the beta-functions for the diagonal entries (or Yukawa couplings) [118, 119]. For simplicity, we use the label F to represent each flavor matrix, i.e., Y_F, M_F, D_F^2, V_L^F with $F = U, D$. First of all, we perturb eq. (4.1.17) as follows

$$V_L^F M_F V_L^{F\dagger} = D_F^2 \longrightarrow (V_L^F + \delta V_L^F)(M_F + \delta M_F)(V_L^{F\dagger} + \delta V_L^{F\dagger}) = D_F^2 + \delta D_F^2. \tag{4.1.19}$$

Then, we write the new transformation matrix as $\tilde{V}_L^F = V_L^F + \delta V_L^F = (1+\epsilon)V_L^F$ which implies that $\epsilon^\dagger = -\epsilon$ and $\mathrm{Tr}\,\epsilon = 0$. Keeping terms up to first order in the perturbations, we obtain

$$V_L^F M_F V_L^F - V_L^F M_F V_L^F \epsilon + \epsilon V_L^F M_F V_L^{F\dagger} + V_L^F \delta M_F V_L^{F\dagger} = D_F^2 + \delta D_F^2. \tag{4.1.20}$$

As a result, the variation in the diagonal elements will be given by

$$\delta D_F^2 = \epsilon D_F^2 - D_F^2\epsilon + V_L^F \delta M_F V_L^{F\dagger} = \epsilon D_F^2 - D_F^2\epsilon + V_L^F \beta_{M_F} V_L^{F\dagger}\delta t, \tag{4.1.21}$$

where we have used Eq. (4.1.17). Since the quantity $\epsilon D_F^2 - D_F^2\epsilon$ does not contain elements in the diagonal, it does not contribute to δD_F^2. Thus, the variation of D_F^2 is given by the diagonal elements of $V_L^F \beta_{M_F} V_L^{F\dagger}\delta t$

$$\left(\frac{dD_F^2}{dt}\right)_{ij} = \left(V_L^F \beta_{M_F} V_L^{F\dagger}\right)_{ij}\delta_{ij}, \tag{4.1.22}$$

where there is no summation in i, j. On the other hand, the off-diagonal elements of ϵ are expressed as

$$\epsilon_{ij}^F = \frac{1}{y_i^2 - y_j^2}\left(V_L^F \beta_{M_F} V_L^{F\dagger}\right)_{ij}, \tag{4.1.23}$$

where we have included a superscript F in ϵ since they are different for the up- and down-type quarks. The previous expression is valid only when $y_i^2 \neq y_j^2$. That is, in order to talk about mixing we need to avoid degeneracy in the up (down)-Yukawa couplings. Defining the vectors $y_i = (y_u, y_c, y_t)$, $y_\rho = (y_d, y_s, y_b)$, and working out Eq. (4.1.22) we get

$$\begin{aligned}\frac{dy_i^2}{dt} = &\left[2(Y_2(S) - G_U) + 3y_i^2 - 3\sum_\rho y_\rho^2 |V_{i\rho}|^2\right]\frac{y_i^2}{(4\pi)^2}\varepsilon_1 + \left[3y_i^4 - \frac{5}{2}y_i^2\sum_\rho y_\rho^2|V_{i\rho}|^2\right.\\ &\left. + \frac{11}{2}\sum_\rho y_\rho^4|V_{i\rho}|^2 + 2A_{UU}y_i^2 + 2A_{UD}\sum_\rho y_\rho^2|V_{i\rho}|^2 + 2B_U\right]\frac{y_i^2}{(4\pi)^4}\varepsilon_2 + 2f_y y_i^2,\end{aligned} \tag{4.1.24}$$

$$\begin{aligned}\frac{dy_\rho^2}{dt} = &\left[2(Y_2(S) - G_D) + 3y_\rho^2 - 3\sum_i y_i^2 |V_{i\rho}|^2\right]\frac{y_\rho^2}{(4\pi)^2}\varepsilon_1 + \left[3y_\rho^4 - \frac{5}{2}y_\rho^2\sum_i y_i^2|V_{i\rho}|^2\right.\\ &\left. + \frac{11}{2}\sum_i y_i^4|V_{i\rho}|^2 + 2A_{DD}y_\rho^2 + 2A_{DU}\sum_i y_i^2|V_{i\rho}|^2 + 2B_D\right]\frac{y_\rho^2}{(4\pi)^4}\varepsilon_2 + 2f_y y_\rho^2,\end{aligned} \tag{4.1.25}$$

where we introduced the CKM matrix $V_{i\rho}$ defined by

$$V = V_L^U V_L^{D\dagger} = \begin{pmatrix} V_{ud} & V_{us} & V_{ub} \\ V_{cd} & V_{cs} & V_{cb} \\ V_{td} & V_{ts} & V_{tb}\end{pmatrix}. \tag{4.1.26}$$

As a consequence, some of the quantities defined before become

$$Y_2(S) = 3\sum_i y_i^2 + 3\sum_\rho y_\rho^2, \tag{4.1.27}$$

$$\chi_4(S) = \tfrac{9}{4}\Big[3\sum_i y_i^4 + 3\sum_\rho y_\rho^4 - \tfrac{2}{3}\sum_{i,\rho}|V_{i\rho}|^2 y_i^2 y_\rho^2\Big], \tag{4.1.28}$$

$$Y_4(S) = (\tfrac{17}{12}g_1^2 + \tfrac{9}{4}g_2^2 + 8g_3^2)\sum_i y_i^2 + (\tfrac{5}{12}g_1^2 + \tfrac{9}{4}g_2^2 + 8g_3^2)\sum_\rho y_\rho^2. \tag{4.1.29}$$

It is interesting to see that the gravitational corrections appear only in the running of the diagonal elements of Y_F, they are absent in the ϵ_{ij}^F

$$\begin{aligned}(y_i^2 - y_j^2)\epsilon_{ij}^U = &\left[-\frac{3}{2}(y_i^2+y_j^2)\sum_\rho y_\rho^2 V_{i\rho}V_{j\rho}^*\right]\frac{\delta t}{(4\pi)^2}\varepsilon_1 + \left[-\frac{1}{2}y_i^2y_j^2\sum_\rho y_\rho^2 V_{i\rho}V_{j\rho}^*\right.\\ &\left. - (y_i^4+y_j^4)\sum_\rho y_\rho^2 V_{i\rho}V_{j\rho}^* + \frac{11}{4}(y_i^2+y_j^2)\sum_\rho y_\rho^4 V_{i\rho}V_{j\rho}^* + A_{UD}(y_i^2+y_j^2)\sum_\rho y_\rho^2 V_{i\rho}V_{j\rho}^*\right]\frac{\delta t}{(4\pi)^4}\varepsilon_2,\end{aligned} \tag{4.1.30}$$

$$\begin{aligned}(y_\rho^2 - y_\sigma^2)\epsilon_{\rho\sigma}^D = &\left[-\frac{3}{2}(y_\rho^2+y_\sigma^2)\sum_i y_i^2 V_{i\rho}^*V_{i\sigma}\right]\frac{\delta t}{(4\pi)^2}\varepsilon_1 + \left[-\frac{1}{2}y_\rho^2y_\sigma^2\sum_i y_i^2 V_{i\rho}^*V_{i\sigma}\right.\\ &\left. - (y_\rho^4+y_\sigma^4)\sum_i y_i^2 V_{i\rho}^*V_{i\sigma} + \frac{11}{4}(y_\rho^2+y_\sigma^2)\sum_i y_i^4 V_{i\rho}^*V_{i\sigma} + A_{DU}(y_\rho^2+y_\sigma^2)\sum_i y_i^2 V_{i\rho}^*V_{i\sigma}\right]\frac{\delta t}{(4\pi)^4}\varepsilon_2,\end{aligned} \tag{4.1.31}$$

where $i \neq j$ and $\rho \neq \sigma$. The quantities ϵ_{ij}^F are useful because they help us finding the running of the matrix $V_{i\rho}$. Since we can redefine the phases of the quarks in the Lagrangian, we have the freedom of changing V to PVQ where P and Q are diagonal phase matrices. Therefore, we will have different forms of parametrizing the CKM matrix V. In order to work with quantities that are independent of any parametrization, we study the running of $|V_{i\rho}|^2$. Using the definition of V, and taking its infinitesimal variation, we find that

$$\delta V_{i\rho} = \epsilon_{ij}^U V_{j\rho} - V_{i\beta}\epsilon_{\beta\rho}^D. \tag{4.1.32}$$

Then, the variation of $|V_{i\rho}|^2$ is

$$\delta|V_{i\rho}|^2 = \epsilon_{ij}^U V_{j\rho}V_{i\rho}^* - V_{i\beta}\epsilon_{\beta\rho}^D V_{i\rho}^* + \epsilon_{ij}^{U*}V_{j\rho}^*V_{i\rho} - V_{i\beta}^*\epsilon_{\beta\rho}^{D*}V_{i\rho}, \tag{4.1.33}$$

where there is no sum neither on i nor on ρ. Working out a bit the expression, we find that

$$\begin{aligned}\delta|V_{i\rho}|^2 = &(\epsilon_{ii}^U + \epsilon_{ii}^{U*})|V_{i\rho}|^2 - (\epsilon_{\rho\rho}^D + \epsilon_{\rho\rho}^{D*})|V_{i\rho}|^2\\ &+ \sum_{j\neq i}(\epsilon_{ij}^U V_{j\rho}V_{i\rho}^* + \epsilon_{ij}^{U*}V_{j\rho}^*V_{i\rho}) - \sum_{\beta\neq\rho}(V_{i\beta}\epsilon_{\beta\rho}^D V_{i\rho}^* + V_{i\beta}^*\epsilon_{\beta\rho}^{D*}V_{i\rho}).\end{aligned} \tag{4.1.34}$$

Since the matrices ϵ^F are antihermitian, their diagonal entries are purely imaginary. Then, the first two terms in the previous expression vanish, and the variation of the squared CKM elements is simply

$$\delta|V_{i\rho}|^2 = \sum_{j\neq i}(\epsilon^U_{ij}V_{j\rho}V^*_{i\rho} + \epsilon^{U*}_{ij}V^*_{j\rho}V_{i\rho}) - \sum_{\beta\neq\rho}(V_{i\beta}\epsilon^D_{\beta\rho}V^*_{i\rho} + V^*_{i\beta}\epsilon^{D*}_{\beta\rho}V_{i\rho}). \tag{4.1.35}$$

We see that we do not need to know the diagonal entries of ϵ^F, the running of the CKM elements are fully determined by Eqs. (4.1.30) and (4.1.31). Thus, the beta functions for $|V_{i\rho}|^2$ up to two-loops are given by

$$\begin{aligned}
\frac{d|V_{i\rho}|^2}{dt} = &-\frac{3}{2}\left[\sum_{\beta,j\neq i}\frac{y_i^2+y_j^2}{y_i^2-y_j^2}y_\beta^2 V_{i\beta}V^*_{j\beta}V_{j\rho}V^*_{i\rho} + \sum_{\beta,j\neq i}\frac{y_i^2+y_j^2}{y_i^2-y_j^2}y_\beta^2 V^*_{i\beta}V_{j\beta}V^*_{j\rho}V_{i\rho}\right.\\
&\left.\sum_{j,\beta\neq\rho}\frac{y_\rho^2+y_\beta^2}{y_\rho^2-y_\beta^2}y_j^2 V^*_{j\beta}V_{j\rho}V_{i\beta}V^*_{i\rho} + \sum_{j,\beta\neq\rho}\frac{y_\rho^2+y_\beta^2}{y_\rho^2-y_\beta^2}y_j^2 V_{j\beta}V^*_{j\rho}V^*_{i\beta}V_{i\rho}\right]\frac{\varepsilon_1}{(4\pi)^2}\\
&-\left[\sum_{\beta,j\neq i}\frac{1}{y_i^2-y_j^2}\left(\tfrac{1}{2}y_i^2y_j^2 + (y_i^4+y_j^4) - \tfrac{11}{4}(y_i^2+y_j^2)y_\beta^2 - A_{UD}(y_i^2+y_j^2)\right)y_\beta^2 V_{i\beta}V^*_{j\beta}V_{j\rho}V^*_{i\rho}\right.\\
&+\sum_{\beta,j\neq i}\frac{1}{y_i^2-y_j^2}\left(\tfrac{1}{2}y_i^2y_j^2 + (y_i^4+y_j^4) - \tfrac{11}{4}(y_i^2+y_j^2)y_\beta^2 - A_{UD}(y_i^2+y_j^2)\right)y_\beta^2 V^*_{i\beta}V_{j\beta}V^*_{j\rho}V_{i\rho}\\
&+\sum_{j,\beta\neq\rho}\frac{1}{y_\rho^2-y_\beta^2}\left(\tfrac{1}{2}y_\rho^2y_\beta^2 + (y_\rho^4+y_\beta^4) - \tfrac{11}{4}(y_\rho^2+y_\beta^2)y_j^2 - A_{DU}(y_\rho^2+y_\beta^2)\right)y_j^2 V^*_{j\beta}V_{j\rho}V_{i\beta}V^*_{i\rho}\\
&\left.+\sum_{j,\beta\neq\rho}\frac{1}{y_\rho^2-y_\beta^2}\left(\tfrac{1}{2}y_\rho^2y_\beta^2 + (y_\rho^4+y_\beta^4) - \tfrac{11}{4}(y_\rho^2+y_\beta^2)y_j^2 - A_{DU}(y_\rho^2+y_\beta^2)\right)y_j^2 V_{j\beta}V^*_{j\rho}V^*_{i\beta}V_{i\rho}\right]\frac{\varepsilon_2}{(4\pi)^4}
\end{aligned} \tag{4.1.36}$$

In the following, we will study in detail the effects of the gravitational corrections encoded in (f_g, f_y) for one, two and three generations of quarks. By doing so, we will understand better how the fixed points arise, and how the predictions come about. We start from the heaviest generation and then we include the lighter ones. Additionally, we focus on the one-loop expressions since the fixed-point values appear to be in the perturbative regime. Stability checks at two loops are done throughout the analysis of the fixed-point solutions. We find that there are no substantial modifications from one to two loops. The identification of fixed points at one and two loops in the following sections translates in a modification of the parameter f_y by 2%

4.2. One generation

The one generation case is important because it is here where we see the interplay between the two parameters f_g and f_y. The number of Yukawa couplings is just two, so the full set of beta functions is composed by the gauge sector

$$\beta_{g_1} = \frac{1}{16\pi^2}\frac{41}{6}g_1^3 - f_g\, g_1, \quad \beta_{g_2} = -\frac{1}{16\pi^2}\frac{19}{6}g_2^3 - f_g\, g_2, \quad \beta_{g_3} = -\frac{1}{16\pi^2}7g_3^3 - f_g\, g_3, \tag{4.2.1}$$

and the Yukawa sector

$$\beta_{y_t} = \frac{y_t}{16\pi^2}\left(\frac{9}{2}y_t^2 + \frac{3}{2}y_b^2 - \frac{17}{12}g_1^2 - \frac{9}{4}g_2^2 - 8g_3^2\right) - f_y\, y_t, \tag{4.2.2}$$

$$\beta_{y_b} = \frac{y_b}{16\pi^2}\left(\frac{9}{2}y_b^2 + \frac{3}{2}y_t^2 - \frac{5}{12}g_1^2 - \frac{9}{4}g_2^2 - 8g_3^2\right) - f_y\, y_b. \tag{4.2.3}$$

We want now to look for non-trivial fixed points solutions for the full system. As we explained in Chapter 1, the existence of a non-trivial UV fixed point might provide IR predictions. Therefore, it might be possible to predict, for instance, the hierarchy present in the top and bottom Yukawa couplings. This is in fact possible [49], and the dynamics is very interesting. We start by noting that in order to have real fixed-point values in the gauge sector, we need to specify the sign of f_g. We can have either $f_g > 0$ or $f_g < 0$. In the former case, we can have AS in the g_1 coupling, in the latter g_2 and g_3 can become AS. In order to choose the sign for f_g we note that the main difference between β_{y_t} and β_{y_b} lies in the $U(1)$ contribution. Therefore, in order to have non-degenerate y_{t*} and y_{b*}, we should have a non-vanishing value for the g_1 at the fixed point. With g_2 and g_3 equal to zero at the fixed point, we have the following set of possible fixed-point solutions in the subsystem $(y_t,\, y_b,\, g_1)$

$$y_{t*} = 0\,, \qquad y_{b*} = 0\,, \qquad g_{1*} = 0\,, \tag{4.2.4}$$

$$y_{t*} = \sqrt{\frac{32\pi^2\, f_y}{9}}\,, \qquad y_{b*} = 0\,, \qquad g_{1*} = 0\,, \tag{4.2.5}$$

$$y_{t*} = 0\,, \qquad y_{b*} = \sqrt{\frac{32\pi^2\, f_y}{9}}\,, \qquad g_{1*} = 0\,, \tag{4.2.6}$$

$$y_{t*} = \sqrt{\frac{16\pi^2\, f_y}{3}}\,, \qquad y_{b*} = \sqrt{\frac{16\pi^2\, f_y}{3}}\,, \qquad g_{1*} = 0\,, \tag{4.2.7}$$

$$y_{t*} = 0\,, \qquad y_{b*} = 0\,, \qquad g_{1*} = 4\pi\sqrt{\frac{6\, f_g}{41}}\,, \tag{4.2.8}$$

$$y_{t*} = \frac{4\pi}{3}\sqrt{\frac{17\, f_g}{41} + 2f_y}\,, \qquad y_{b*} = 0\,, \qquad g_{1*} = 4\pi\sqrt{\frac{6\, f_g}{41}}\,, \tag{4.2.9}$$

$$y_{t*} = 0\,, \qquad y_{b*} = \frac{4\pi}{3}\sqrt{\frac{5\, f_g}{41} + 2f_y}\,, \qquad g_{1*} = 4\pi\sqrt{\frac{6\, f_g}{41}}\,, \tag{4.2.10}$$

$$y_{t*} = 2\pi\sqrt{\frac{23\, f_g}{123} + \frac{2\, f_y}{3}}\,, \qquad y_{b*} = 2\pi\sqrt{-\frac{f_g}{123} + \frac{2\, f_y}{3}}\,, \qquad g_{1*} = 4\pi\sqrt{\frac{6\, f_g}{41}}\,. \tag{4.2.11}$$

We see that, for $g_1 = 0$, the fixed-point solutions in the Yukawa sector have the symmetry $y_{t*} \leftrightarrow y_{b*}$. The second fixed point is studied in [47], the fifth fixed point in [48], and the last one in [49]. It is the last fixed point the one we use for our discussion. It will help us explain the mechanism that is used in the subsequent sections of this chapter. We already noticed that, in order to have non-trivial solutions for the Yukawa couplings, we need a non-zero $U(1)$ gauge coupling. In particular, for the fixed-point solution in (4.2.11) we have

$$y_{t*}^2 - y_{b*}^2 = \frac{1}{3} g_{1*}^2 \,. \tag{4.2.12}$$

We observe that $g_{1*} \neq 0$ implies $y_{t*} > y_{b*}$. The crucial question now is to know whether $y_{t*} > y_{b*}$ predicts the right IR values once we follow the running down to low energies. For our interesting fixed point, the number of irrelevant directions is equal to three, so in principle we have three IR predictions. However, since we have two free parameters f_g and f_y, by simple counting we end up with only one true prediction. (In a more general setting, where f_g and f_y are determined from first principles, we actually have 3 predictions. For now, f_g and f_y are adjustable). We choose the ratio between y_t and y_b as the quantity to be the predicted. Starting the flow around the fixed point we look for values of f_g and f_y such that y_b/y_t at $k = M_t$ coincides with the experimental value. The value of f_g is determined by analysing the flow of g_1. Since the beta function for this coupling is simple, we can solve analytically the equation and choose f_g such that we get the correct value for g_1 in the IR. With the value of $f_g = 9.7 \times 10^{-3}$ we find that $f_y = 1.192 \times 10^{-4}$ generates the ratio $y_b/y_t = 0.0246$ which is close to the experimental value $y_b/y_t = 0.0242$. In Fig. 4.1 we can see the flow of the couplings. We observe that the hierarchy between y_t and y_b is not inverted or disminished substantially along the RG flow. Therefore, we conclude that gravity can be the source of the big gap observed in the top and bottom quark masses. The question now is whether we can extend this pattern to other families. Once we consider more than one generation of quarks, the notion of mixing enters the discussion. In the next section, we explore the two-generations case.

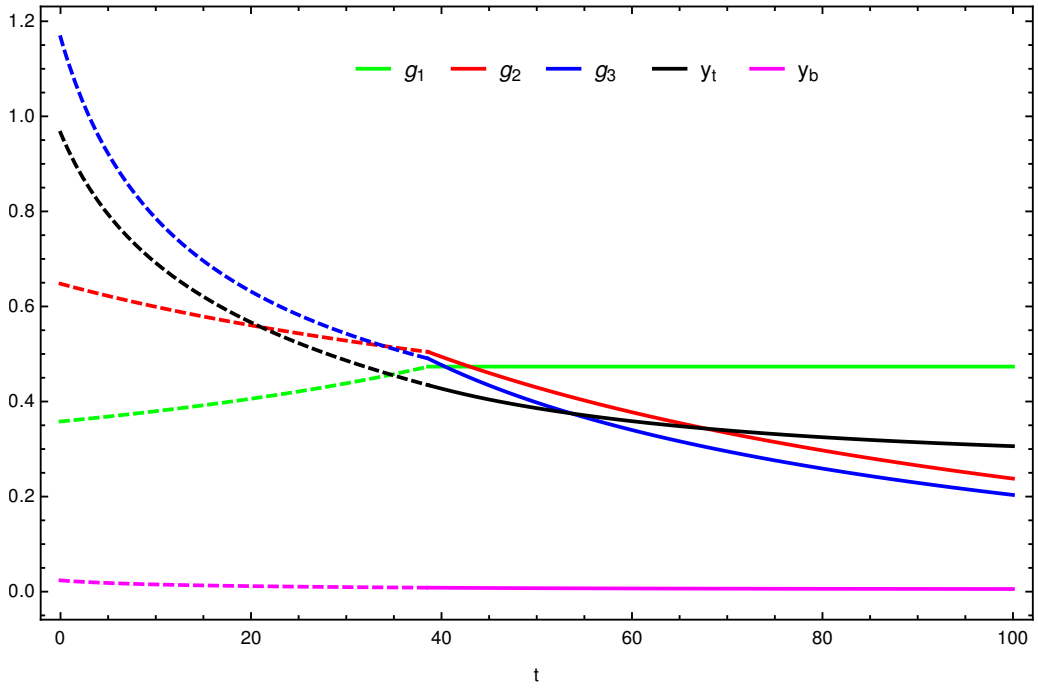

Figure 4.1: RG trajectory emanating from the asymptotically safe fixed point (4.2.11). The dashed lines correspond to the SM running, while the solid lines contain the f-corrections.

4.3. Two generations

In this case, we take the two heaviest generations, i.e., $y_i = (y_t, y_c)$ and $y_\rho = (y_b, y_s)$. As a consequence, the matrix characterizing the relative orientation between the bases that diagonalize Y_U and Y_D is

$$V = \begin{bmatrix} V_{tb} & V_{ts} \\ V_{cb} & V_{cs} \end{bmatrix}. \tag{4.3.1}$$

The mixing matrix has in general 4 entries but there exists only one physical parameter that characterizes it, we call W the free parameter. We define $|V_{tb}|^2 = W$, and therefore, via the unitary property of V, we have that $|V_{ts}|^2 = 1 - W$, $|V_{cb}|^2 = 1 - W$ and $|V_{cs}|^2 = W$. Since we study the flow of the squared CKM elements, it is useful to construct a matrix made of the squares of each entry of the CKM matrix

$$V_2 = \left[\{|V_{ij}|^2\}\right] = \begin{bmatrix} W & 1-W \\ 1-W & W \end{bmatrix}. \tag{4.3.2}$$

The 1-loop beta function for our CKM parameter is given by

$$\frac{dW}{dt} = -3(1-W)W\left[\frac{y_t^2+y_c^2}{y_t^2-y_c^2}(y_b^2-y_s^2)+\frac{y_b^2+y_s^2}{y_b^2-y_s^2}(y_t^2-y_c^2)\right]\frac{1}{(4\pi)^2}. \tag{4.3.3}$$

We see that $W=1$ corresponds to the case of no mixing ($V=\mathbb{1}$) among quarks belonging to different generations. On the other hand, $W=0$ is seen as the situation of maximal mixing. However, in the particle physics jargon, $W=0,1$ correspond both to minimal mixing, being maximal mixing the case of $W=1/2$. Now, taking into account the running of the mixing parameter, the beta functions for y_t and y_b are

$$\beta_{y_t} = \frac{y_t}{16\pi^2}\left(\frac{9}{2}y_t^2+\frac{3}{2}y_b^2\,(2-W)+\frac{3}{2}y_s^2\,(1+W)+3y_c^2-\frac{9}{4}g_2^2-8g_3^2-\frac{17}{12}g_1^2\right)-f_y\,y_t, \tag{4.3.4}$$

$$\beta_{y_b} = \frac{y_b}{16\pi^2}\left(\frac{9}{2}y_b^2+\frac{3}{2}y_t^2\,(2-W)+3y_s^2+\frac{3}{2}y_c^2\,(1+W)-\frac{9}{4}g_2^2-8g_3^2-\frac{5}{12}g_1^2\right)-f_y\,y_b. \tag{4.3.5}$$

The beta functions for the quarks of the second generation are obtained by the interchange $(t,b)\leftrightarrow(c,s)$. As it was explained in Sec. 4.2, the sign of f_g is chosen such that g_1 acquires a non-trivial value at the fixed point. Therefore, we take here $g_{1*}=4\pi\sqrt{\frac{6\,f_g}{41}}$, $g_{2*}=0$ and $g_{3*}=0$. For this configuration of gauge couplings, we obtain two lines of fixed points and the list of 24 isolated fixed points, see Appendix E. There are solutions with $W*=0,1$, but also non-trivial CKM configurations. In order to select the promising fixed points, we impose certain general conditions on the solutions. First, knowing the value of f_g, we look for solutions that have real couplings. This translates into conditions on f_y. In some cases, there are no values of f_y for which all the couplings in a fixed-point solution are real. Those solutions are automatically excluded, in particular the cases where we have a non-trivial W_*. Then, we select the cases for which y_{t*} and y_{b*} are different from zero. Otherwise, we would never be able to reach $y_t>y_b$ and $y_c>y_s$ in the IR due to the poles in (4.3.3). Thus, we end up with only four possibilities, namely, fixed points $1b$, $1c$, $2b$, $3a$ and the line (E.0.2). Finally, we check whether there are actually values of f_y for which $y_{t*}>y_{c*}$ and $y_{b*}>y_{s*}$. It turns out that the fixed point $(1c)$ is excluded, while $(1b)$ and the line predict a $y_{c*}\gtrsim 0.0747$ which is always larger than $y_c(M_{pl})=0.273$. This makes impossible a correct IR matching. Thus, we end up with only two truly fixed points. In this section, as well as in the next one, we explore the properties of the lines of fixed points . However, these lines disappear at two loops and beyond. They are just an artifact of the loop expansion. Therefore, they are not as interesting as the isolated fixed points in our discussion. In Appendix F we explain how the lines and planes (surfaces in general) of fixed points . Moreover, following the results of [120, 121], we study the relation between surfaces of fixed points and RG invariants at one-loop order (combinations of couplings that are constant along the RG flow).

We have the fixed point of Eq. (4.2.11) that we rewrite here for convenience

$$y_{t*} = 2\pi\sqrt{\frac{23\,f_g}{123} + \frac{2\,f_y}{3}}\,, \quad y_{b*} = 2\pi\sqrt{-\frac{f_g}{123} + \frac{2\,f_y}{3}}\,, \quad y_{c*} = 0\,, \quad y_{s*} = 0\,. \tag{4.3.6}$$

The fixed-point analysis taking all the couplings into account tells us that one of the irrelevant directions is aligned with y_s. Being y_s zero at the fixed point, it remains zero at all energy scales. This is clearly not desired because we know that $m_s \neq 0$. On the other hand, as a promising candidate, we have the fixed point with $W_* = 0$ and

$$y_{t*} = \frac{4\pi}{\sqrt{15}}\sqrt{f_g + 2f_y}, \quad y_{b*} = \frac{4\pi}{\sqrt{615}}\sqrt{-19f_g + 82f_y}\,, \quad y_{c*} = 0\,, \quad y_{s*} = 0\,. \tag{4.3.7}$$

In order to show the power of our mechanism and the phenomenological viability of (4.3.7), we study the RG flow of the Yukawa couplings and W. Additionally, we compute the ratio y_b/y_t in the IR. In this case, the number of irrelevant directions is 3, and we are able to obtain the ratio 0.0225. This value is close to the expected result $y_b/y_t = 0.0242$. Since y_c and y_c are asymptotically free couplings, they cannot be predicted. They are just adjusted to the experimental values in the IR. In Fig. 4.2, we can see the running of the Yukawa couplings and the parameter W. We conclude then that it is possible to render the SM with two generations of quark Yukawa couplings UV finite. Moreover, it is conceivable to decrease the number of free parameters of the SM via the existence of a fixed point whose critical dimension surface is less than the number of couplings. In particular, we are able to generate the small ratio between the top and bottom quark masses $m_b/m_t = 0.0225$. We do not display here the RG running of the gauge couplings. It is already shown in Fig. 4.1.

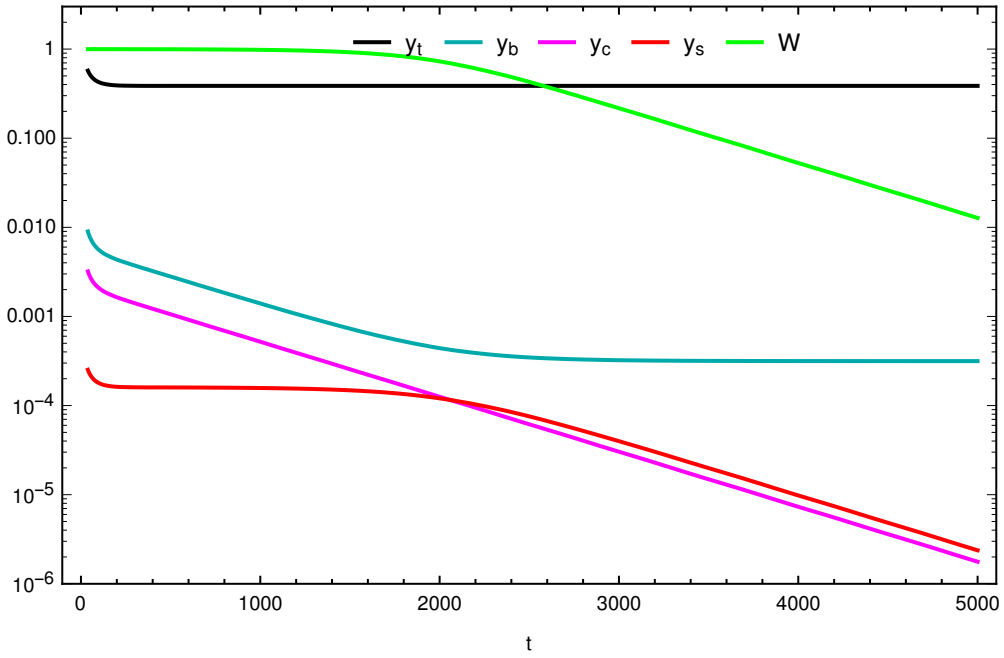

Figure 4.2: RG trajectory emanating from the asymptotically safe fixed point (4.3.7).

4.4. Three generations

For three generations of quarks, the CKM matrix contains only 4 physical elements. In this work, we parametrize the entries of V by using the four quantities $X = |V_{ud}|^2$, $Y = |V_{us}|^2$, $Z = |V_{cd}|^2$ and $W = |V_{cs}|^2$. Then, the matrix of the squared CKM elements takes the form

$$V_2 = \left[\{|V_{ij}|^2\}\right] = \begin{bmatrix} X & Y & 1-X-Y \\ Z & W & 1-Z-W \\ 1-X-Z & 1-Y-W & X+Y+Z+W-1 \end{bmatrix} . \tag{4.4.1}$$

Working out Eq. (4.1.36), we find the beta functions for these parameters

$$\begin{aligned}\frac{dX}{dt} = -\frac{3}{(4\pi)^2}\Bigg[&\frac{y_u^2+y_c^2}{y_u^2-y_c^2}\left\{(y_d^2-y_b^2)XZ + \frac{(y_b^2-y_s^2)}{2}(W(1-X)+X-(1-Y)(1-Z))\right\}\\ &+\frac{y_u^2+y_t^2}{y_u^2-y_t^2}\left\{(y_d^2-y_b^2)X(1-X-Z) + \frac{(y_b^2-y_s^2)}{2}((1-Y)(1-Z)-X(1-2Y)-W(1-X))\right\}\\ &+\frac{y_d^2+y_s^2}{y_d^2-y_s^2}\left\{(y_u^2-y_t^2)XY + \frac{y_t^2-y_c^2}{2}(W(1-X)+X-(1-Y)(1-Z))\right\}\\ &+\frac{y_d^2+y_b^2}{y_d^2-y_b^2}\left\{(y_u^2-y_t^2)X(1-X-Y) + \frac{y_t^2-y_c^2}{2}((1-Y)(1-Z)-X(1-2Z)-W(1-X))\right\}\Bigg]\end{aligned} \tag{4.4.2}$$

$$\begin{aligned}\frac{dY}{dt} = -\frac{3}{(4\pi)^2}\Bigg[&\frac{y_u^2+y_c^2}{y_u^2-y_c^2}\left\{\frac{(y_b^2-y_d^2)}{2}(W(1-X)+X-(1-Y)(1-Z)) + (y_s^2-y_b^2)YW\right\}\\ &+\frac{y_u^2+y_t^2}{y_u^2-y_t^2}\left\{\frac{(y_b^2-y_d^2)}{2}((1-Y)(1-Z)-W(1-X)-X(1-2Y)) + (y_s^2-y_b^2)Y(1-Y-W)\right\}\\ &+\frac{y_s^2+y_d^2}{y_s^2-y_d^2}\left\{(y_u^2-y_t^2)XY + \frac{y_t^2-y_c^2}{2}(W(1-X)+X-(1-Y)(1-Z))\right\}\\ &+\frac{y_s^2+y_b^2}{y_s^2-y_b^2}\left\{(y_u^2-y_t^2)Y(1-X-Y) + \frac{(y_c^2-y_t^2)}{2}(W(1-X-2Y)+X-(1-Z)(1-Y))\right\}\Bigg]\end{aligned} \tag{4.4.3}$$

$$\begin{aligned}\frac{dZ}{dt} = -\frac{3}{(4\pi)^2}\Bigg[&\frac{y_c^2+y_u^2}{y_c^2-y_u^2}\left\{(y_d^2-y_b^2)XZ + \frac{(y_b^2-y_s^2)}{2}(W(1-X)+X-(1-Z)(1-Y))\right\}\\ &+\frac{y_c^2+y_t^2}{y_c^2-y_t^2}\left\{(y_d^2-y_b^2)Z(1-X-Z) + \frac{(y_s^2-y_b^2)}{2}(W(1-X-2Z)+X-(1-Y)(1-Z))\right\}\\ &+\frac{y_d^2+y_s^2}{y_d^2-y_s^2}\left\{\frac{(y_u^2-y_t^2)}{2}((1-Y)(1-Z)-X-W(1-X)) + (y_c^2-y_t^2)ZW\right\}\\ &+\frac{y_d^2+y_b^2}{y_d^2-y_b^2}\left\{\frac{(y_t^2-y_u^2)}{2}((1-Z)(1-Y)-W(1-X)-X(1-2Z)) + (y_c^2-y_t^2)Z(1-Z-W)\right\}\Bigg]\end{aligned} \tag{4.4.4}$$

$$\begin{aligned}\frac{dW}{dt} = -\frac{3}{(4\pi)^2}\Bigg[&\frac{y_c^2+y_u^2}{y_c^2-y_u^2}\left\{(y_s^2-y_b^2)WY + \frac{(y_b^2-y_d^2)}{2}((1-X)W+X-(1-Y)(1-Z))\right\}\\ &+\frac{y_c^2+y_t^2}{y_c^2-y_t^2}\left\{(y_s^2-y_b^2)W(1-Y-W) + \frac{(y_b^2-y_d^2)}{2}((1-Y)(1-Z)-X-W(1-X-2Z))\right\}\\ &+\frac{y_s^2+y_d^2}{y_s^2-y_d^2}\left\{(y_c^2-y_t^2)WZ + \frac{(y_t^2-y_u^2)}{2}Z((1-X)W+X-(1-Y)(1-Z))\right\}\\ &+\frac{y_s^2+y_b^2}{y_s^2-y_b^2}\left\{(y_c^2-y_t^2)W(1-Z-W) + \frac{(y_t^2-y_u^2)}{2}((1-Y)(1-Z)-X-W(1-X-2Y))\right\}\Bigg]\end{aligned} \tag{4.4.5}$$

The standard parametrization of the quark mixing is generally given in terms of the angles θ_{12}, θ_{13}, θ_{23} and δ. Using our variables, the mixing angles are written as

$$\theta_{12} = \arctan\sqrt{\frac{Y}{X}} \tag{4.4.6}$$

$$\theta_{13} = \arccos\sqrt{X+Y} \tag{4.4.7}$$

$$\theta_{23} = \arcsin\sqrt{\frac{1-W-Z}{X+Y}} \tag{4.4.8}$$

$$\delta = \arccos\frac{(X+Y)^2Z - Y(X+Y+Z+W-1) - X(1-W-Z)(1-X-Y)}{2\sqrt{XY(1-X-Y)(1-Z-W)(X+Y+Z+W-1)}} \tag{4.4.9}$$

4.4.1. Fixed points of the CKM matrix

We know that the equations (4.4.2-4.4.5) do not admit solutions with degenerate up or down Yukawa couplings. Therefore, for every solution we should have $y_i \neq y_j$ $(i,j = u,c,t)$ and $y_\rho \neq y_\gamma$ $(\rho,\gamma = d,s,b)$. However, the complexity of the CKM beta functions does not allow us to find analytic solutions for the full set of equations (i.e., gauge, Yukawa and CKM beta function simultaneously). Then, we look for particular cases that seem more interesting and easier to analyse. We take first the cases for which each factor inside the curly brackets in equations (4.4.2-4.4.5) vanishes. It turns out that there are only 6 CKM configurations for which all the CKM beta functions vanish independently of the values of the Yukawa couplings. These configurations for V_2 correspond to the matrices

$$M_{123} = \begin{bmatrix} 1 & 0 & 0 \\ 0 & 1 & 0 \\ 0 & 0 & 1 \end{bmatrix} , \quad M_{132} = \begin{bmatrix} 1 & 0 & 0 \\ 0 & 0 & 1 \\ 0 & 1 & 0 \end{bmatrix} , \quad M_{321} = \begin{bmatrix} 0 & 0 & 1 \\ 0 & 1 & 0 \\ 1 & 0 & 0 \end{bmatrix} ,$$

$$M_{213} = \begin{bmatrix} 0 & 1 & 0 \\ 1 & 0 & 0 \\ 0 & 0 & 1 \end{bmatrix} , \quad M_{312} = \begin{bmatrix} 0 & 0 & 1 \\ 1 & 0 & 0 \\ 0 & 1 & 0 \end{bmatrix} , \quad M_{231} = \begin{bmatrix} 0 & 1 & 0 \\ 0 & 0 & 1 \\ 1 & 0 & 0 \end{bmatrix} . \tag{4.4.10}$$

We observe these matrices also provide a faithful representation of the permutation group of three objects. Hence, the solutions for each of these configurations will be related by permutations. The second, third and fourth are odd permutations corresponding to interchanging two families, whereas the other three correspond to cyclic permutations. The matrix M_{123} represents the case of no mixing, where each up-type quark interacts only with the corresponding down-type quark. In the standard terminology the other cases are also referred to as "no mixing", because each up-type quark interacts only with one down-type quark, although possibly belonging to a different family.

4.4.2. Fixed-point structure of the Yukawa couplings.

We can now insert the CKM fixed-point matrices of Eq. (4.4.10) in the Yukawa beta functions. The resulting fixed-point equations can be solved analytically, yielding 392 solutions for each choice of V_2. In order to stay away from poles in the beta functions for the CKM matrix elements, we note that the number of zero Yukawa couplings in each solution cannot be greater than two. Otherwise, there will always exist two vanishing Yukawa belonging to either the up y_i or down set y_ρ. On the other hand, non-vanishing fixed-point values for the Yukawa couplings must not exhibit degeneracies between up-type and down-type quarks. This rules out a large number of solutions. Altogether end up with only 16 solutions for each choice of CKM matrix. Of these, six are isolated fixed points, nine are lines of fixed points and one is a plane of fixed points. Finally we can discard the six isolated solutions and three lines of fixed points, since they all involve some negative squared Yukawa coupling (this is valid as long as $f_g > 0$).

We give here the remaining seven solutions for the case $V_2 = M_{123}$ ($X_* = W_* = 1$, $Y_* = Z_* = 0$). The plane solution is given by

$$\begin{aligned} y_{u*}^2 &= \frac{4\pi^2}{123}(47f_g - 82f_y) - y_{c*}^2 - y_{t*}^2\ , \quad y_{s*}^2 = -\frac{32f_g\pi^2}{41} + y_{c*}^2\ , \\ y_{d*}^2 &= \frac{4\pi^2}{123}(23f_g - 82f_y) - y_{c*}^2 - y_{t*}^2, \quad y_{b*}^2 = -\frac{32f_g\pi^2}{41} + y_{t*}^2\ . \end{aligned} \tag{4.4.11}$$

The lines of fixed points are presented in Table 4.1. The Yukawa beta functions with the mixing matrix $V_2 = M_{abc}$, with $(a, b, c) \neq (1, 2, 3)$ are obtained from those of the case $V_2 = M_{123}$ by multiplying the down-type quarks with the matrix M_{abc}^{-1}. Thus, all the fixed points of the Yukawa couplings for any $V_2 = M_{abc}$ can be obtained from the ones described in (4.4.11) and Table 4.1 by just permuting the values of the down-type Yukawa couplings. We will therefore not repeat them here.

	y_u^2	y_c^2	y_t^2	y_d^2	y_s^2	y_b^2
1	$\frac{4\pi^2}{123}(35f_g - 82f_y) - y_t^2$	0	y_t^2	$\frac{4\pi^2}{123}(11f_g - 82f_y) - y_t^2$	0	$-\frac{32f_g\pi^2}{41} + y_t^2$
2	$\frac{4\pi^2}{123}(23f_g - 82f_y) - y_t^2$	$\frac{32f_g\pi^2}{41}$	y_t^2	$-\frac{4\pi^2}{123}(f_g + 82f_y) - y_t^2$	0	$-\frac{32f_g\pi^2}{41} + y_t^2$
3	$\frac{32f_g\pi^2}{41}$	$\frac{4\pi^2}{123}(23f_g - 82f_y) - y_t^2$	y_t^2	0	$-\frac{4\pi^2}{123}(f_g + 82f_y) - y_t^2$	$-\frac{32f_g\pi^2}{41} + y_t^2$
4	0	$\frac{4\pi^2}{123}(35f_g - 82f_y) - y_t^2$	y_t^2	0	$\frac{4\pi^2}{123}(11f_g - 82f_y) - y_t^2$	$-\frac{32f_g\pi^2}{41} + y_t^2$
5	$\frac{4\pi^2}{123}(35f_g - 82f_y) - y_c^2$	y_c^2	0	$\frac{4\pi^2}{123}(11f_g - 82f_y) - y_c^2$	$-\frac{32f_g\pi^2}{41} + y_c^2$	0
6	$\frac{4\pi^2}{123}(23f_g - 82f_y) - y_c^2$	y_c^2	$\frac{32f_g\pi^2}{41}$	$-\frac{4\pi^2}{123}(f_g + 82f_y) - y_c^2$	$-\frac{32f_g\pi^2}{41} + y_c^2$	0

Table 4.1: Lines of fixed points in the Yukawa sector for the case $V_2 = M_{123}$. The fixed point symbol $*$ in all the Yukawa couplings is understood.

We now examine whether these solutions feature interesting properties from a phenomeno-

logical point of view. Since the value of f_g is fixed by the running of the g_1, we have the free parameter f_y that can be used to set the values of the Yukawa couplings at the fixed point. For the lines of fixed points we also have the free parameter y_{t*} or y_{c*}, but we do not to impose conditions on those quantities in order to see if they can be indirectly determined. This would result in a lower number of free parameters. We start by demanding that $y_{t*} > y_{c*} > y_{u*}$ and $y_{b*} > y_{s*} > y_{d*}$, because the poles in Eq. (4.4.2)-(4.4.5) imply that a "wrong" ordering at the fixed point cannot be undone by the RG flow. Note that we do not require specific values of the Yukawa couplings. After analyzing all the solutions in (4.4.11) and Tab. 4.1, plus their permutations, we find that only the case with proper no-mixing ($X_* = 1$, $Y_* = 0$, $Z_* = 0$, $W_* = 1$) produces fixed points respecting the right ordering in the couplings. In particular, we are left with the plane (4.4.11) and the solutions 3 - 4 in Tab. 4.1. The conditions on the ordering of Yukawa couplings at the fixed point translates in a constrained parameter space for the quantities f_y and y_{t*} (y_{c*}). However, for the allowed region of parameter space, we find that the the resulting values for the couplings at the fixed point are much higher than its corresponding values at the Planck scale. Thus, an agreement with measured quark masses becomes impossible due to the slow running of the Yukawa coupling. For instance, for the up quark we have that $y_{u*} \gtrsim 0.273$, while at the Planck scale $y_c(M_{pl}) = 5.079 \times 10^{-6}$. On the other hand, we find that the CKM elements seem to remain frozen at their fixed-point value. This is due to the low number of relevant directions. In total, there are only two relevant directions, these basically correspond to the gauge couplings g_2 and g_3. The number of marginal directions is equal to two, whereas the number of irrelevant directions sums up to nine. These irrelevant directions mix all the Yukawa couplings and CKM elements, so we cannot conclude that one specific coupling is irrelevant. However, the RG flow analysis shows us that the CKM remain frozen at their fixed-point value. Therefore, we conclude that none of the fixed points arising from Tab. 4.1 is of phenomenological interest.

In the analysis above, the beta functions of the mixing parameters were zero because the coefficient of each term of the form $y_i^2 - y_j^2$ vanishes independently. In principle there could exist other fixed points where these coefficients are not precisely zero but cancel one another. At such fixed points the mixing angles could be different from $n\pi/2$, $n \in \mathbb{R}$. These fixed points are harder to find because the beta functions of the mixing parameters cannot be solved independently of the ones of the Yukawa coupling.

We adopt the following search strategy. As before, the first step is to solve the beta functions of the gauge couplings and to retain only the fixed point $g_{1*} > 0$, $g_{2*} = 0 = g_{3*}$. Then, leaving X, Y, Z, W arbitrary, we solve the beta functions of the Yukawa couplings. This results in 64 fixed-point solutions depending parametrically on X, Y, Z, W, f_g and f_y. There are always solutions containing at least one zero coupling, and only one solution with all the Yukawa couplings non-trivial. As stated before, in order to avoid the poles in the CKM beta functions,

we note that the maximum number of zeros that we can have in each solution is equal to two. The presence of more than two zeros will always implies that two up (or down) Yukawa couplings are degenerate. Then, out of the 64 solutions, we isolate those having at most two vanishing Yukawa couplings. Thus, we end up with 16 possibilities. The case with all Yukawa couplings non-trivial has some degenerate couplings, so we ignore it. For the other 15 solutions, we realize that only the lightest generation can have a zero value at the fixed-point. Otherwise, as it has been stated along the text, the correct ordering in the Yukawa sector cannot be achieved in the IR. Thus, we find that there are only 3 solutions that have to be taken into account. These 3 solutions are pugged back into the CKM beta functions to obtain a system of four differential equations with four variables, $\beta_{X,Y,Z,W}(X,Y,Z,W)$. These new beta functions are quite involved so it is not possible to find an analytic solution. We therefore study the system numerically. Since f_g is fixed by the running of g_1, we only have f_y as a free parameter. We take 4 different values for f_y that are close to the one used in the two generations case, $f_y \sim 2.2475 \times 10^{-3}$. In order to solve the system of equations, we make use of the option FindRoot in the software Mathematica. We construct a 4-dimensional grid of 9^4 points around which we look for the roots of the CKM beta functions. Eliminating the degenerate solutions for X, Y, Z and W, we replace back the resulting 1410 configurations in the expressions for the Yukawa couplings $y_j(X,Y,Z,W)$. Analyzing this set of solutions for the Yukawa couplings, we realize that there are no non-degenerate and real solutions. Thus, we conclude that it is unlikely to find fixed-point solutions with non-trivial CKM values and real Yukawa couplings. Although we do not possess the complete set of solutions, the previous analysis supports our statements on the non-existence of CKM values beyond those reported in Tab. 4.1.

4.4.3. Phenomenologically viable fixed points

In the preceding sections we have assumed that the fixed-point values of two up-type or down-type Yukawa couplings cannot be equal, in order to avoid the singularities in the beta functions of the CKM elements. However, there might be an exception to it: fixed points with equal up-type or down-type Yukawa coupling can be approached asymptotically, as long as one avoids directions along which the two couplings become equal. In the following, we take this path and look for phenomenologically interesting configurations having more than two zero Yukawa couplings.

We assume here that y_c, y_s, y_d and y_u go to zero values towards the fixed point along a trajectory that avoids $y_c = y_u$ and $y_s = y_d$. That is, these couplings emanate from zero at very high energies and flow towards their observed values in the IR in the phenomenologically viable ordering $y_c > y_u$ and $y_s > y_d$. For $y_u \to 0, y_d \to 0, y_s \to 0, y_c \to 0$, the set of equations

simplifies greatly, allowing analytical solutions for y_t, y_b, and the CKM elements. We obtain two substantially distinct group of solutions. The first one given by the Yukawa couplings in Eq. (4.3.6), plus two possible CKM configuration: an isolated fixed point ($X_* = 0$, $Y_* = 1$, $Z_* = 1$, $W_* = 0$), and a line of fixed points ($X_* = 1 - \delta$, $Y_* = \delta$, $Z_* = \delta$, $W_* = 1 - \delta$) parameterized by a number $\delta \in [0, 1]$. On the other hand, the second solution, corresponding to (4.3.7). It admits four different CKM sets of fixed points, ($X_* = 1$, $Y_* = 0$, $Z_* = 0$, $W_* = 0$), ($X_* = 0$, $Y_* = 1$, $Z_* = 0$, $W_* = 0$), ($X_* = 0$, $Y_* = 0$, $Z_* = 1$, $W_* = 0$) or ($X_* = 0$, $Y_* = 0$, $Z_* = 0$, $W_* = 1$). From this set of outcomes, we focus on the last expression since that is the one that carries more phenomenologically interesting properties. Namely, we take the top and bottom Yukawa given in Eq. (4.3.7) plus the following matrix of squared CKM elements

$$V_2 = \begin{bmatrix} 0 & 0 & 1 \\ 0 & 1 & 0 \\ 1 & 0 & 0 \end{bmatrix} . \tag{4.4.12}$$

Using $f_y \simeq 22476 \times 10^{-3}$, the flow from the UV to the IR results in values that match $y_b(k_{\rm IR}) = 0.024$, $y_c(k_{\rm IR}) = 0.0073$, $y_s(k_{\rm IR}) = 5.5 \times 10^{-4}$, $y_u(k_{\rm IR}) = 1.2 \times 10^{-5}$, $y_d(k_{\rm IR}) = 2.7 \times 10^{-5}$ with $k_{\rm IR} = 173\,\text{GeV}$ with a percentage error of around 1%, only y_t turns out to be much larger than required at low energies, $y_t(k_{\rm IR}) = 1.07$. The values that we use for the Yukawa couplings to benchmark our results correspond to a tree-level matching of the current PDG values [122]. Although it is well-known that there can be a significant difference between the tree-level and the one-loop matching conditions, the former is sufficient for our purposes. We do not aim at quantitative accuracy, but only at establishing that the approximate mass-patterns of the quark sector could (partially) arise from an interacting fixed point. The overestimation of the top mass was already seen in the two- and one- generations case. In Fig. 4.3, we show the running of the Yukawa couplings down to the IR starting from very high energies.

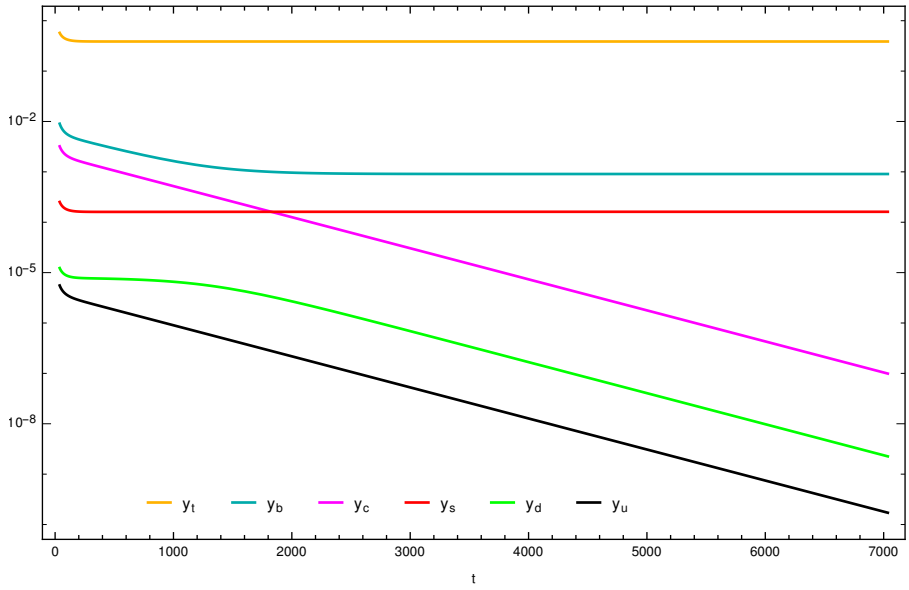

Figure 4.3: Running of the full set of Yukawa couplings from the far UV to $k = 173GeV$.

It is worth noting the particular behavior of y_s. Its flow appears to be determined by a non-trivial fixed point. However, a closer look actually reveals a slow running towards zero. It is also important to note the crossing of y_c and y_s, which is compatible with the pole-structure in the beta functions that only excludes equality of up-type or down-type quarks, respectively. The RG flow of the CKM elements is shown in Fig. (4.4). Their very slow running follows from tiny prefactors in the set of beta functions.

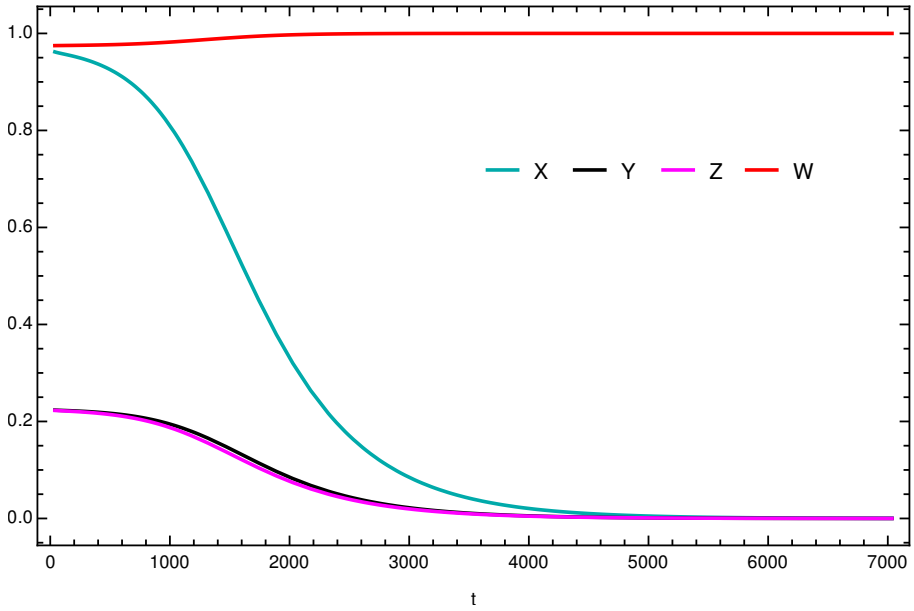

Figure 4.4: RG flow of the CKM elements in the case of $y_u \to 0, y_d \to 0, y_s \to 0, y_c \to 0$ in the far UV.

Conclusions

Asymptotically Safe theories seem to be more attractive than ordinary theories since the number of arbitrary or free parameters is generally smaller. Therefore, we can take Asymptotic Safety as a guiding principle to construct fundamental theories of nature. As such, we have attempted to continue the line of recent studies on Gauge-Yukawa systems and, in particular, extensive gravitational research. The mechanism generating non-trivial fixed points in these two approaches is very distinct in nature. The first one deals with physics from the the electroweak scale to the Planck scale. It also relies on perturbation theory and the fixed points arise from the balance between two-loops and one-loop terms in the gauge beta functions. The other one deals with Planck scale physics and beyond. In this case, the fixed points arise as the cancellation of one-loop and zero-loop terms.

In the case of physics below the Planck scale, that is, without the inclusion of gravity, we scan matter extensions in order to render the gauge couplings UV finite. In particular, the evolution of the $U(1)$ gauge coupling was expected to be asymptotically safe. A systematic search of possible extensions of the SM based on vector-like fermions charged under the SM groups, carrying various representations and coming in several copies (generations) shows that there are no fixed points in the β-functions that satisfy the minimal criteria to make them perturbatively stable and therefore physical. In other words, the presence of a large number of vector-like fermions make the loop coefficients of the beta functions large, which turns the models into highly non-perturbative.

We conclude that it is not possible, at least within the models we have studied, to extend the SM up to arbitrarily high energies in perturbation theory. This result might indicate that the search must be enlarged to include models with BSM fields more complicated than vector-like fermions. However, since vector-like fermions are actually just a proxy for more general matter fields, this does not seem too promising a line of inquiry. Another possibility is to embed the

SM gauge groups in a larger group before AS becomes manifest [13].

A completely different possibility is that the Landau pole is cured by gravity. In this scenario, we take into account the absence of new discoveries in the current particle colliders. That is, we assume that there are no new degrees of freedom from the TeV scale up to the Planck scale. If there is nothing between these two energy scales, we can in principle observe the imprint of gravity in the SM couplings at low energies. In fact, the modifications of the running in the SM couplings can be used to remove the Landau pole in the $U(1)$ sector. Moreover, it also gives us extra information that is not known a priori from the usual formulation of the SM. For the parametrized gravitational corrections that we considered in this thesis, we learned how the gravitational effects come into play. The introduction of non-trivial fixed points in the quark Yukawa sector of the theory opens the door for interesting low energy predictions. In particular, we saw that the generation of a gap between the heaviest quarks is possible while keeping the other couplings free. Even though the we are not able to explain all the details in the mass pattern of the quark sector, we can appreciate the power of Asymptotic Safety. Thus, following the lines written above, we can use Asymptotic Safety as a guiding principle in constructing fundamental theories of nature.

Bibliography

[1] K. G. Wilson. **Renormalization group and critical phenomena. 1. Renormalization group and the Kadanoff scaling picture**. *Phys. Rev.*, B4:3174–3183, 1971.

[2] S. Weinberg. **Ultraviolet divergences in quantum theories of gravitation**. In *General Relativity: An Einstein Centenary Survey*, pages 790–831. 1980.

[3] H. Gies and M. M. Scherer. **Asymptotic safety of simple Yukawa systems**. *Eur. Phys. J.*, C66:387–402, 2010.

[4] H. Gies, S. Rechenberger, and M. M. Scherer. **Towards an Asymptotic-Safety Scenario for Chiral Yukawa Systems**. *Eur. Phys. J.*, C66:403–418, 2010.

[5] M. Fabbrichesi, R. Percacci, A. Tonero, and O. Zanusso. **Asymptotic safety and the gauged SU(N) nonlinear σ-model**. *Phys. Rev.*, D83:025016, 2011.

[6] F. Bazzocchi, M. Fabbrichesi, R. Percacci, A. Tonero, and L. Vecchi. **Fermions and Goldstone bosons in an asymptotically safe model**. *Phys. Lett.*, B705:388–392, 2011.

[7] M. Fabbrichesi, R. Percacci, A. Tonero, and L. Vecchi. **The Electroweak S and T parameters from a fixed point condition**. *Phys. Rev. Lett.*, 107:021803, 2011.

[8] H. Gies, S. Rechenberger, M. M. Scherer, and L. Zambelli. **An asymptotic safety scenario for gauged chiral Higgs-Yukawa models**. *Eur. Phys. J.*, C73:2652, 2013.

[9] D. F. Litim and F. Sannino. **Asymptotic safety guaranteed**. *JHEP*, 12:178, 2014.

[10] A. Codello, M. Safari, G. P. Vacca, and O. Zanusso. **Functional perturbative RG and CFT data in the ϵ-expansion**. *Eur. Phys. J.*, C78(1):30, 2018.

[11] A. D. Bond and D. F. Litim. **Theorems for Asymptotic Safety of Gauge Theories**. *Eur. Phys. J.*, C77(6):429, 2017. [Erratum: Eur. Phys. J.C77,no.8,525(2017)].

[12] D. F. Litim, M. Mojaza, and F. Sannino. **Vacuum stability of asymptotically safe gauge-Yukawa theories**. *JHEP*, 01:081, 2016.

[13] B. Bajc and F. Sannino. **Asymptotically Safe Grand Unification**. *JHEP*, 12:141, 2016.

[14] A. D. Bond, G. Hiller, K. Kowalska, and D. F. Litim. **Directions for model building from asymptotic safety**. *JHEP*, 08:004, 2017.

[15] R. Mann, J. Meffe, F. Sannino, T. Steele, Z.-W. Wang, and C. Zhang. **Asymptotically Safe Standard Model via Vectorlike Fermions**. *Phys. Rev. Lett.*, 119(26):261802, 2017.

[16] G. M. Pelaggi, A. D. Plascencia, A. Salvio, F. Sannino, J. Smirnov, and A. Strumia. **Asymptotically Safe Standard Model Extensions?** *Phys. Rev.*, D97(9):095013, 2018.

[17] G. M. Pelaggi, F. Sannino, A. Strumia, and E. Vigiani. **Naturalness of asymptotically safe Higgs**. *Front.in Phys.*, 5:49, 2017.

[18] M. Gell-Mann and F. E. Low. **Quantum electrodynamics at small distances**. *Phys. Rev.*, 95:1300–1312, 1954.

[19] M. Gockeler, R. Horsley, V. Linke, Paul E. L. Rakow, G. Schierholz, and H. Stuben. **Is there a Landau pole problem in QED?** *Phys. Rev. Lett.*, 80:4119, 1998.

[20] G. Degrassi, S. Di Vita, J. Elias-Miro, J. R. Espinosa, G. F. Giudice, G. Isidori, and A. Strumia. **Higgs mass and vacuum stability in the Standard Model at NNLO**. *JHEP*, 08:098, 2012.

[21] D. Barducci, M. Fabbrichesi, C. M. Nieto, R. Percacci, and V. Skrinjar. **In search of a UV completion of the standard model — 378,000 models that don't work**. *JHEP*, 11:057, 2018.

[22] M. Reuter. **Nonperturbative evolution equation for quantum gravity**. *Phys. Rev.*, D57:971–985, 1998.

[23] M. Reuter and F. Saueressig. **Renormalization group flow of quantum gravity in the Einstein-Hilbert truncation**. *Phys. Rev.*, D65:065016, 2002.

[24] O. Lauscher and M. Reuter. **Ultraviolet fixed point and generalized flow equation of quantum gravity**. *Phys. Rev.*, D65:025013, 2002.

[25] D. F. Litim. **Fixed points of quantum gravity**. *Phys. Rev. Lett.*, 92:201301, 2004.

[26] A. Codello, R. Percacci, and C. Rahmede. **Investigating the Ultraviolet Properties of Gravity with a Wilsonian Renormalization Group Equation**. *Annals Phys.*, 324:414–469, 2009.

[27] D. Benedetti, P. F. Machado, and F. Saueressig. **Asymptotic safety in higher-derivative gravity**. *Mod. Phys. Lett.*, A24:2233–2241, 2009.

[28] P. Donà, A. Eichhorn, and R. Percacci. **Matter matters in asymptotically safe quantum gravity**. *Phys. Rev.*, D89(8):084035, 2014.

[29] K. Falls, D. F. Litim, K. Nikolakopoulos, and C. Rahmede. **A bootstrap towards asymptotic safety**. 2013.

[30] D. Becker and M. Reuter. **En route to Background Independence: Broken split-symmetry, and how to restore it with bi-metric average actions**. *Annals Phys.*, 350:225–301, 2014.

[31] H. Gies, B. Knorr, S. Lippoldt, and F. Saueressig. **Gravitational Two-Loop Counterterm Is Asymptotically Safe**. *Phys. Rev. Lett.*, 116(21):211302, 2016.

[32] N. Christiansen, K. Falls, J. M. Pawlowski, and M. Reichert. **Curvature dependence of quantum gravity**. *Phys. Rev.*, D97(4):046007, 2018.

[33] R. Percacci. **An Introduction to Covariant Quantum Gravity and Asymptotic Safety**, volume 3 of *100 Years of General Relativity*. World Scientific, 2017.

[34] K. Falls, C. R. King, D. F. Litim, K. Nikolakopoulos, and C. Rahmede. **Asymptotic safety of quantum gravity beyond Ricci scalars**. *Phys. Rev.*, D97(8):086006, 2018.

[35] A. Eichhorn. **Status of the asymptotic safety paradigm for quantum gravity and matter**. *Found. Phys.*, 48(10):1407–1429, 2018.

[36] A. Eichhorn, S. Lippoldt, J. M. Pawlowski, M. Reichert, and M. Schiffer. **How perturbative is quantum gravity?** *Phys. Lett.*, B792:310–314, 2019.

[37] A. Eichhorn. **An asymptotically safe guide to quantum gravity and matter**. *Front. Astron. Space Sci.*, 5:47, 2019.

[38] M. Reuter and F. Saueressig. **Quantum Gravity and the Functional Renormalization Group**. Cambridge University Press, 2019.

[39] O. Zanusso, L. Zambelli, G. P. Vacca, and R. Percacci. **Gravitational corrections to Yukawa systems**. *Phys. Lett.*, B689:90–94, 2010.

[40] A. Eichhorn, A. Held, and J. M. Pawlowski. **Quantum-gravity effects on a Higgs-Yukawa model**. *Phys. Rev.*, D94(10):104027, 2016.

[41] Y. Hamada and M. Yamada. **Asymptotic safety of higher derivative quantum gravity non-minimally coupled with a matter system**. *JHEP*, 08:070, 2017.

[42] A. Eichhorn and A. Held. **Viability of quantum-gravity induced ultraviolet completions for matter**. *Phys. Rev.*, D96(8):086025, 2017.

[43] M. Shaposhnikov and C. Wetterich. **Asymptotic safety of gravity and the Higgs boson mass**. *Phys. Lett.*, B683:196–200, 2010.

[44] J.-E. Daum, U. Harst, and M. Reuter. **Running Gauge Coupling in Asymptotically Safe Quantum Gravity**. *JHEP*, 01:084, 2010.

[45] U. Harst and M. Reuter. **QED coupled to QEG**. *JHEP*, 05:119, 2011.

[46] N. Christiansen and A. Eichhorn. **An asymptotically safe solution to the U(1) triviality problem**. *Phys. Lett.*, B770:154–160, 2017.

[47] A. Eichhorn and A. Held. **Top mass from asymptotic safety**. *Phys. Lett.*, B777:217–221, 2018.

[48] A. Eichhorn and F. Versteegen. **Upper bound on the Abelian gauge coupling from asymptotic safety**. *JHEP*, 01:030, 2018.

[49] A. Eichhorn and A. Held. **Mass difference for charged quarks from asymptotically safe quantum gravity**. *Phys. Rev. Lett.*, 121(15):151302, 2018.

[50] T. J. Hollowood. **Renormalization Group and Fixed Points in Quantum Field Theory**. *Swansea, UK: Springer Briefs in Physics*, 2013.

[51] D. G. C. McKeon and C. Zhao. **Multiple Couplings and Renormalization Scheme Ambiguities**. 2017.

[52] M. H. Goroff and A. Sagnotti. **The Ultraviolet Behavior of Einstein Gravity**. *Nucl. Phys.*, B266:709–736, 1986.

[53] A. E. M. van de Ven. **Two loop quantum gravity**. *Nucl. Phys.*, B378:309–366, 1992.

[54] J. F. Donoghue. **Leading quantum correction to the Newtonian potential**. *Phys. Rev. Lett.*, 72:2996–2999, 1994.

[55] J. F. Donoghue. **General relativity as an effective field theory: The leading quantum corrections**. *Phys. Rev.*, D50:3874–3888, 1994.

[56] J. F. Donoghue. **The effective field theory treatment of quantum gravity**. *AIP Conf. Proc.*, 1483(1):73–94, 2012.

[57] K. S. Stelle. **Renormalization of Higher Derivative Quantum Gravity**. *Phys. Rev.*, D16:953–969, 1977.

[58] E. S. Fradkin and A. A. Tseytlin. **Renormalizable asymptotically free quantum theory of gravity**. *Nucl. Phys.*, B201:469–491, 1982.

[59] I. G. Avramidi and A. O. Barvinsky. **Asymptotic Freedom In Higher Derivative Quantum Gravity**. *Phys. Lett.*, 159B:269–274, 1985.

[60] D. Dou and R. Percacci. **The running gravitational couplings**. *Class. Quant. Grav.*, 15:3449–3468, 1998.

[61] W. Souma. **Nontrivial ultraviolet fixed point in quantum gravity**. *Prog. Theor. Phys.*, 102:181–195, 1999.

[62] J. Laiho and D. Coumbe. Evidence for Asymptotic Safety from Lattice Quantum Gravity. *Phys. Rev. Lett.*, 107:161301, 2011.

[63] C. Wetterich. **Exact evolution equation for the effective potential**. *Phys. Lett.*, B301:90–94, 1993.

[64] U. Ellwanger. **FLow equations for N point functions and bound states**. *Z. Phys.*, C62:503–510, 1994. [,206(1993)].

[65] T. R. Morris. **The Exact renormalization group and approximate solutions**. *Int. J. Mod. Phys.*, A9:2411–2450, 1994.

[66] T. R. Morris. **Large curvature and background scale independence in single-metric approximations to asymptotic safety**. *JHEP*, 11:160, 2016.

[67] R. Percacci and G. P. Vacca. **The background scale Ward identity in quantum gravity**. *Eur. Phys. J.*, C77(1):52, 2017.

[68] P. Labus, T. R. Morris, and Z. H. Slade. **Background independence in a background dependent renormalization group**. *Phys. Rev.*, D94(2):024007, 2016.

[69] N. Ohta. **Background Scale Independence in Quantum Gravity**. *PTEP*, 2017(3):033E02, 2017.

[70] C. M. Nieto, R. Percacci, and V. Skrinjar. **Split Weyl transformations in quantum gravity**. *Phys. Rev.*, D96(10):106019, 2017.

[71] H. Gies, B. Knorr, and S. Lippoldt. **Generalized Parametrization Dependence in Quantum Gravity**. *Phys. Rev.*, D92(8):084020, 2015.

[72] N. Ohta, R. Percacci, and G. P. Vacca. **Renormalization Group Equation and scaling solutions for f(R) gravity in exponential parametrization**. *Eur. Phys. J.*, C76(2):46, 2016.

[73] G. P. De Brito, N. Ohta, A. D. Pereira, A. A. Tomaz, and M. Yamada. **Asymptotic safety and field parametrization dependence in the $f(R)$ truncation**. *Phys. Rev.*, D98(2):026027, 2018.

[74] K. G. Falls, D. F. Litim, and J. Schröder. **Aspects of asymptotic safety for quantum gravity**. *Phys. Rev.*, D99(12):126015, 2019.

[75] K. Falls, D. F. Litim, K. Nikolakopoulos, and C. Rahmede. **Further evidence for asymptotic safety of quantum gravity**. *Phys. Rev.*, D93(10):104022, 2016.

[76] G. Narain and R. Percacci. Renormalization Group Flow in Scalar-Tensor Theories. I. *Class. Quant. Grav.*, 27:075001, 2010.

[77] P. Labus, R. Percacci, and G. P. Vacca. **Asymptotic safety in $O(N)$ scalar models coupled to gravity**. *Phys. Lett.*, B753:274–281, 2016.

[78] J. Biemans, A. Platania, and F. Saueressig. **Renormalization group fixed points of foliated gravity-matter systems**. *JHEP*, 05:093, 2017.

[79] A. Eichhorn and S. Lippoldt. **Quantum gravity and Standard-Model-like fermions**. *Phys. Lett.*, B767:142–146, 2017.

[80] S. Folkerts, D. F. Litim, and J. M. Pawlowski. **Asymptotic freedom of Yang-Mills theory with gravity**. *Phys. Lett.*, B709:234–241, 2012.

[81] A. Eichhorn, A. Held, and C. Wetterich. **Quantum-gravity predictions for the fine-structure constant**. *Phys. Lett.*, B782:198–201, 2018.

[82] K.-y. Oda and M. Yamada. **Non-minimal coupling in Higgs–Yukawa model with asymptotically safe gravity**. *Class. Quant. Grav.*, 33(12):125011, 2016.

[83] H. Osborn. **Derivation of a four dimensional c-theorem for renormaliseable quantum field theories**. *Physics Letters B*, 222(1):97, 1989.

[84] J. L. Cardy. **Is there a c-theorem in four dimensions?** *Physics Letters B*, 215(4):749, 1988.

[85] I. Jack and H. Osborn. **Analogs of the c-theorem for four-dimensional renormalisable field theories**. *Nuclear Physics B*, 343(3):647, 1990.

[86] H. Osborn. **Weyl consistency conditions and a local renormalisation group equation for general renormalisable field theories**. *Nuclear Physics B*, 363(2):486, 1991.

[87] O. Antipin, M. Gillioz, J. Krog, E. Mølgaard, and F. Sannino. **Standard Model Vacuum Stability and Weyl Consistency Conditions**. *JHEP*, 08:034, 2013.

[88] A. D. Bond, D. F. Litim, G. Medina Vazquez, and T. Steudtner. **UV conformal window for asymptotic safety**. *Phys. Rev.*, D97(3):036019, 2018.

[89] D. J. Gross and F. Wilczek. **Ultraviolet Behavior of Nonabelian Gauge Theories**. *Phys. Rev. Lett.*, 30:1343–1346, 1973. [,271(1973)].

[90] H. D. Politzer. **Reliable Perturbative Results for Strong Interactions?** *Phys. Rev. Lett.*, 30:1346–1349, 1973. [,274(1973)].

[91] T. P. Cheng, E. Eichten, and L.-F. Li. **Higgs Phenomena in Asymptotically Free Gauge Theories**. *Phys. Rev.*, D9:2259, 1974.

[92] D. J. Gross and F. Wilczek. **Asymptotically Free Gauge Theories - I**. *Phys. Rev.*, D8:3633–3652, 1973.

[93] W. E. Caswell. **Asymptotic Behavior of Nonabelian Gauge Theories to Two Loop Order**. *Phys. Rev. Lett.*, 33:244, 1974.

[94] O. V. Tarasov and A. A. Vladimirov. **Two Loop Renormalization of the Yang-Mills Theory in an Arbitrary Gauge**. *Sov. J. Nucl. Phys.*, 25:585, 1977. [Yad. Fiz.25,1104(1977)].

[95] D. R. T. Jones. **The Two Loop beta Function for a G(1) x G(2) Gauge Theory**. *Phys. Rev.*, D25:581, 1982.

[96] M. E. Machacek and M. T. Vaughn. **Two Loop Renormalization Group Equations in a General Quantum Field Theory. 1. Wave Function Renormalization**. *Nucl. Phys.*, B222:83, 1983.

[97] M. Fischler and J. Oliensis. **Two Loop Corrections to the Evolution of the Higgs-Yukawa Coupling Constant**. *Phys. Lett.*, 119B:385, 1982.

[98] M. E. Machacek and M. T. Vaughn. **Two Loop Renormalization Group Equations in a General Quantum Field Theory. 2. Yukawa Couplings**. *Nucl. Phys.*, B236:221, 1984.

[99] I. Jack and H. Osborn. **Background Field Calculations in Curved Space-time. 1. General Formalism and Application to Scalar Fields**. *Nucl. Phys.*, B234:331–364, 1984.

[100] M. E. Machacek and M. T. Vaughn. **Two Loop Renormalization Group Equations in a General Quantum Field Theory. 3. Scalar Quartic Couplings**. *Nucl. Phys.*, B249:70, 1985.

[101] C. Ford, I. Jack, and D. R. T. Jones. **The Standard model effective potential at two loops**. *Nucl. Phys.*, B387:373–390, 1992. [Erratum: Nucl. Phys.B504,551(1997)].

[102] H. Arason, D. J. Castano, B. Keszthelyi, S. Mikaelian, E. J. Piard, Pierre Ramond, and B. D. Wright. **Renormalization group study of the standard model and its extensions. 1. The Standard model**. *Phys. Rev.*, D46:3945–3965, 1992.

[103] M. Luo, H. Wang, and Y. Xiao. **Two loop renormalization group equations in general gauge field theories**. *Phys. Rev.*, D67:065019, 2003.

[104] M. Luo and Y. Xiao. **Two loop renormalization group equations in the standard model**. *Phys. Rev. Lett.*, 90:011601, 2003.

[105] T. Curtright. **Three loop charge renormalization effects due to quartic scalar selfintercations**. *Phys. Rev.*, D21:1543, 1980.

[106] A. G. M. Pickering, J. A. Gracey, and D. R. T. Jones. **Three loop gauge beta function for the most general single gauge coupling theory**. *Phys. Lett.*, B510:347–354, 2001. [Erratum: Phys. Lett.B535,377(2002)].

[107] L. N. Mihaila, J. Salomon, and M. Steinhauser. **Gauge Coupling Beta Functions in the Standard Model to Three Loops**. *Phys. Rev. Lett.*, 108:151602, 2012.

[108] L. Mihaila. **Three-loop gauge beta function in non-simple gauge groups**. *PoS*, RADCOR2013:060, 2013.

[109] L. Mihaila. to appear.

[110] K. G. Chetyrkin and M. F. Zoller. **Three-loop β-functions for top-Yukawa and the Higgs self-interaction in the Standard Model**. *JHEP*, 06:033, 2012.

[111] A. V. Bednyakov, A. F. Pikelner, and V. N. Velizhanin. **Yukawa coupling beta-functions in the Standard Model at three loops**. *Phys. Lett.*, B722:336–340, 2013.

[112] A. V. Bednyakov, A. F. Pikelner, and V. N. Velizhanin. **Higgs self-coupling beta-function in the Standard Model at three loops**. *Nucl. Phys.*, B875:552–565, 2013.

[113] N. A. Dondi, F. Sannino, and V. Prochazka. **Conformal Data of Fundamental Gauge-Yukawa Theories**. 2017.

[114] A. D. Bond, D. F. Litim, G. Medina Vazquez, and T. Steudtner. **UV conformal window for asymptotic safety**. *Phys. Rev.*, D97(3):036019, 2018.

[115] B. Holdom. **Large N flavor beta-functions: a recap**. *Phys. Lett.*, B694:74–79, 2011.

[116] M. Cirelli, N. Fornengo, and A. Strumia. **Minimal dark matter**. *Nucl. Phys.*, B753:178, 2006.

[117] E. W. Kolb, D. J. H. Chung, and A. Riotto. **WIMPzillas!** *AIP Conf. Proc.*, 484(1):91–105, 1999. [,592(1999)].

[118] K. Sasaki. **Renormalization Group Equations for the Kobayashi-Maskawa Matrix**. *Z. Phys.*, C32:149–152, 1986.

[119] K. S. Babu. **Renormalization Group Analysis of the Kobayashi-Maskawa Matrix**. *Z. Phys.*, C35:69, 1987.

[120] P. F. Harrison, R. Krishnan, and W. G. Scott. **Exact One-Loop Evolution Invariants in the Standard Model**. *Phys. Rev.*, D82:096004, 2010.

[121] T. Feldmann, T. Mannel, and S. Schwertfeger. **Renormalization Group Evolution of Flavour Invariants**. *JHEP*, 10:007, 2015.

[122] M. Tanabashi et al. **Review of Particle Physics**. *Phys. Rev.*, D98(3):030001, 2018.

[123] D. M. Hofman and J. Maldacena. **Conformal collider physics: Energy and charge correlations**. *JHEP*, 05:012, 2008.

[124] M. J. Duff. **Observations on Conformal Anomalies**. *Nucl. Phys.*, B125:334–348, 1977.

Appendices

Appendix A

Analysis of marginal couplings

Here we prove the statement, made in Section 1.3, that when the marginal couplings are associated to vanishing gauge couplings, the behavior of the flow at quadratic order is determined by the coefficients P_{iii}.

The general form of the gauge β-functions is

$$\beta_i = (A^i + B^i_r \alpha_r + C^i_{rs} \alpha_r \alpha_s)\, \alpha_i^2, \tag{A.0.1}$$

where A^i, B^i_r and C^i_{rs} represent the one, two and three-loops coefficients. Their contribution to the stability matrix is given by

$$M_{ij} = \left.\frac{\partial \beta_i}{\partial \alpha_j}\right|_{\alpha_i^*} = (B^i_j + 2\, C^i_{jr} \alpha^*_r)\, \alpha_i^{*2} + 2\, (A^i + B^i_r \alpha^*_r + C^i_{rs} \alpha^*_r \alpha^*_s)\, \alpha^*_i \delta_{ij}. \tag{A.0.2}$$

We see that if $\alpha_i^* = 0$, the row i will have zeros in all the entries. This does not happen for the Yukawa interactions, whose NLO β-functions have the form $\beta_{Y_i} = (D^i_r \alpha_r + F^i_{rs} \alpha_r \alpha_s)\alpha_i$. Then, the contribution to the stability matrix reads

$$M_{ij} = \left.\frac{\partial \beta_{Y_i}}{\partial \alpha_j}\right|_{\alpha_i^*} = (D^i_j + 2F^i_{jr} \alpha^*_r)\alpha^*_i + (D^i_r \alpha^*_r + F^i_{rs} \alpha^*_r \alpha^*_s)\delta_{ij}, \tag{A.0.3}$$

where we see that if $\alpha_i^* = 0$, the last piece will be in general different from zero. Consequently, we do not have a row of zeros. The fact of having rows of zeros implies that $detM = 0$. Thus, the matrix M is singular and there exist vectors $\mathbf{x}$ such that $A\mathbf{x} = 0\mathbf{x}$. As a result, M has the eigenvalue $\lambda = 0$ with multiplicity given by the number of zero rows.

Suppose we have a fixed point with two gauge couplings equal to zero. Then the stability matrix will have two zero rows, that we can assume to be the last two. This implies that

the $n-2$ eigenvectors corresponding to $\lambda_i \neq 0$ have the form $\mathbf{V}^i = [V_1^i, V_2^i, \ldots, V_{n-2}^i, 0, 0]$. The eigenvectors for $\lambda = 0$ lie in a 2-dimensional plane. There is a freedom in choosing these vectors, and we can take them to have the form $\mathbf{V}^{n-1} = [V_1^{n-1}, V_2^{n-1}, \ldots, V_{n-2}^{n-1}, V_{n-1}^{n-1}, 0]$, $\mathbf{V}^n = [V_1^n, V_2^n, \ldots, V_{n-2}^n, 0, V_n^n]$. Moreover, the entries V_{n-1}^{n-1}, V_n^n can be taken to be positive without loss of generality. Thus, the transformation matrix constructed with the eigenvectors of M takes the form

$$S = \begin{bmatrix} V_1^1 & V_1^2 & \ldots & V_1^{n-2} & V_1^{n-1} & V_1^n \\ V_2^1 & V_2^2 & \ldots & V_2^{n-2} & V_2^{n-1} & V_2^n \\ \vdots & \vdots & \ddots & \vdots & \vdots & \vdots \\ V_{n-2}^1 & V_{n-2}^2 & \ldots & V_{n-2}^{n-2} & V_{n-2}^{n-1} & V_{n-2}^n \\ 0 & 0 & \ldots & 0 & V_{n-1}^{n-1} & 0 \\ 0 & 0 & \ldots & 0 & 0 & V_n^n \end{bmatrix} \tag{A.0.4}$$

This implies that

$$S^{-1} = \begin{bmatrix} a_{1,1} & a_{1,2} & \ldots & a_{1,n-2} & a_{1,n-1} & a_{1,n} \\ a_{2,1} & a_{2,2} & \ldots & a_{2,n-2} & a_{2,n-1} & a_{2,n} \\ \vdots & \vdots & \ddots & \vdots & \vdots & \vdots \\ a_{n-2,1} & a_{n-2,2} & \ldots & a_{n-2,n-2} & a_{n-2,n-1} & a_{n-2,n} \\ 0 & 0 & \ldots & 0 & b & 0 \\ 0 & 0 & \ldots & 0 & 0 & c \end{bmatrix} \tag{A.0.5}$$

where we have labelled $a_{i,j}$ the non-zero entries and we have called $b = 1/V_{n-1}^{n-1}$, $c = 1/V_n^n$. Now, when we compute the form of the new variables $z_i = S_{ij}^{-1} y_j = S_{ij}^{-1}(\alpha_j - \alpha_j^*)$, we observe that two of the new coordinates are just proportional to the asymptotically free variables, namely $z_{n-1} = b \cdot y_{n-1} = b \cdot \alpha_{n-1}$, $z_n = c \cdot y_n = c \cdot \alpha_n$. This result has an important effect in the analysis. For the gauge β-functions,

$$\begin{aligned} P_{ijk} = \left.\frac{\partial^2 \beta_i}{\partial \alpha_j \alpha_k}\right|_{\alpha_i^*} =& 2\, C_{jk}^i \alpha_i^{*2} + 2\left(B_j^i + 2\, C_{jr}^i \alpha_r^*\right) \alpha_i^* \delta_{ik} + 2\left(B_k^i + 2 C_{kr}^i \alpha_r^*\right) \alpha_i^* \delta_{ij} \\ &+ 2\left(A^i + B_r^i \alpha_r^* + C_{rs}^i \alpha_r^* \alpha_s^*\right) \delta_{ij} \delta_{ik} \end{aligned} \tag{A.0.6}$$

which in the case of the AF couplings reduces to

$$P_{ijk} = 2\left(A^i + B_r^i \alpha_r^* + C_{rs}^i \alpha_r^* \alpha_s^*\right) \delta_{ij} \delta_{ik} \ . \tag{A.0.7}$$

We conclude that in order to know if a marginal coupling is relevant or irrelevant we need only check the sign of P_{iii}. If $P_{iii} < 0$, the coupling is marginally relevant. If $P_{iii} > 0$, the coupling is marginally irrelevant.

Appendix B

Conformal field theory and central charges

The CFT at a given fixed point is characterized by two local functions: c and a. We refer to them collectively as central charges or CFT functions. They appear in the matrix element of the trace of the energy-momentum tensor of the theory as $\langle T^{\mu}_{\mu} \rangle = cW^2 - aE_4 + \cdots$, where W is the Weyl tensor, E_4 is the Euler density, and ellipses denote operators constructed from the fields in the theory. A function related to the CFT function a, often denoted $\tilde{a}$, was proven to be monotonically decreasing following the RG flow from a UV fixed point to an IR one [83, 85]. In fact, the RG flow of the $\tilde{a}$-function is related to the dynamics by means of the β-functions of the theory; it is given by

$$\mu \frac{\partial \tilde{a}}{\partial \mu} = -\chi_{ij} \beta^i \beta^j \,, \tag{B.0.1}$$

where χ_{ij} is known as the Zamolodchikov metric. Evaluated at a fixed point, $\tilde{a}$ reduces to the a-function.

In all of the models studied in this paper there is only a UV fixed point present, whereas dynamics in the IR is not known. Nevertheless, central charges of the UV fixed points can still be used to test whether the fixed points are reliable.

In any CFT, both a and c have to be positive, and their ratio has to satisfy the so-called *collider bounds* [123], namely

$$\frac{1}{3} \leq \frac{a}{c}\Big|_{FP} \leq \frac{31}{18} \,. \tag{B.0.2}$$

In perturbation theory, central charges are expanded in series

$$\tilde{a} = \tilde{a}_{free} + \frac{\tilde{a}^{(1)}}{(4\pi)^2} + \frac{\tilde{a}^{(2)}}{(4\pi)^4} + ... \tag{B.0.3}$$

$$c = c_{free} + \frac{c^{(1)}}{(4\pi)^4} + ... \ , \tag{B.0.4}$$

and since free-field theory contributions are positive [124],

$$\tilde{a}_{free} = \frac{1}{(4\pi)^2}\frac{n_s + 11/2\, n_w + 62\, n_v}{360} \tag{B.0.5}$$

$$c_{free} = \frac{1}{(4\pi)^2}\frac{1/6\, n_s + n_w + 2\, n_v}{20} \tag{B.0.6}$$

(n_s, n_w, and n_v referring to scalar, Weyl and vector degrees of freedom, respectively), the positivity of the CFT functions is ensured in perturbation theory.

There is a correlation between critical exponents and the change in central charges, which for the a-function can be explained as follows. At the fixed point we have,

$$\tilde{a}^* = a^* = a_{free} + \frac{1}{4}\sum_i b_i \chi_{g_i g_i} \alpha_i^* (1 + A_i \alpha_i^*) \tag{B.0.7}$$

where i runs over simple gauge groups, $b_1 = B_1, b_2 = -B_2, b_3 = -B_3$ are the one-loop coefficients of the gauge beta functions, and $\chi_{g_i g_i}$ and A_i are components of the Zamolodchikov metric, see [113]. One-loop critical exponent follows from $\beta_i = \pm B_i \alpha_i^2$ ($+$ for the group $U(1)$, $-$ otherwise), and reads $\theta^{1L} = 2 b_i \alpha_i^*$. Then,

$$\delta a = \frac{a^* - a_{free}}{a_{free}} = \frac{1}{8 a_{free}} \sum_i \theta_i^{1L} \chi_{g_i g_i} (1 + A_i \alpha_i^*) \ , \tag{B.0.8}$$

which explains the correlation.

Appendix C

All the fixed points in the 210 approximation scheme

In Table C.1 we list all the distinct zeroes of the β-functions in the 210 approximation scheme for all the models discussed in the text and for the SM. There are altogether 32 zeroes, with the Gaussian fixed point appearing with multiplicity four (this is the reason for missing fixed point P_{20}, P_{27}, P_{32}, which are copies of P_1).

The column labelled by $N_f = 0$ contains the values of α_1^*, α_2^*, α_3^*, α_t^* for the matter content of the SM (the coupling α_y^* does not appear in the SM). In this case the fixed points all come in pairs. When $N_f \neq 0$ this degeneracy is lifted and all the fixed points are different.

Note that the fixed points can be roughly divided in two classes. The fixed points with $\alpha_1^* = 0$ have coordinates α_i^* independent of Y. The remaining fixed points have coordinates that in general depend on all the quantum numbers.

	α_1^*	α_2^*	α_3^*	α_t^*	α_y^*	$N_f = 0$
P_1	0	0	0	0	0	$(0,0,0,0)$
P_2	0	$\alpha_2^*(p,q,\ell)$	$\alpha_3^*(p,q,\ell)$	0	$\alpha_y^*(p,q,\ell)$	$\left(0,\frac{499}{617},-\frac{319}{2468},0\right)$
P_3	0	$\alpha_2^*(p,q,\ell)$	$\alpha_3^*(p,q,\ell)$	$\alpha_t^*(p,q,\ell)$	$\alpha_y^*(p,q,\ell)$	$\left(0,\frac{1226}{1411},-\frac{189}{1411},\frac{277}{1411}\right)$
P_4	0	$\alpha_2^*(p,q,\ell)$	$\alpha_3^*(p,q,\ell)$	0	0	$\left(0,\frac{499}{617},-\frac{319}{2468},0\right)$
P_5	0	$\alpha_2^*(p,q,\ell)$	$\alpha_3^*(p,q,\ell)$	$\alpha_t^*(p,q,\ell)$	0	$\left(0,\frac{1226}{1411},-\frac{189}{1411},\frac{277}{1411}\right)$
P_6	$\alpha_1^*(p,q,\ell,Y)$	$\alpha_2^*(p,q,\ell,Y)$	$\alpha_3^*(p,q,\ell,Y)$	0	$\alpha_y^*(p,q,\ell,Y)$	$\left(-\frac{7938}{9257},\frac{9841}{9257},-\frac{5395}{37028},0\right)$
P_7	$\alpha_1^*(p,q,\ell,Y)$	$\alpha_2^*(p,q,\ell,Y)$	$\alpha_3^*(p,q,\ell,Y)$	$\alpha_t^*(p,q,\ell,Y)$	$\alpha_y^*(p,q,\ell,Y)$	$\left(-\frac{121821}{142153},\frac{151229}{142153},-\frac{41441}{284306},\frac{427}{142153}\right)$
P_8	0	0	$\alpha_3^*(p,q,\ell)$	$\alpha_t^*(p,q,\ell)$	$\alpha_y^*(p,q,\ell)$	$\left(0,0,-\frac{9}{38},-\frac{8}{19}\right)$
P_9	0	0	$\alpha_3^*(p,q,\ell)$	0	$\alpha_y^*(p,q,\ell)$	$\left(0,0,-\frac{7}{26},0\right)$
P_{10}	0	0	$\alpha_3^*(p,q,\ell)$	$\alpha_t^*(p,q,\ell)$	0	$\left(0,0,-\frac{9}{38},-\frac{8}{19}\right)$
P_{11}	0	0	$\alpha_3^*(p,q,\ell)$	0	0	$\left(0,0,-\frac{7}{26},0\right)$
P_{12}	$\alpha_1^*(p,q,\ell,Y)$	0	$\alpha_3^*(p,q,\ell,Y)$	0	$\alpha_y^*(p,q,\ell,Y)$	$\left(-\frac{225}{943},0,-\frac{1079}{3772}\right)$
P_{13}	$\alpha_1^*(p,q,\ell,Y)$	0	$\alpha_3^*(p,q,\ell,Y)$	$\alpha_t^*(p,q,\ell,Y)$	$\alpha_y^*(p,q,\ell,Y)$	$\left(-\frac{7266}{16847},0,-\frac{4286}{16847},-\frac{9907}{16847}\right)$
P_{14}	$\alpha_1^*(p,q,\ell,Y)$	0	$\alpha_3^*(p,q,\ell,Y)$	0	0	$\left(-\frac{225}{943},0,-\frac{1079}{3772}\right)$
P_{15}	$\alpha_1^*(p,q,\ell,Y)$	0	$\alpha_3^*(p,q,\ell,Y)$	$\alpha_t^*(p,q,\ell,Y)$	0	$\left(-\frac{7266}{16847},0,-\frac{4286}{16847},-\frac{9907}{16847}\right)$
P_{16}	0	$\alpha_2^*(p,q,\ell)$	0	0	$\alpha_y^*(p,q,\ell)$	$\left(0,\frac{19}{35},0,0\right)$
P_{17}	0	$\alpha_2^*(p,q,\ell)$	0	$\alpha_t^*(p,q,\ell)$	$\alpha_y^*(p,q,\ell)$	$\left(0,\frac{38}{61},0,\frac{19}{61}\right)$
P_{18}	0	$\alpha_2^*(p,q,\ell)$	0	0	0	$\left(0,\frac{19}{35},0,0\right)$
P_{19}	0	$\alpha_2^*(p,q,\ell)$	0	$\alpha_t^*(p,q,\ell)$	0	$\left(0,\frac{38}{61},0,\frac{19}{61}\right)$
P_{21}	$\alpha_1^*(p,q,\ell,Y)$	0	0	0	0	$\left(-\frac{123}{199},0,0,0\right)$
P_{22}	$\alpha_1^*(p,q,\ell,Y)$	0	0	$\alpha_t^*(p,q,\ell,Y)$	0	$\left(-\frac{2214}{3293},0,0,-\frac{697}{3293}\right)$
P_{23}	$\alpha_1^*(p,q,\ell,Y)$	0	0	$\alpha_t^*(p,q,\ell,Y)$	$\alpha_y^*(p,q,\ell,Y)$	$\left(-\frac{2214}{3293},0,0,-\frac{697}{3293}\right)$
P_{24}	$\alpha_1^*(p,q,\ell,Y)$	0	0	0	$\alpha_y^*(p,q,\ell,Y)$	$\left(-\frac{123}{199},0,0,0\right)$
P_{25}	$\alpha_1^*(p,q,\ell,Y)$	$\alpha_2^*(p,q,\ell,Y)$	0	0	$\alpha_y^*(p,q,\ell,Y)$	$\left(-\frac{1461}{1559},\frac{1222}{1559},0,0\right)$
P_{26}	$\alpha_1^*(p,q,\ell,Y)$	$\alpha_2^*(p,q,\ell,Y)$	0	$\alpha_t^*(p,q,\ell,Y)$	$\alpha_y^*(p,q,\ell,Y)$	$\left(-\frac{21627}{23569},\frac{515}{637},0,\frac{2719}{23569}\right)$
P_{28}	$\alpha_1^*(p,q,\ell,Y)$	$\alpha_2^*(p,q,\ell,Y)$	0	0	0	$\left(-\frac{1461}{1559},\frac{1222}{1559},0,0\right)$
P_{29}	$\alpha_1^*(p,q,\ell,Y)$	$\alpha_2^*(p,q,\ell,Y)$	0	$\alpha_t^*(p,q,\ell,Y)$	0	$\left(-\frac{21627}{23569},\frac{515}{637},0,\frac{2719}{23569}\right)$
P_{30}	$\alpha_1^*(p,q,\ell,Y)$	$\alpha_2^*(p,q,\ell,Y)$	$\alpha_3^*(p,q,\ell,Y)$	0	0	$\left(-\frac{7938}{9257},\frac{9841}{9257},-\frac{5395}{37028},0\right)$
P_{31}	$\alpha_1^*(p,q,\ell,Y)$	$\alpha_2^*(p,q,\ell,Y)$	$\alpha_3^*(p,q,\ell,Y)$	$\alpha_t^*(p,q,\ell,Y)$	0	$\left(-\frac{121821}{142153},\frac{151229}{142153},-\frac{41441}{284306},\frac{427}{142153}\right)$

Table C.1: Only the highlighted fixed points appear in the tables in the main text. The column $N_f = 0$ contains the values for the SM.

Appendix D

Coefficients of the β-functions in the 321 expansion

The β-function in eqs. (3.6.7)–(3.6.9) contain a number of coefficients that we collect in this appendix. The BSM fermions enter in the running of α_t via the coefficients

$$B_{t1} = Y^2 N_f d_{R_2} d_{R_3},\ B_{t2} = S_{R_2} N_f d_{R_3},\ B_{t3} = S_{R_3} N_f d_{R_2}. \tag{D.0.1}$$

For the BSM Yukawa coupling, besides the terms in Eq. (3.6.6), we have the coefficients

$$\begin{aligned}
V &= \frac{1}{2}N_f^2 + 3\,N_f d_{R_2} d_{R_3}, & V_1 &= 2\,(8\,N_f + 5\,d_{R_2} d_{R_3}) Y^2,\\
V_2 &= 2\,(8\,N_f + 5\,d_{R_2} d_{R_3}) C_{R_2}, & V_3 &= 2\,(8\,N_f + 5\,d_{R_2} d_{R_3}) C_{R_3},\\
W_1 &= \left(\frac{211}{3} - 6Y^2 + \frac{40}{3} Y^2 N_f d_{R_2} d_{R_3}\right) Y^2, & W_{12} &= 12\,Y^2 C_{R_2},\\
W_2 &= \left(-\frac{257}{3} - 6C_{R_2} + \frac{40}{3} N_f S_{R_2} d_{R_3}\right) C_{R_2}, & W_{23} &= 12\,C_{R_2} C_{R_3},\\
W_3 &= \left(-154 - 6C_{R_3} + \frac{40}{3} N_f S_{R_3} d_{R_2}\right) C_{R_3} & W_{13} &= 12\,Y^2 C_{R_3}.
\end{aligned} \tag{D.0.2}$$

The gauge β-functions get more contributions. These are split in two classes: the Yukawa contributions:

$$
\begin{aligned}
K_{y1} &= 6\,Y^2 N_f^3 d_{R_2} d_{R_3} + 7 Y^2 N_f^2 d_{R_2}^2 d_{R_3}^2, & K_{11} &= 6\,Y^4 N_f^2 d_{R_2} d_{R_3},\\
K_{12} &= 6\,Y^2 C_{R_2} N_f^2 d_{R_2} d_{R_3}, & K_{13} &= 6\,Y^2 C_{R_3} N_f^2 d_{R_2} d_{R_3},\\
K_{y2} &= 2\,C_{R_2} N_f^3 d_{R_2} d_{R_3} + \frac{7}{3} C_{R_2} N_f^2 d_{R_2}^2 d_{R_3}^2, & K_{21} &= 2\,Y^2 C_{R_2} N_f^2 d_{R_2} d_{R_3},\\
K_{22} &= 16\,C_{R_2} N_f^2 d_{R_2} d_{R_3} + 2\,C_{R_2}^2 N_f^2 d_{R_2} d_{R_3}, & K_{23} &= 2\,C_{R_2} C_{R_3} N_f^2 d_{R_2} d_{R_3},\\
K_{y3} &= \frac{3}{4} C_{R_3} N_f^3 d_{R_2} d_{R_3} + \frac{7}{8} C_{R_3} N_f^2 d_{R_2}^2 d_{R_3}^2, & K_{31} &= \frac{3}{4} Y^2 C_{R_3} N_f^2 d_{R_2} d_{R_3},\\
K_{33} &= 9\,C_{R_3} N_f^2 d_{R_2} d_{R_3} + \frac{3}{4} C_{R_3}^2 N_f^2 d_{R_2} d_{R_3} & K_{32} &= \frac{3}{4} C_{R_2} C_{R_3} N_f^2 d_{R_2} d_{R_3},
\end{aligned}
\tag{D.0.3}
$$

and the gauge contributions, which contain the diagonal terms

$$
\begin{aligned}
M_{11} &= \frac{388613}{2592} + \frac{4405}{162} N_f Y^2 d_{R_2} d_{R_3} + \frac{463}{9} N_f Y^4 d_{R_2} d_{R_3}\\
&\quad + 4 N_f Y^6 d_{R_2} d_{R_3} + \frac{88}{9} N_f^2 Y^6 d_{R_2}^2 d_{R_3}^2,\\
M_{22} &= \frac{324953}{864} + \frac{13411}{54} N_f S_{R_2} d_{R_3} + \frac{533}{9} N_f C_{R_2} S_{R_2} d_{R_3} - 4 N_f C_{R_2}^2 S_{R_2} d_{R_3}\\
&\quad - \frac{632}{27} N_f^2 S_{R_2}^2 d_{R_3}^2 - \frac{88}{9} C_{R_2} N_f^2 S_{R_2}^2 d_{R_3}^2,\\
M_{33} &= 65 + \frac{6242}{9} N_f S_{R_3} d_{R_2} + \frac{322}{3} N_f C_{R_3} S_{R_3} d_{R_2} - 4 N_f C_{R_3}^2 S_{R_3} d_{R_2}\\
&\quad - \frac{316}{9} N_f^2 S_{R_3}^2 d_{R_2}^2 - \frac{88}{9} C_{R_3} N_f^2 S_{R_3}^2 d_{R_2}^2,
\end{aligned}
\tag{D.0.4}
$$

as well as mixed coefficients

$$
\begin{aligned}
M_{12} &= \frac{205}{48} - 8\,C_{R_2} N_f Y^4 d_{R_2} d_{R_3}, \qquad M_{13} = \frac{274}{27} + 8\,C_{R_3} N_f Y^4 d_{R_2} d_{R_3},\\
M_{21} &= \frac{291}{16} + 32\,Y^2 N_f S_{R_2} d_{R_3} - 8\,Y^2 C_{R_2} N_f S_{R_2} d_{R_3},\\
M_{23} &= 78 + 32\,C_{R_3} N_f S_{R_2} d_{R_3} - 8\,C_{R_2} C_{R_3} N_f S_{R_2} d_{R_3},\\
M_{31} &= \frac{154}{9} + 48\,Y^2 N_f S_{R_3} d_{R_2} - 8\,Y^2 C_{R_3} N_f S_{R_3} d_{R_2},\\
M_{32} &= 42 + 48\,C_{R_2} N_f S_{R_3} d_{R_2} - 8\,C_{R_2} C_{R_3} N_f S_{R_3} d_{R_2},\\
G_{23} &= 2 + 8\,C_{R_2} C_{R_3} N_f Y^2 d_{R_2} d_{R_3}, \quad G_{13} = \frac{2}{3} + 8\,Y^2 C_{R_3} N_f S_{R_2} d_{R_3},\\
G_{12} &= \frac{1}{4} + 8\,Y^2 C_{R_2} N_f S_{R_3} d_{R_2},
\end{aligned}
\tag{D.0.5}
$$

$$
\begin{aligned}
H_{11} &= \frac{1315}{32} + \frac{245}{9} C_{R_2} N_f Y^2 d_{R_2} d_{R_3} - 4\, C_{R_2}^2 N_f Y^2 d_{R_2} d_{R_3} + \frac{23}{2} N_f S_{R_2} d_{R_3} \\
&\quad - \frac{88}{9} C_{R_2} N_f^2 Y^2 S_{R_2} d_{R_2} d_{R_3}^2, \\
G_{11} &= 198 + \frac{178}{3} C_{R_3} N_f Y^2 d_{R_2} d_{R_3} - 4\, C_{R_3}^2 N_f Y^2 d_{R_2} d_{R_3} - \frac{968}{27} N_f S_{R_3} d_{R_2} \\
&\quad - \frac{88}{9} C_{R_3} N_f^2 Y^2 S_{R_3} d_{R_2}^2 d_{R_3}, \\
H_{22} &= \frac{5597}{288} + \frac{23}{6} N_f Y^2 d_{R_2} d_{R_3} + \frac{463}{9} Y^2 N_f S_{R_2} d_{R_3} + 4 N_f Y^4 S_{R_2} d_{R_3} \\
&\quad + \frac{88}{9} N_f^2 Y^4 S_{R_2} d_{R_2} d_{R_3}^2, \\
G_{22} &= 162 + \frac{178}{3} C_{R_3} N_f S_{R_2} d_{R_3} - 4\, C_{R_3}^2 N_f S_{R_2} d_{R_3} - \frac{88}{3} N_f S_{R_3} d_{R_2} \\
&\quad - \frac{88}{9} C_{R_3} N_f^2 S_{R_2} S_{R_3} d_{R_2} d_{R_3}, \\
H_{33} &= \frac{2615}{108} + \frac{121}{27} N_f Y^2 d_{R_2} d_{R_3} + \frac{463}{9} Y^2 N_f S_{R_3} d_{R_2} + 4 N_f Y^4 S_{R_3} d_{R_2} \\
&\quad + \frac{88}{9} N_f^2 Y^4 S_{R_3} d_{R_3} d_{R_2}^2, \\
G_{33} &= \frac{109}{4} - 11 N_f S_{R_2} d_{R_3} + \frac{245}{9} C_{R_2} N_f S_{R_3} d_{R_2} - 4\, C_{R_2}^2 N_f S_{R_3} d_{R_2} \\
&\quad - \frac{88}{9} C_{R_2} N_f^2 S_{R_2} S_{R_3} d_{R_2} d_{R_3},
\end{aligned}
\tag{D.0.6}
$$

Appendix E

Complete set of fixed points for two generations of quarks

Lines of fixed points

The lines of fixed points are parametrized by the coupling y_{t*}^2. The first one corresponds to the proper no-mixing case

$$\begin{aligned} y_{c*}^2 &= \frac{140 f_g \pi^2}{123} + \frac{8 f_y \pi^2}{3} - y_{t*}^2, \quad y_{s*}^2 = -\frac{32 f_g \pi^2}{41} + y_{t*}^2 \ , \\ y_{b*}^2 &= \frac{44 f_g \pi^2}{123} + \frac{8 f_y \pi^2}{3} - y_{t*}^2, \quad W_* = 0 \ . \end{aligned} \tag{E.0.1}$$

The second one has completely the opposite configuration for the CKM matrix

$$\begin{aligned} y_{c*}^2 &= \frac{140 f_g \pi^2}{123} + \frac{8 f_y \pi^2}{3} - y_{t*}^2, \quad y_{b*}^2 = -\frac{32 f_g \pi^2}{41} + y_{t*}^2 \ , \\ y_{s*}^2 &= \frac{44 f_g \pi^2}{123} + \frac{8 f_y \pi^2}{3} - y_{t*}^2, \quad W_* = 1 \ . \end{aligned} \tag{E.0.2}$$

We see that solution (E.0.2) is obtained from (E.0.1) by permuting $y_{b*} \leftrightarrow y_{s*}$. Similartly, the solutions of the table in the next page are related by permutations. For all the groups of solutions, we can take the fixed points a and b as representatives, and obtain c and d by the simultaneous permutations $y_{t*} \leftrightarrow y_{c*}$ and $y_{b*} \leftrightarrow y_{s*}$. Moreover, for the groups $1-4$ we can relate solutions with 0 and 1 by permuting either $y_{t*} \leftrightarrow y_{c*}$ or $y_{t*} \leftrightarrow y_{c*}$. These relations arise from the symmetries in the beta functions once we use any of the particular values of W_* given in the last column of the following table.

FP	$y^2_{t\star}$	$y^2_{c\star}$	$y^2_{b\star}$	$y^2_{s\star}$	W_*
1a	$\frac{4}{123}\left(11f_g+82f_y\right)\pi^2$	$\frac{32}{41}f_g\pi^2$	0	$\frac{4}{123}\left(-13f_g+82f_y\right)\pi^2$	0
1b	$\frac{4}{123}\left(11f_g+82f_y\right)\pi^2$	$\frac{32}{41}f_g\pi^2$	$\frac{4}{123}\left(-13f_g+82f_y\right)\pi^2$	0	1
1c	$\frac{32}{41}f_g\pi^2$	$\frac{4}{123}\left(11f_g+82f_y\right)\pi^2$	$\frac{4}{123}\left(-13f_g+82f_y\right)\pi^2$	0	0
1d	$\frac{32}{41}f_g\pi^2$	$\frac{4}{123}\left(11f_g+82f_y\right)\pi^2$	0	$\frac{4}{123}\left(-13f_g+82f_y\right)\pi^2$	1
2a	$\frac{4}{123}\left(23f_g+82f_y\right)\pi^2$	0	0	$\frac{4}{123}\left(-f_g+82f_y\right)\pi^2$	0
2b	$\frac{4}{123}\left(23f_g+82f_y\right)\pi^2$	0	$\frac{4}{123}\left(-f_g+82f_y\right)\pi^2$	0	1
2c	0	$\frac{4}{123}\left(23f_g+82f_y\right)\pi^2$	$\frac{4}{123}\left(-f_g+82f_y\right)\pi^2$	0	0
2d	0	$\frac{4}{123}\left(23f_g+82f_y\right)\pi^2$	0	$\frac{4}{123}\left(-f_g+82f_y\right)\pi^2$	1
3a	$\frac{16}{15}\left(f_g+2f_y\right)\pi^2$	0	$\frac{16}{615}\left(-19f_g+82f_y\right)\pi^2$	0	0
3b	$\frac{16}{15}\left(f_g+2f_y\right)\pi^2$	0	0	$\frac{16}{615}\left(-19f_g+82f_y\right)\pi^2$	1
3c	0	$\frac{16}{15}\left(f_g+2f_y\right)\pi^2$	0	$\frac{16}{615}\left(-19f_g+82f_y\right)\pi^2$	0
3d	0	$\frac{16}{15}\left(f_g+2f_y\right)\pi^2$	$\frac{16}{615}\left(-19f_g+82f_y\right)\pi^2$	0	1
4a	$\frac{4}{123}\left(35f_g+82f_y\right)\pi^2$	0	$-\frac{32}{41}f_g\pi^2$	$\frac{4}{123}\left(11f_g+82f_y\right)\pi^2$	0
4b	$\frac{4}{123}\left(35f_g+82f_y\right)\pi^2$	0	$\frac{4}{123}\left(11f_g+82f_y\right)\pi^2$	$-\frac{32}{41}f_g\pi^2$	1
4c	0	$\frac{4}{123}\left(35f_g+82f_y\right)\pi^2$	$\frac{4}{123}\left(11f_g+82f_y\right)\pi^2$	$-\frac{32}{41}f_g\pi^2$	0
4d	0	$\frac{4}{123}\left(35f_g+82f_y\right)\pi^2$	$-\frac{32}{41}f_g\pi^2$	$\frac{4}{123}\left(11f_g+82f_y\right)\pi^2$	1
5a	$\frac{8}{1107}\left(87f_g+246f_y-s\right)\pi^2$	$\frac{8}{1107}\left(87f_g+246f_y+s\right)\pi^2$	$\frac{16}{1107}\left(-43f_g+82f_y\right)\pi^2$	0	$-\frac{-43f_g+82f_y-s}{86f_g-164f_y}$
5b	$\frac{8}{1107}\left(87f_g+246f_y+s\right)\pi^2$	$\frac{8}{1107}\left(87f_g+246f_y-s\right)\pi^2$	$\frac{16}{1107}\left(-43f_g+82f_y\right)\pi^2$	0	$-\frac{-43f_g+82f_y+s}{86f_g-164f_y}$
5c	$\frac{8}{1107}\left(87f_g+246f_y-s\right)\pi^2$	$\frac{8}{1107}\left(87f_g+246f_y+s\right)\pi^2$	0	$\frac{16}{1107}\left(-43f_g+82f_y\right)\pi^2$	$-\frac{-43f_g+82f_y+s}{86f_g-164f_y}$
5d	$\frac{8}{1107}\left(87f_g+246f_y+s\right)\pi^2$	$\frac{8}{1107}\left(87f_g+246f_y-s\right)\pi^2$	0	$\frac{16}{1107}\left(-43f_g+82f_y\right)\pi^2$	$-\frac{-43f_g+82f_y-s}{86f_g-164f_y}$
6a	$\frac{16}{1107}\left(65f_g+82f_y\right)\pi^2$	0	$\frac{8}{1107}\left(-21f_g+246f_y-r\right)\pi^2$	$\frac{8}{1107}\left(-21f_g+246f_y+r\right)\pi^2$	$\frac{65f_g+82f_y-r}{130f_g+164f_y}$
6b	$\frac{16}{1107}\left(65f_g+82f_y\right)\pi^2$	0	$\frac{8}{1107}\left(-21f_g+246f_y+r\right)\pi^2$	$\frac{8}{1107}\left(-21f_g+246f_y-r\right)\pi^2$	$\frac{65f_g+82f_y+r}{130f_g+164f_y}$
6c	0	$\frac{16}{1107}\left(65f_g+82f_y\right)\pi^2$	$\frac{8}{1107}\left(-21f_g+246f_y-r\right)\pi^2$	$\frac{8}{1107}\left(-21f_g+246f_y+r\right)\pi^2$	$\frac{65f_g+82f_y+r}{130f_g+164f_y}$
6d	0	$\frac{16}{1107}\left(65f_g+82f_y\right)\pi^2$	$\frac{8}{1107}\left(-21f_g+246f_y+r\right)\pi^2$	$\frac{8}{1107}\left(-21f_g+246f_y-r\right)\pi^2$	$\frac{65f_g+82f_y-r}{130f_g+164f_y}$

Table E.1: Fixed point solutions in the Yukawa sector for the gauge coupling fixed points $g^2_{1\star}=\frac{96}{41}f_g\pi^2$ and $g^2_{2\star}=0=g^2_{3\star}$. The square roots s and r are given by $s=\sqrt{3741f_g^2+3444f_gf_y-20172f_y^2}$ and $r=\sqrt{1365f_g^2-14268f_gf_y-20172f_y^2}$.

Appendix F

Surfaces of fixed points and 1-loop RG invariants

In this Appendix, we discuss the relation between the existence of surfaces of fixed points and RG invariants along the flow. In particular, we will see how the existence of surfaces of fixed points can help us finding the 1-loop RG invariants in the quark Yukawa system of the Standard Model. We start by mentioning previous results on RG and flavor invariants. Being, Y_U and Y_D the up - and down - Yukawa matrices, it is easy to show that the following two quantities are invariant along the RG flow [120, 121]

$$I_{(1)} = \frac{Tr(M_U M_D)}{(det(M_U M_D))^{1/3}}, \quad I_{(2)} = Tr((M_U M_D)^{-1})(det(M_U M_D))^{1/3}, \tag{F.0.1}$$

where $M_U = Y_U Y_U^\dagger$ and $M_D = Y_D Y_D^\dagger$. In the diagonalized basis, we have

$$I_{(1)} = \sum_{i\rho} \frac{y_i^2 y_\rho^2 |V_{i\rho}|^2}{(y_t y_c y_u y_b y_s y_d)^{2/3}}, \quad I_{(2)} = (y_t y_c y_u y_b y_s y_d)^{2/3} \sum_{i\rho} y_i^{-2} y_\rho^{-2} |V_{i\rho}|^2. \tag{F.0.2}$$

These are invariants for the flow in the 10-dimensional space of the Yukawas and the CKM elements X, Y, Z, W. If we evaluate X, Y, Z, W at a fixed point, $I_{(1)}$ and $I_{(1)}$ are invariant for the flow in the 6-dimensional space of the Yukawa couplings only.

For instance, when the mixing matrix is equal to the identity ($X = 1, Y = 0, Z = 0, W = 1$), the invariants in (F.0.2) become

$$I_{(1)} = \frac{(y_t^2 y_b^2 + y_c^2 y_s^2 + y_u^2 y_d^2)}{(y_t y_c y_u y_b y_s y_d)^{2/3}}, \quad I_{(2)} = (y_t y_c y_u y_b y_s y_d)^{2/3} \left(\frac{1}{y_t^2 y_b^2} + \frac{1}{y_c^2 y_s^2} + \frac{1}{y_u^2 y_d^2} \right). \tag{F.0.3}$$

However one can show that each term in these sums is an invariant by itself:

$$U_1 = \frac{y_u^2 y_d^2}{y_t y_c y_b y_s}, \quad U_2 = \frac{y_c^2 y_s^2}{y_t y_u y_b y_d}, \quad U_3 = \frac{y_t^2 y_b^2}{y_c y_u y_s y_d}. \tag{F.0.4}$$

Let us see now how we can obtain these invariants when we know the surface of fixed points .

For any of the 6 particular CKM configurations we have considered, and the gauge fixed point ($g_1 = \sqrt{96 f_g \pi^2/41}$, $g_2 = 0$, $g_3 = 0$), the structure of the Yukawa beta functions at one loop take the form

$$\beta_{y_j^2} = y_j^2 h_j(y_k^2), \tag{F.0.5}$$

where h_j are linear functions of the couplings y_k^2. Surfaces of fixed points arise when at least one of these functions h_j are not independent. When looking for non-trivial fixed points, we have to solve the system of equations $h_j = 0$. Thus, when the h_i's are linearly dependent we have infinitely many solutions. Hence the appearance of surfaces of fixed points.

In general, an RG invariant is a quantity I that satisfies $\frac{d}{dk} I = 0$. In terms of the beta functions of the couplings

$$0 = \beta_{y_j^2} \partial_j I = y_j^2 h_j \partial_j I. \tag{F.0.6}$$

We take for the moment the case of n couplings y_j. Then, if there are some dependent function h_j, let us say h_{n-1} and h_n, we have that

$$h_{n-1} = \sum_{i=1}^{n-2} A_i h_i, \quad h_n = \sum_{i=1}^{n-2} B_i h_i. \tag{F.0.7}$$

Consequently, eq. (F.0.6) becomes

$$\sum_{j=1}^{n-2} (y_j^2 \partial_j I + y_{n-1}^2 A_j \partial_{n-1} I + y_n^2 B_j \partial_n I) h_j = 0. \tag{F.0.8}$$

Since by assumption the $n-2$ functions h_j are linearly independent, each of their coefficients must vanish separately. This means that any function of the variable

$$W = \frac{(y_1^2)^{A_1+B_1} (y_2^2)^{A_2+B_2} \dots (y_{n-2}^2)^{A_{n-2}+B_{n-2}}}{y_{n-1}^2 y_n^2}. \tag{F.0.9}$$

is an RG invariant.

For example, in the case considered above ($X = 1$, $Y = 0$, $Z = 0$, $W = 1$) we have the linear relations

$$h_t = h_u + h_d - h_b, \quad h_c = h_u + h_d - h_s. \tag{F.0.10}$$

or $A_u = 1$, $A_b = -1$, $A_s = 0$, $A_d = 1$, $B_u = 1$, $B_b = 0$, $B_s = -1$, $B - d = 1$, so we see that W coincides with $(U_1)^2$. (Obviously any function of an invariant is an invariant).

But we can also write

$$h_t = h_u + h_d - h_b, \quad h_c = h_u + h_d - h_s, \tag{F.0.11}$$

and

$$h_t = h_u + h_d - h_b, \quad h_c = h_u + h_d - h_s. \tag{F.0.12}$$

which are obtained from the previous linear relation by the permutations ($u \leftrightarrow c$, $d \leftrightarrow s$) and ($u \leftrightarrow t$, $d \leftrightarrow b$). These give rise to the invariants U_2 and U_3.

So we see that the surfaces of FPs and the one-loop invariants both originate from linear relations between the beta functions. If we allow one coupling to be zero, the number of equations decrease and then we will have only one linear relation. As a result, we obtain a line of fixed points.